EVALUATION OF ROTORCRAFT SYSTEM IDENTIFICATION APPROACHES

A THESIS SUBMITTED TO
THE GRADUATE SCHOOL OF NATURAL AND APPLIED SCIENCES
OF
MIDDLE EAST TECHNICAL UNIVERSITY

BY

SERKAN KAYMAK

IN PARTIAL FULFILLMENT OF THE REQUIREMENTS
FOR
THE DEGREE OF MASTER OF SCIENCE
IN
AEROSPACE ENGINEERING

FEBRUARY 2013

Approval of the thesis:

EVALUATION OF ROTORCRAFT SYSTEM IDENTIFICATION APPROACHES

submitted by **SERKAN KAYMAK** in partial fulfillment of the requirements for the degree of **Master of Science in Aerospace Engineering Department, Middle East Technical University** by,

Prof. Dr. Canan Özgen
Dean, Graduate School of **Natural and Applied Sciences**   _____

Prof. Dr. Ozan Tekinalp
Head of Department, **Aerospace Engineering**   _____

Prof. Dr. Ozan Tekinalp
Supervisor, **Aerospace Engineering**
Aerospace Engineering Dept., METU   _____

Asst. Prof. Dr. Ali Türker Kutay
Co-Supervisor, **Aerospace Engineering**
Aerospace Engineering Dept., METU   _____

Examining Committee Members:

Prof. Dr. Ozan Tekinalp
Aerospace Engineering Dept., METU   _____

Prof. Dr. M. Kemal Özgören
Mechanical Engineering Dept., METU   _____

Prof. Dr. Yusuf Özyörük
Aerospace Engineering Dept., METU   _____

Asst. Prof. Dr. Ali Türker KUTAY
Aerospace Engineering Dept., METU   _____

Asst. Prof. Dr. İlkay Yavrucuk
Aerospace Engineering Dept., METU   _____

Date: _____

I hereby declare that all information in this document has been obtained and presented in accordance with academic rules and ethical conduct. I also declare that, as required by these rules and conduct, I have fully cited and referenced all material and results that are not original to this work.

Name, Surname: Serkan Kaymak

Signature:

ABSTRACT

EVALUATION OF ROTORCRAFT SYSTEM IDENTIFICATION APPROACHES

Kaymak, Serkan

M. Sc., Department of Aerospace Engineering

Supervisor   : Prof. Dr. Ozan Tekinalp

Co-Supervisor   : Asst. Prof. Dr. Ali Türker Kutay

February 2013, 90 pages

This thesis addresses rotorcraft system identification approaches and estimating the stability and control parameters for linear system identification of a helicopter in hover. Output error and least square methods are used for the system identification. Inputs of the system identification analysis are obtained from the nonlinear helicopter model written in FLIGHTLAB commercial software environment. A linear helicopter model is used for identification. For validation, results obtained from identified helicopter model are compared with FLIGHTLAB's nonlinear simulation results by employing different inputs which are not used in the identification procedure.

Keywords: Helicopter, UH-60, simulation, system identification, output error method, least square method, mathematical modeling, FLIGHTLAB, standard deviation, coefficient of determination

ÖZ

HELİKOPTER SİSTEM TANIMLAMA YAKLAŞIMLARININ DEĞERLENDİRİLMESİ

Kaymak, Serkan

Yüksek Lisans, Havacılık ve Uzay Mühendisliği Bölümü

Tez Yöneticisi   : Prof. Dr. Ozan Tekinalp

Ortak Tez Yöneticisi   : Asst. Prof. Dr. Ali Türker Kutay

Şubat 2013, 90 sayfa

Bu tez helikopter sistem tanımlama yaklaşımlarının kullanılarak hover koşulunda helikopterin doğrusal sistem tanımlama modelindeki kararlılık ve kontrol parametrelerinin elde edilmesini içermektedir. Sistem tanımlaması zaman düzleminde Çıkış Hatası ve En Küçük Kareler yöntemleri kullanılarak gerçekleştirilmiştir. Sistem tanımlama analizi girdileri, ticari bir yazılım olan FLIGHTLAB ortamında doğrusal olmayan helikopter modeli kullanılarak elde edilmiştir. Bulunan sistem parametreleri ile oluşturulan doğrusal helikopter modelinden elde edilen sonuçların FLIGHTLAB yazılımından elde edilen sonuçlar ile karşılaştırılması ile doğrusal helikopter tanımlama modelinin doğrulaması yapılmıştır.

Anahtar kelimeler: Helikopter, UH-60, simülasyon, sistem tanımlama, çıkış hatası yöntemi, en küçük kareler yöntemi, matematiksel modelleme, FLIGHTLAB, Standard sapma, tespit katsayıları

To my close friends,
to my family and
to peace,

ACKNOWLEDGEMENTS

TABLE OF CONTENTS

LIST OF TABLES

TABLES

LIST OF FIGURES

FIGURES

LIST OF SYMBOLS

L	Roll moment
M	Pitch moment
N	Yaw Moment
X	Force on X-direction
Y	Force on Y-direction
Z	Force on Z-direction
a	Lift curve slope
β_0	Coning angle
β_{1c}	Longitudinal flapping angle
β_{1s}	Lateral flapping angle
c	Chord
g	Gravitational acceleration
m	Mass
v_0	Inflow ratio
x	Displacement in X-direction
y	Displacement in Y-direction
z	Displacement in Z-direction
γ	Lock number
σ	Solidity
ρ	Air density
φ	Roll angle
θ	Pitch angle
V	Velocity vector in body axis
u, v, w	Velocity components in body axis
ω	Angular velocity vector in body axis
p, q, r	Angular velocity components in body axis
I	Inertia matrix
I_{xx}	Rolling moment of inertia in body axis
I_{xy}	XY product of inertia in body axis
I_{xz}	XZ product of inertia in body axis
I_{yz}	YZ product of inertia in body axis
J	Cost function
y	Output vector
z	Measurement vector
x	State vector
δ_{long}	Longitudinal control input

δ_{lat}	Lateral control input
δ_{coll}	Collective control input
δ_{pedal}	Pedal control input

Subscripts:

i, j	General indices
$long$	Longitudinal
lat	Lateral
$coll$	Collective
b	Blade
0	Initial Condition
tot	Total

Other parameters are clearly defined wherever applicable.

CHAPTER 1

INTRODUCTION

1.1   BACKGROUND

System identification is a multidisciplinary and iterative process to determine the mathematical model of a system by using the input and output data of the system. System can be defined in different areas, such as biology, chemistry, economics, civil, electrical and mechanical engineering, automobiles, ships and flight vehicles. In this thesis flight vehicle, specifically helicopter, system identification, is addressed. Proper identification methods are examined, and identification of helicopter using simulation results is carried out.

What is System Identification?

Zadeh [1] defined the system identification technically in 1962 as: "the determination, on the basis of observation of input and output, of a system within a specified class of system to which the system under test is equivalent." According to this definition, it can be said that system identification process is basically composed of data gathering, appropriate system mathematical model and test. While the system is being tested, input and output data are collected and by using these data system mathematical model can be determined.

A simple definition was made by Iliff [2] in 1994 as: "Given the answer, what are the questions, i.e., look at the results and try to figure out what situation caused those results." Moreover Ljung [3] described the system identification in 1997 as: "The process of going from observed data to a mathematical model is fundamental in science and engineering. In the control area this process has been termed System Identification and objective is then to find dynamical models (difference or differential equations) from observed input and output signals."

System identification is multi-disciplinary. It is also an inverse problem of obtaining a description of a system. Figure 1- 1 shows the basic description of the system identification. Inputs and outputs are known. They are obtained from simulation data. However system and/or parameters of the system are not known. Aim of the system identification is to find the parameters of the system by using known inputs and outputs. In this thesis, unknown system is the helicopter.
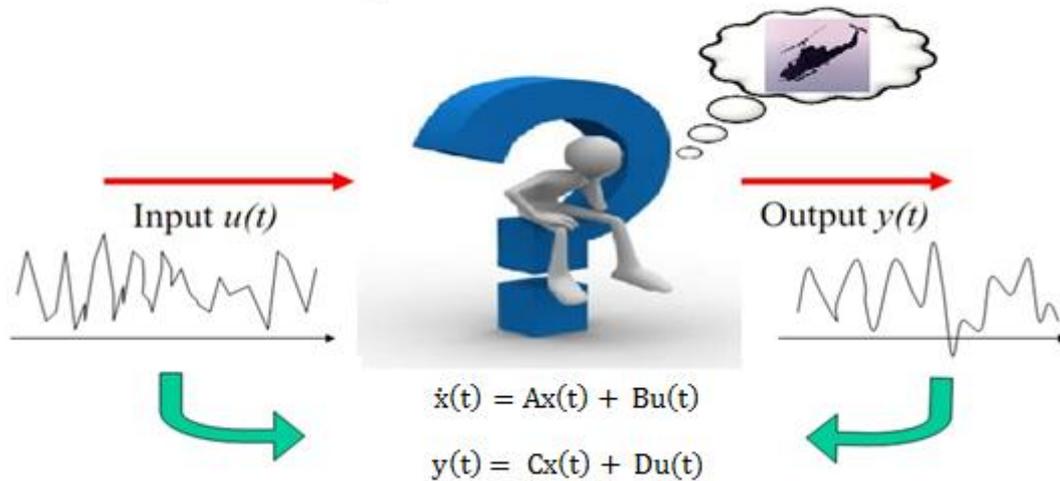
Figure 1- 1 : System Identification

Process

The general approach of the system identification process can be described as in Figure 1- 2. To excite the desired rotorcraft modes during the flight test, specific control inputs are designed. Responses of the rotorcraft to these inputs are measured and recorded. By comparing the model predicted response and the flight measured response, desired model parameters are estimated.

A coordinated approach to flight vehicle system identification can be divided into three major parts [4]:

- Instrumentation and Filters: For the flight testing, data gathering is very important. Flight data is gathered by using the flight data acquisition system. Flight data acquisition system can be composed of the ground and/or airvehicle based recording equipment. Instrumentation and filters are part of the data gathering process. In order to obtain the high data quality, instrumentation and filters are properly used.
- Flight Test Technique: Flight test maneuvers should be determined according to dynamic response of the airvehicle. In order to excite the airvehicle dynamic modes, suitable inputs should be cover the frequency range of interest. Hence, the case of optimal input design of the airvehicle may be required.
- Analysis of Flight Data: In order to analyze the flight data, mathematical model of the airvehicle and system identification method should be properly chosen. Unknown parameters are estimated by minimizing the response error. Initial unknown parameter values can be used to obtain the best solution for the identification process.

Jatagoankar [4] explained the most important aspects of system identification, namely "Quad-M" basics. Quad-M consists of the maneuvers, measurements, models and methods. Each of that is the requirement for the system identification procedure. Figure 1- 2 shows the Quad-M requirements to identify the unknown system or unknown parameters.

Maneuvers: Design of the control input in order to excite all modes of the airvehicle dynamic system that will be identified.

Measurements: Selection of instrumentation and filters for high accuracy data acquisition.

Models: Mathematical model of the unknown system should be selected.

Methods: Time domain or frequency domain system identification methods are used to identify the system. In this part, more suitable estimation method is selected. A priori parameter values and/or constraints of the parameters are also used for obtaining the best estimation results.
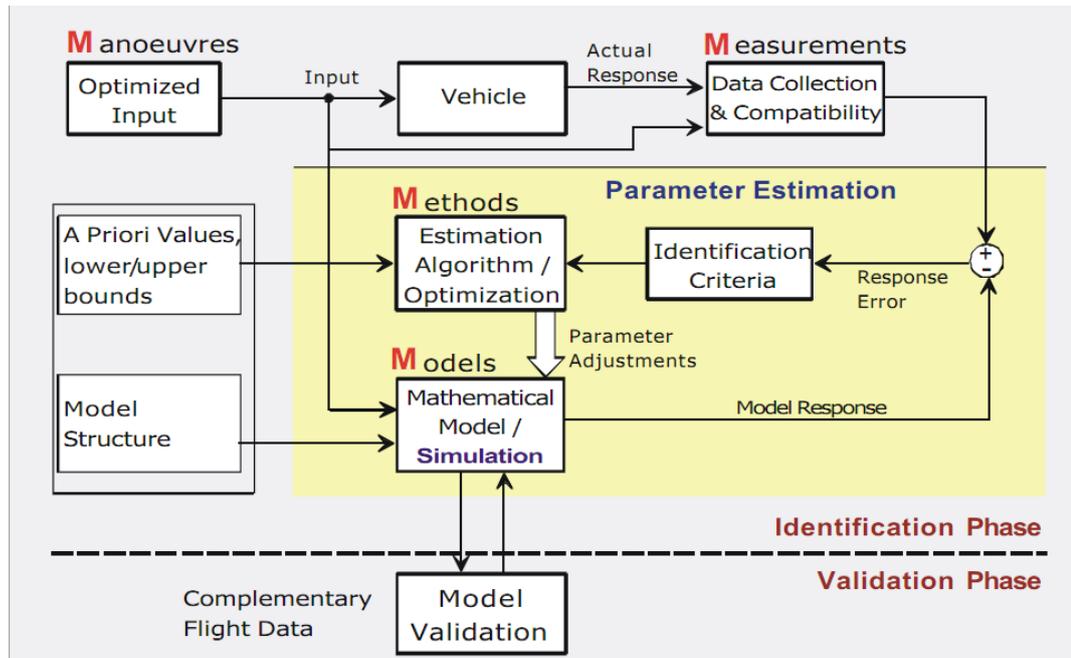
Figure 1- 2 : Quad-M Basics of Flight Vehicle System Identification [4]

Test Inputs

Proper control input design is important, because the accuracy and reliability of parameter estimation depends on the amount of the information available in the flight vehicle response. In general, optimal control input means best excitation of the frequency range of interest. Optimal control inputs should be the ones which maximize the information content for minimum maneuver time and minimum peak response. There are some limitations to design optimal input because input design process is based on a prior knowledge of the model structure and dynamic response characteristics. If the system model structure and dynamic mode characteristics are not known, rough guesses can be used for a good initial estimate to design the optimal inputs. [4, 5]

Based on these practical considerations, several signals can be found in literature, e.g. step, doublet, multistep 3-2-1-1, Mehra, Schulz, Delft University of Technology (DUT) and Langley inputs. Although the 3-2-1-1, Mehra, Langley and DUT inputs are more efficient, the doublet input is often used due to its simplicity. Since the multistep 3-2-1-1 signal is easily realizable and relatively easy to fly manually by pilots, this signal remains as the one most accepted by the

3

flight test community. Moreover the 3-2-1-1 signal and its variants have been highly successful in time-domain system identification applications such as Maximum Likelihood method. [4] Figure 1- 3 shows the spectral density of the step, doublet, 3-2-1-1 and improved 3-2-1-1 inputs with respect to normalized frequency, $\omega\Delta t$. It can be seen that 3-2-1-1 input has wider frequency range according to other signals at the Figure 1- 3.

Another optimal input well suited for identification of transfer function models and frequency domain identification methods is the "Schroder-phase signal". This signal composed of multi frequency wave form. It has large number of harmonics at equal frequency spacing. Schroder-phase signal has also a very flat power spectral density. Hence this signal is used for especially frequency domain identification methods. This signal is also called "frequency sweep input signal". However relatively long maneuver times can be required for applying this input. It is has also restriction with single axis excitation. Moreover, airvehicle can be easily departed from the trim condition by applying this input to airvehicle. In addition, during the sweep testing, critical flight incidence resulting from aero-servo-elastic interactions and exceeding the permissible loads should be avoided [4, 5]. At the Figure 1- 4, example of the frequency sweep input can be seen. From Figure 1- 3 and Figure 1- 4, it can be seen that frequency sweep input is applied to longer time than 3-2-1-1 input.
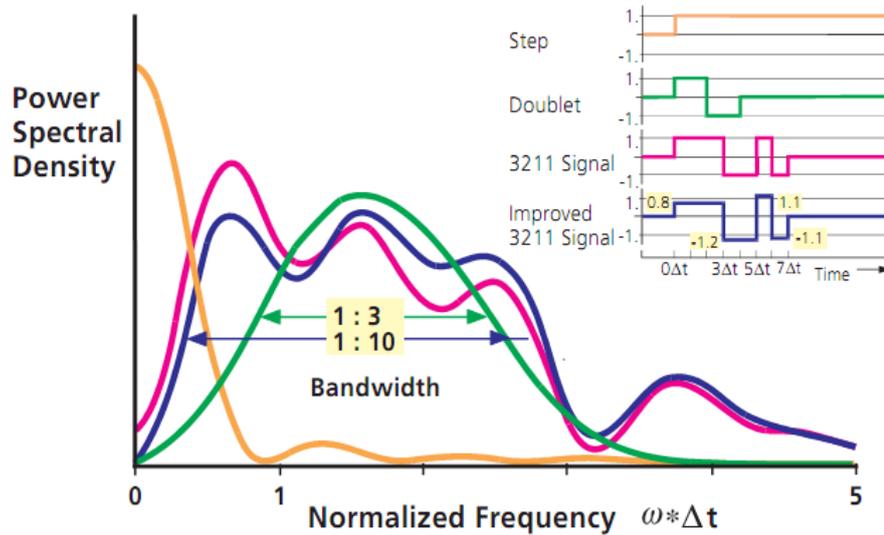
Figure 1- 3 : Comparison of the different input signals [4]
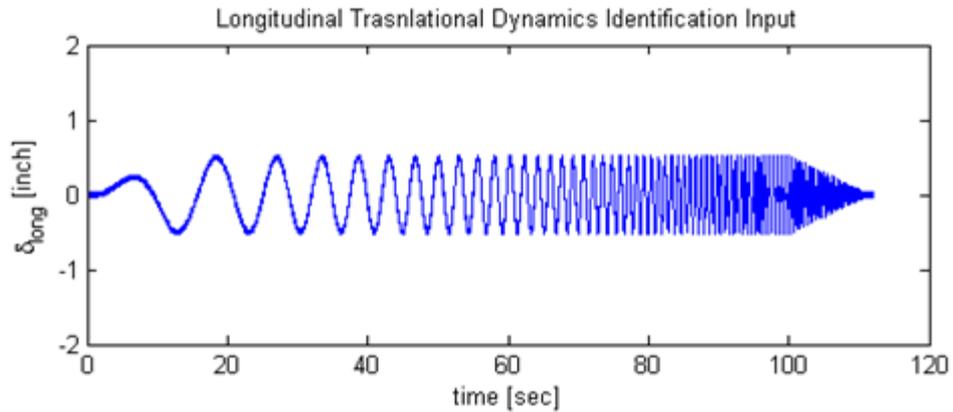
Figure 1- 4 : Frequency sweep input

In this thesis, time domain system identification methods, output error and least square methods, are used. Multistep 3-2-1-1 and sine sweep inputs are employed to excite the rotorcraft. Detailed explanations are done in the related parts.

Applications and Examples

In the literature, a lot of examples for system identification of different kinds of systems could be found, but the examples presented in this thesis are related to air vehicles. System identification results are used for validation and update of simulation models, handling quality analyses and automatic flight control design applications.

In 1972 Taylor and Iliff [6] tried to obtain a generic algorithm and develop a code for linear and constant coefficient systems and also to give an example of the determination of the lateral-directional aerodynamic derivatives of the aircraft. They claimed that linear regression methods such as least square and Shinbrot's method, are good to match the measured response well, however there is a convergence problem, making it difficult to solve the equations because they are nonlinear. They showed that by using the modified Newton Raphson method (quasilinearization) this problem may be eliminated. In the same year they explained this phenomenon in another article [7]. In this study five different methods, namely simplified equations, analog matching, least square, Shinbrot's method and modified Newton-Raphson method, were used to determine the stability derivatives of the state equations of three different aircrafts, which are a light general aviation airplane, a large supersonic airplane and a lifting body vehicle. They encountered convergence difficulties when there were more than a few unknowns, but modified Newton-Raphson method was used to succeed in solving the convergence problem. Another important advantage of this method is that it does not necessarily measure all components of the state variables and their time derivatives. [7]

Another application of the system identification on air vehicle systems is simulation development and validation. In 2001 Cicolani, Sahai, Tischler and et al. published an article related to flight test methods and results, and the simulation model and validation results for UH-60A and UH-60A with slung load [8]. In this article, identification computations are done by using the CIFER software for interactive frequency domain analysis and frequency sweep input is used. By using the system identification technique, bandwidth and phase delay parameters are obtained. These parameters are important for modern specification of the handling quality.

Rotorcraft System Identification

5

The identification of flight vehicle dynamic models from test data has some difficulties, namely limitations of the flight-data measurement systems, test inputs, signal to noise ratio, and test record length. Identification of rotorcraft is perhaps more challenging than other system identification processes. Because these vehicles have a wide range of possible configurations, from small ducted fun to tilt-rotor aircraft, single and tandem helicopters, and helicopter slung-load configurations. [4, 5, 8] Many rotorcrafts exhibit a high-order dynamic response because of the tightly coupled dynamics of the fuselage, rotors, inflow, engine, etc. so that typical low order approximations of fixed-wing aircraft responses do not apply. Inputs in one axis generally produce responses of comparable magnitude in all axes, referred to cross coupling. Therefore decoupled longitudinal and lateral responses, as in fixed wing, are not valid. Other difficulties are due to high signal to noise ratio for near hovering maneuvers, unstable pitch and roll dynamics, and high levels of noise in the measurements caused by vibration and atmospheric disturbances [5].

1.2   FLIGHTLAB

FLIGHTLAB is a commercial software program developed by ART for modeling and simulation of dynamic air vehicle systems. It supports modeling of dynamic systems from a predefined library of modeling components. Each component is an independent dynamic element such as a spring, a damper, an airfoil section etc. These components can be interconnected in arbitrary architectures to model any desired dynamic system. Vehicle specific values can be assigned as the parameters of the components, allowing a wide range of complex models to be built from a common library of modeling components that have been pre-defined, programmed and tested for reliability. FLIGHTLAB also provides the possibility of modifying the basic modeling components and model templates and building new components by using SCOPE which is a high level module of the FLIGHTLAB. [9]

FLIGHTLAB simulations consist of two procedures, building a model by using FLME (Flightlab Model Editor) and CSGE (Control System Graphical Editor) and performing analysis and simulation of the model by using XANALYSIS (Analysis and Simulation Model). FLME is a data entry tool for entering rotorcraft simulation data. CSGE is an Icon-based two dimensional graphical editor like MATLAB SIMULINK that provides the user with the ability to design and build control system schematics in block diagrams. XANALYSIS is an X-windows based graphical user interface for the analysis of dynamic system models built under the FLIGHTLAB environment [9].

In 2011 Vitale, Genito, Federico and Corraro [10] from Italian Aerospace Research Center, CIRA, published an article which is related to rotorcraft identification using the hybrid approach from flight data. In this study case the flight vehicle is UH-60 Black Hawk helicopter. To apply the system identification procedure, instead of flight data, simulated data generated by FLIGHTLAB was used. Similarly, in this thesis FLIGHTLAB software environment is used for flight data generation. FLIGHTLAB nonlinear simulation results are used to compare the system identification analyses results; moreover, these results are also used to evaluate the system identification approaches.
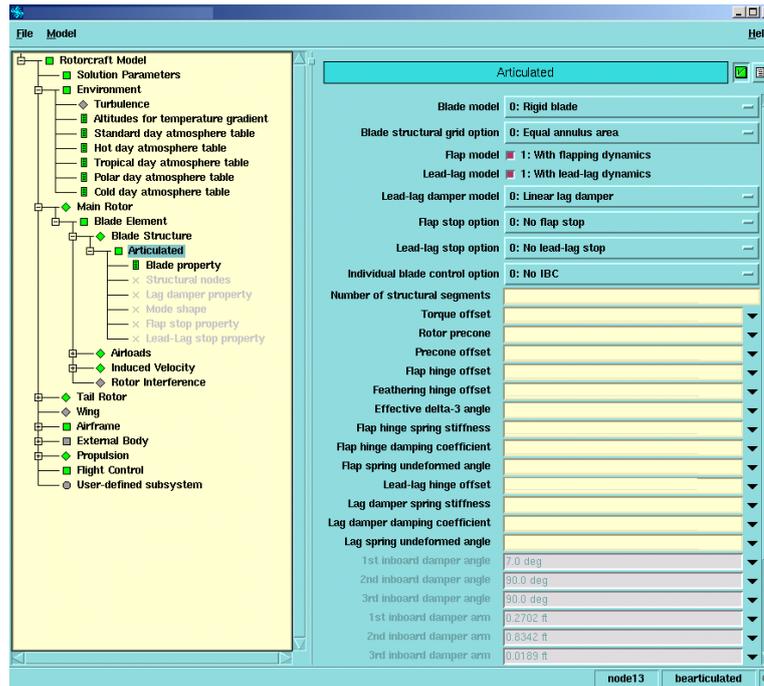
Figure 1- 5 : FLIGHTLAB FLME Editor

1.3 UH-60 HELICOPTER

The word helicopter is adapted from the French hélicoptère, coined by Gustave de Ponton d'Amecourt in 1861, which originates from the Greek helix/helik- (ἕλιξ) = "twisted, curved" and pteron (πτερόν) = "wing" [11].

Helicopters are categorized as rotary wing type aircraft, because their lifting and controlling means are their rotor systems. Helicopters can go forward, sideward, up and down like aircrafts, in addition to these, they can do some extra special maneuvers namely hover, backward flight, vertical take-off and landing. However, helicopters have some limitations on speed and altitude.

In this thesis, for the system identification analysis, flight data are generated from the nonlinear UH-60 Black Hawk helicopter model in the FLIGHTLAB software environment. Model consists of a main rotor, tail rotor, airframe, aerodynamic surfaces and tail propulsion components.

Main rotor of the UH-60 is modeled as articulated rotor system including flapping and lead-lag motions and blade element method (BEM) is used for modeling. Rotor inflow is modeled with Peters-He Six State inflow. Tail rotor is a disk rotor model with collective control only. Airframe and aerodynamic surface modeling is modeled with parametric tables of force and moments. UH-60 has two General Electric turboshaft engines, T700-GE-700. Engines have Digital Electronic Control Unit (DECU) and Hydro Mechanical Unit (HMU). [12]

7

Figure 1- 6 : UH-60 Helicopter

The simple control system is composed of longitudinal and lateral cyclic, collective and pedal controls. Control inputs are transferred to rotor swashplate mechanism by mechanical linkages and hydraulic servos. Outputs of the cockpit pilot controls are transmitted by mechanical linkage to pilot assist servos to mixing unit. Then these inputs are summed and coupled by mixing unit and outputs of the mixing unit are carried by mechanical linkage to main and tail rotor controls.

The UH-60 helicopter has also an Automatic Flight Control System which is composed of Stability Augmentation System (SAS), Trim, Flight Path Stabilization System (FPS) and Stabilator System. The UH-60 incorporates two SAS systems to help maintain a stable platform in flight. SAS 1 is an analog system and SAS 2 is a digital system. Both provide short term rate dampening in the pitch, roll, and yaw axes. Operation of the two SAS is essentially the same. SAS 2 has self-diagnostic capabilities where SAS 1 does not. The FPS system provides long term rate dampening in the pitch, roll, and yaw axes. FPS provides basic autopilot functions using the trim actuators to maintain attitude in the pitch and roll axes, and heading hold/turn coordination in the yaw axis. The trim system is comprised of three trim actuators. The roll and yaw trim actuators are electro-mechanical, and the pitch trim assembly is electro-hydromechanical. The trim system by itself provides a force gradient in the pitch, roll, and yaw axes. The stabilator is a variable angle of incidence airfoil that enhances the handling qualities and longitudinal control of the aircraft. The automatic mode of operation positions the stabilator to the best angle of attack for existing flight conditions [12].

1.4   OBJECTIVE OF THE THESIS

One of the goals of this thesis is to generate a linear helicopter system identification model at hover condition. This model has some simplifications and assumptions, which are explained in Chapter 2. Beside of that, main goal of this thesis is to identify helicopter stability derivatives and to evaluate and determine the system identification approach for helicopters and finally to compare the results with "nonlinear simulation data". As an outcome of this thesis, identified simulation model can be used for stability, control and handling quality analysis, designing control system and also updating the simulation models.

1.5   SCOPE OF THE THESIS

The following chapter is devoted to explain the development of a general system identification model for helicopters. In chapter 3, two time domain system identification methods which are output error and least square methods are presented. These methods are applied to the identification of a

helicopter based on data obtained from FLIGHTLAB software. The linear system identification model obtained is compared with the non-linear simulation, and discussions on the success of the approach are presented. The last chapter summarizes the finding of this thesis. Future work is also given.

CHAPTER 2

MODELS FOR THE IDENTIFICATION OF HELICOPTER FLIGHT MECHANICS

In this section, linear system identification models of different order and complexity are presented. Because the rotor provides the lift and controls the helicopter, rotor dynamics and rotor body coupling modeling are very important parts of the system identification model. For a classical fixed wing aircraft, longitudinal and lateral coupled dynamics can be ignored and uncoupled dynamics of these can be examined separately, since fixed wing aircrafts do not have highly coupled dynamics. However, helicopters have highly coupled dynamics and this is the most important point to obtain a high fidelity helicopter simulation model. Many studies in the literature [4, 5, 13, 14, 15, 16] about helicopter system identification modeling and simulations show that the low order system identification models have a good fit with the on-axis flight test data but do not have a very good correlation with the off-axes. Moreover, these models do not reflect high frequency responses as good as the higher order system identification models. This phenomenon is especially crucial for designing the high gain stability and control augmentation systems. Regarding these, low order models can also be used for simple simulation and stability analysis [16, 17]. Therefore, depending on helicopter rotor dynamics and aim of the work, different kind of higher order models were used by Jatagaonkar [4], Tischler [5], Fletchler [18, 8], Mettler [13], Zivan [19], Ivler [15] etc.

In addition to the classical low order 6 degree of freedom (DoF) quasi-steady model, Jatagaonkar [4] also defined an extended model which includes the rotor body dynamics especially for time domain system identification applications. Figure 2- 1 shows the extended model structure. The state matrix consists of the fuselage, rotor and rotor-body coupling terms. Tischler [5] defined a hybrid model which also takes into account rotor body dynamics, coning inflow dynamics and yaw engine dynamics. In addition to these models, Fletchler [18] defined a 14 degree of freedom model which contains 6 rigid body degrees of freedom, main rotor longitudinal and lateral flapping and lead-lag dynamics, vertical dynamic inflow, main rotor engine angular rate, engine torque and engine fuel flow. These models have a good correlation on the off-axis flight data response and also provide the high frequency compatibility to design the stability and control system. In the sense of these the expectation is that the higher order model is better than the low order model. However, in 1982, Hansen [20] examined 3 different order models for CH-53A helicopter. First model included the conventional 6 degree of freedom rigid body dynamics and second order tip-path plane dynamics. The second model consisted of the amended 6 degree of rigid body dynamics, second order coning and first order tip-path plane dynamics. The third 8 degree of freedom model included 6 degree of freedom rigid body and a simplified tip-path plane tilt dynamics. As a result of this work, Hansen concluded that amended 9 degree of freedom model has better predictions of the helicopter off-axis response and usable bandwidth, whereas 8 degree of freedom model provides the better short-period eigenvalues and with many stability derivatives.
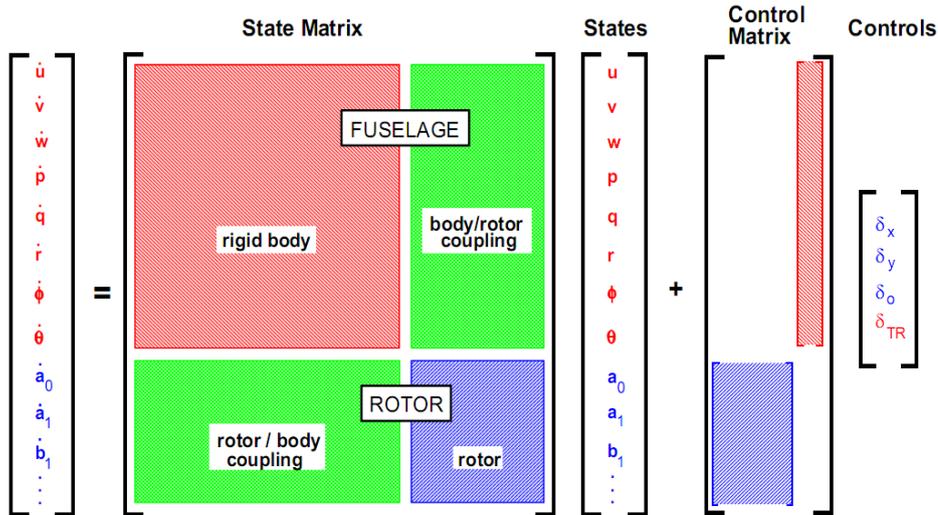
Figure 2- 1 : Extended Helicopter Model Structure [4]

2.1   FORCES AND MOMENTS ACTING ON A HELICOPTER IN FLIGHT

There are many helicopter configurations with different sizes and shapes. Fuselage can be in different sizes and shapes depending on helicopter mission. Also the aerodynamic force and moments applied on the fuselage can be assumed as classical aircraft rigid body aerodynamic force and moments. The main rotor is the most important part of the helicopter and there may be either single or two as in tandem rotor and coaxial rotor. The main rotor provides the lift force and also controls the helicopter by the swashplate mechanism. Anti-torque system can be tail rotor, fan-in-tail, NOTAR, another main rotor. As a classic helicopter, UH-60 which is utilized in this thesis, has a tail rotor configuration. The horizontal stabilizer can be considered as a wing and it provides the lift to help the longitudinal stability of the helicopter especially in the forward flight regime. Moreover, the vertical tail may also be considered as a wing that helps the directional stability of the helicopter. Figure 2- 2 shows the forces and moments acting on the helicopter [17]. Forces are indicated in X, Y, Z directions and for each force component is denoted by subscript of the first letter of the component. For example, main rotor X force is denoted as X_M and horizontal stabilizer Z force is denoted as Z_H. Moments are indicated as L, M and N according to X, Y and Z axes, respectively. Also their notation is the same as the forces. In addition to these force and moments, there are highly coupled interactions between the main rotor and other components, namely fuselage, tail rotor, horizontal stabilizer and vertical fin and also engine governor dynamics.

Helicopter, has a varying mass and flies in the non-stationary air so that the force and moment components acting on its body are changing with aerodynamic, propulsive and gravitational forces. Because of these situations when aerospace vehicles are modeled, some simplifications are done to simplify the calculations. These assumptions, as listed by Morelli [21] are follows:

- The vehcile is a rigid body
- The air is at rest relative to the earth
- The earth is fixed in inertial space
- The earth surface is flat
- Gravity is uniform; vehicle center of gravity is fixed.

12

Force equations are derived from the Newton's Second Law and it is expressed in the inertial frame as follows, [21]

$$F = \frac{d^I m V}{dt} \qquad (2.1)$$

where F is the total external force vector, m is the mass and the V is the translational velocity vector. Here superscript **I** represents the inertial frame. If this formula is converted to body axis coordinate system, it can be rewritten as, [5]

$$\frac{F_{gravity}}{m} + \frac{F_{aero}}{m} = \frac{d^B V}{dt} + (\omega \times V) \qquad (2.2)$$

where F is separated as gravity and aerodynamic forces and **ω** is the body angular velocity. Superscript **B** represents body axis.

The moment equations are also derived by using the Newton's Second Law in the inertial frame as

$$M = \frac{d^I I \omega}{dt} \qquad (2.3)$$

where M is the total external moment vector, **ω** is the angular velocity and I is the inertia tensor of the system. If this formula is converted to body axis coordinate system, it can be rewritten as

$$M_{aero} = \frac{d^B I \omega}{dt} + (\omega \times I \omega) \qquad (2.4)$$

M_{aero} is the external aerodynamic moments vector.

These expressions are converted to body axis coordinate system because measurements are made in the body axis system and inertia tensor **I** is constant in body axes, but it is a function of a time in inertial axes. Thus body axis components of these vectors can be expressed as

$$F = \begin{bmatrix} X \\ Y \\ Z \end{bmatrix} ; \quad M = \begin{bmatrix} L \\ M \\ N \end{bmatrix}$$

$$V = \begin{bmatrix} u \\ v \\ w \end{bmatrix} ; \quad \omega = \begin{bmatrix} p \\ q \\ r \end{bmatrix} ; \quad I = \begin{bmatrix} I_{xx} & -I_{xy} & -I_{xz} \\ -I_{yx} & I_{yy} & -I_{yz} \\ -I_{zx} & -I_{zy} & I_{zz} \end{bmatrix}$$
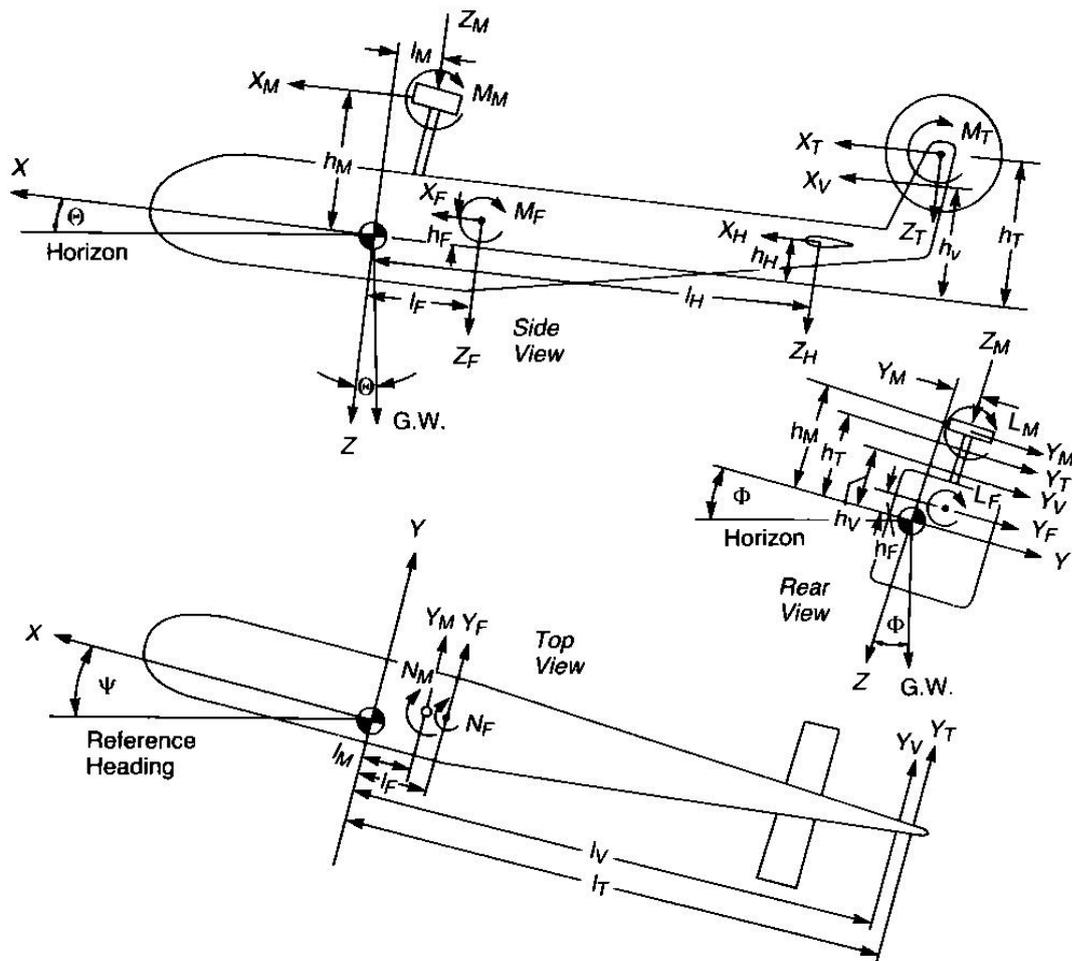
Figure 2- 2 : Forces and Moments Acting on Helicopter [17]

2.2   EQUATIONS OF MOTION FOR HELICOPTER

Forces and moments corresponding to inertia effect associated with accelerations (linear or angular) and combinations of velocities, three force and three moment equations may be written as, [17]

$$X_M + X_T + X_H + X_V + X_F = W\sin\theta + \frac{W}{g}(\ddot{x} - \dot{y}r + \dot{z}q) \tag{2.5}$$

$$Y_M + Y_T + Y_H + Y_V + Y_F = -W\sin\phi + \frac{W}{g}(\ddot{y} + \dot{x}r - \dot{z}p) \tag{2.6}$$

$$Z_M + Z_T + Z_H + Z_V + Z_F = -W\cos\theta + \frac{W}{g}(\ddot{z} - \dot{x}q + \dot{y}p) \tag{2.7}$$

$$L_M + Y_M h_M + Z_M y_M + Y_T h_T + Y_V h_V + Y_F h_F + L_F = I_{xx}\dot{p} - qr\left(I_{yy} - I_{zz}\right) \qquad (2.8)$$

$$M_M - X_M h_M + Z_M l_M + M_T - X_T h_T + Z_T l_T - X_H h_H + Z_H l_H - X_V h_V + M_F$$
$$+ Z_F l_F - X_F h_F = I_{yy}\dot{q} - pr\left(I_{zz} - I_{xx}\right) \qquad (2.9)$$

$$N_M - Y_M l_M - Y_T l_T - Y_V l_V + N_F - Y_F l_F = I_{zz}\dot{r} - pq\left(I_{xx} - I_{yy}\right) \qquad (2.10)$$

These nonlinear equations do not directly include rotor dynamics such as coning, flapping, inflow. By using a "quasi-steady" assumption, number of degrees of freedom is eliminated and forces and moments of the rotor produce instantaneous response to control inputs. This means that time constant for flapping of rotor blades is neglected [17]. This issue is examined in the rotor-body coupling section.

Figure 2- 3 shows the sign convention for the forces, moments, angular displacements, velocities and accelerations according to the body axes coordinate system. Origin of this system is the helicopter center of gravity (cg) and x-axis is pointing forward to nose of the helicopter, y-axis pointing the right when looking to the rear of the helicopter and z-axis down to earth.

For the system identification 6 DoF (degree of freedom) quasi-steady linear models, nonlinear equations of motion are converted to linear equations of motion by using the small perturbation theory. According to this theory, this linear model is only valid for small changes around the trim conditions.

For example, lateral nonlinear force equation can be linearized as follows by using the small angle assumption and also in terms of the stability derivatives.

$$Y = -W\sin\Phi + \frac{W}{g}(\ddot{y} + \dot{x}r - \dot{z}p) \qquad (2.11)$$

This equation can be rewritten by using the small angle assumption in order to linearize the products of the variables.

$$Y = -W\Phi + \frac{W}{g}(\ddot{y} + \dot{x}r - \dot{z}p) \qquad (2.12)$$

$$Y = -W\Phi + \frac{W}{g}(\dot{v} + u_0 r + u r_0 - w_0 p - w p_0) \qquad (2.13)$$

Initial conditions are the trim conditions so the following velocities are zero.

$$q_0 = p_0 = r_0 = 0$$

Moreover, Y lateral force can be written in a Taylor series of the stability and control derivatives multiplying corresponding velocities and control inputs. Stability and control derivatives are partial derivatives of the specific aerodynamic forces and moments with respect to the variations in the states and controls. Stability and control derivatives related to forces can be non-dimensionalized by dividing to aircraft mass and the derivatives related to moments can be non-dimensionalized by dividing to inertias. For example Y_v and L_p can be written as,

$$Y_v \equiv \left(\frac{1}{m}\right)\frac{\partial Y}{\partial v} \qquad (2.14)$$
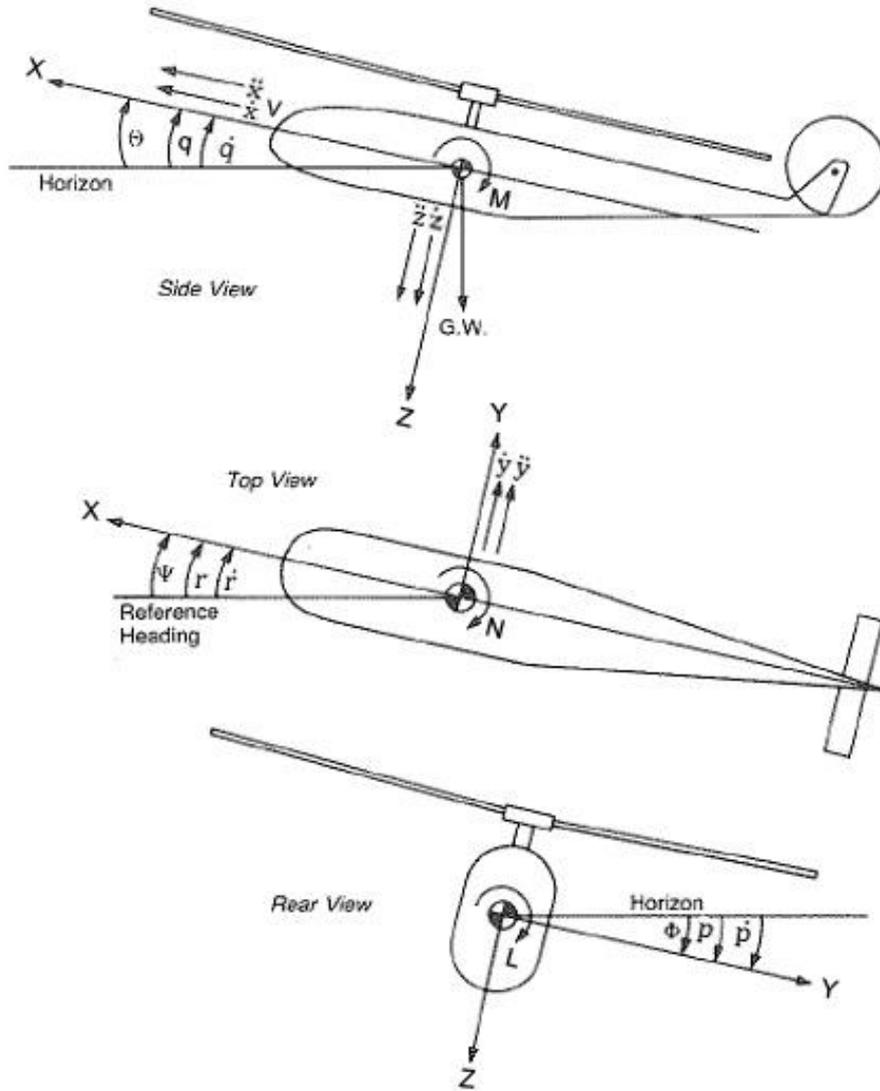
Figure 2- 3 : Parameters in Equations of Motion Sign convention [17]

$$L_p \equiv \left(\frac{1}{I_{xx}}\right)\frac{\partial L}{\partial p} \tag{2.15}$$

$$\begin{aligned} Y = \ & Y_u u + Y_v v + Y_w w + Y_q q + Y_p p + Y_r r + Y_{\theta_o}\theta_0 + Y_{\theta_T}\theta_T + Y_{A_1}A_1 \\ & + Y_{B_1}B_1 \end{aligned} \tag{2.16}$$

Then linear Y lateral force equation can be written as follows,

$$\begin{aligned} & Y_u u + Y_v v + Y_w w + Y_q q + Y_p p + Y_r r + Y_{\theta_o}\theta_0 + Y_{\theta_T}\theta_T + Y_{A_1}A_1 + Y_{B_1}B_1 \\ & + W\Phi + \frac{W}{g}(-\dot{v} - u_0 r + w_0 p) = 0 \end{aligned} \tag{2.17}$$

16

Other forces and moments can be linearized by using the same procedure so that system identification 6 DoF quasi-steady linear model is obtained.

$$\frac{W}{g}\dot{v} = Y_u u + Y_v v + Y_w w + Y_q q + (Y_p + \frac{W}{g}w_0)p + (Y_r - \frac{W}{g}u_0)r + W\Phi \qquad (2.18)$$
$$+ Y_{\theta_o}\theta_0 + Y_{\theta_T}\theta_T + Y_{A_1}A_1 + Y_{B_1}B_1$$

$$\dot{x} = \begin{bmatrix} X_u & X_v & X_w & X_p & X_q - w_0 & X_r + v_0 & 0 & -g \\ Y_u & Y_v & Y_w & Y_p + w_0 & Y_q & Y_r - u_0 & g & 0 \\ Z_u & Z_v & Z_w & Z_p - v_0 & Z_q + u_0 & Z_r & 0 & 0 \\ L_u & L_v & L_w & L_p & L_q & L_r & 0 & 0 \\ M_u & M_v & M_w & M_p & M_q & M_r & 0 & 0 \\ N_u & N_v & N_w & N_p & N_q & N_r & 0 & 0 \\ 0 & 0 & 0 & 1 & 0 & 0 & 0 & 0 \\ 0 & 0 & 0 & 0 & 1 & 0 & 0 & 0 \end{bmatrix} x$$

$$+ \begin{bmatrix} X_{\delta_{long}} & X_{\delta_{lat}} & X_{\delta_{coll}} & X_{\delta_{pedal}} \\ Y_{\delta_{long}} & Y_{\delta_{lat}} & Y_{\delta_{coll}} & Y_{\delta_{pedal}} \\ Z_{\delta_{long}} & Z_{\delta_{lat}} & Z_{\delta_{coll}} & Z_{\delta_{pedal}} \\ L_{\delta_{long}} & L_{\delta_{lat}} & L_{\delta_{coll}} & L_{\delta_{pedal}} \\ M_{\delta_{long}} & M_{\delta_{lat}} & M_{\delta_{coll}} & M_{\delta_{pedal}} \\ N_{\delta_{long}} & N_{\delta_{lat}} & N_{\delta_{coll}} & N_{\delta_{pedal}} \\ 0 & 0 & 0 & 0 \\ 0 & 0 & 0 & 0 \end{bmatrix} u$$

(2.19)

where state vector and input vector are respectively as,

$$x' = \begin{bmatrix} u & v & w & p & q & r & \varphi & \theta \end{bmatrix}$$

$$u = \begin{bmatrix} \delta_{long} & \delta_{lat} & \delta_{coll} & \delta_{pedal} \end{bmatrix}$$

And the output vector is,

$$y' = \begin{bmatrix} u & v & w & p & q & r & \varphi & \theta \end{bmatrix}$$

Here, subscript 0 represents the trim values of the parameters. Hence, total number of the unknown system parameters is 60.

2.3   ROTOR-BODY COUPLING

In order to obtain a linearized 6 DoF helicopter model, quasi steady assumption is used to ignore the rotor lag dynamics for helicopters which have small hinge offset. For helicopters which have large hinge offset, this assumption is not practical and the results of the linearized system may not be good. For this reason, rotor-body coupling dynamics is added to the classical 6 DoF linearized model. In the literature, there are two main modeling approaches of the rotor-body coupling in the literature, namely hybrid modeling and extended rigid-body and rotor modeling [4,5].

These system identification models are suitable for the high frequency response range and also for hover and forward flight regimes. Hybrid model is claimed to lead to an accurate identification in the 0.2 to 30 rad/sec frequency range with good accuracy depending on the achievement of the test. [5]

Hence, if a high bandwidth model is required, the system identification model should be extended. High bandwidth models can be used for the applications of flight mechanics, simulation, autopilot design and handling quality analysis. Hence, system identification model should be determined depending on the purpose of the identification.

Hybrid model structure has the 13 DoF and it can be obtained by extending the classical linear 6 DoF model with [5]

- coupled fuselage/regressive-flap dynamics which has 2 DoF
- coupled inflow-coning dynamics which has 2 DoF
- lead-lag dynamics which has 2 DoF
- engine torque response which has 1 DoF

On the other hand, Jatagaonkar [4] used extended rigid body-rotor and rotor dynamics models with 9 DoF. Moreover depending on the purpose wake, turbulence or any requiring model may be added to this extended model to improve the accuracy.

In this study, 8 DoF linear model, obtained by using the coupled fuselage /regressive-flap dynamics adding to classical 6 DoF, is used to identify UH-60 helicopter in hover case.

2.4   FLAPPING MODEL

Rotor blades have mainly three motions: Flapping, lead-lag and feathering (pitching motion). As shown in Figure 2- 4, flapping motion is the up and down motion of the blade around flapping hinge at the root of the blade. Lead-lag motion is the forward and backward motion of the blade around the lead lag hinge and finally feathering motion can be described as the pitching motion around the feathering hinge.
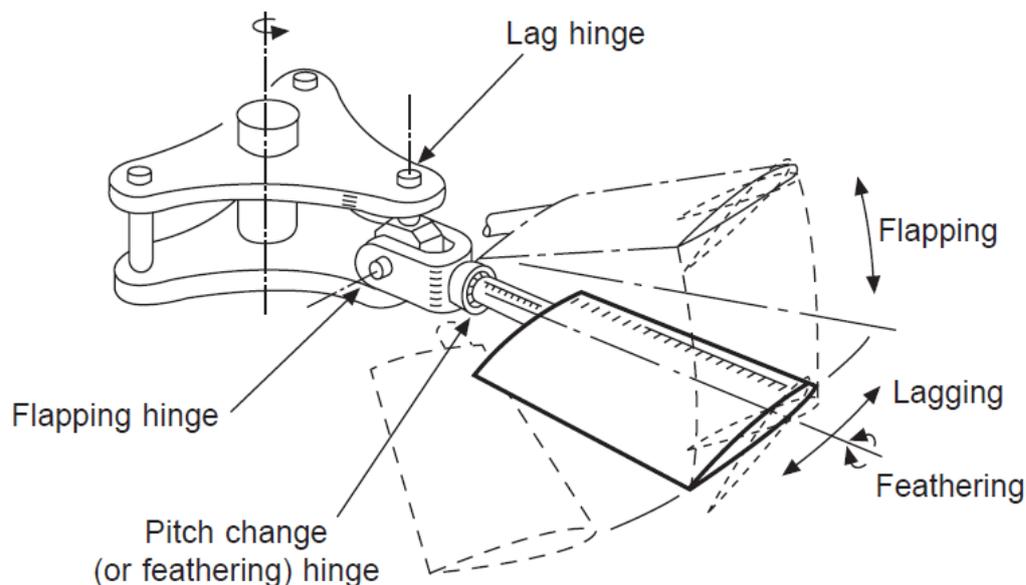
Figure 2- 4 : Hinges of the Articulated Rotor [25]

For high fidelity model applications, especially for designing high bandwidth control systems, effects of the rotor time delay may be added to the classical 6 DoF helicopter model. In the literature, there are many studies about these helicopter flight mechanics models with flapping effects. They are capable of predicting high frequency responses more accurately than the classical 6 DoF models [4, 5, 18, 8, 15, 22].

Rotor motion of the helicopter is modeled as disc or tip-path plane where coupled tip-path plane dynamic equations are derived by Chen [24]. Tip-path plane of motion is described by the conning angle (β_0), longitudinal flapping angle (β_{1c}) and lateral flapping angle (β_{1s}). Figure 2- 5 shows the sign convention of these tip-path plane motions.
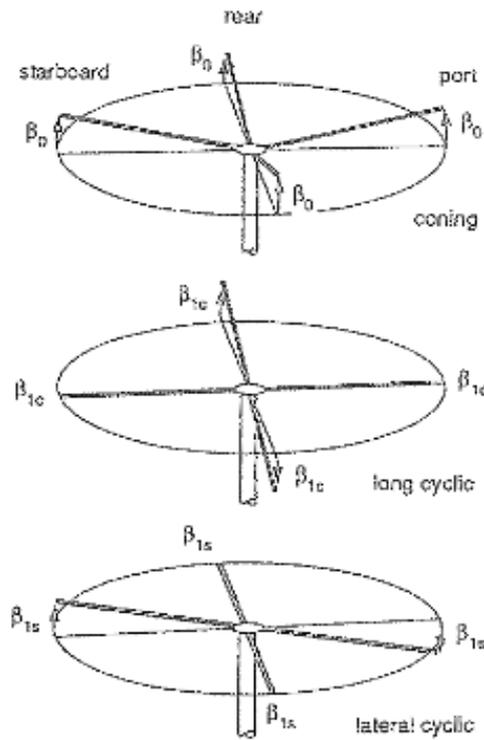
Figure 2- 5 : Rotor Disc Motion [26]

There are two approaches for modeling the flapping dynamics: implicit first order flapping model and explicit second order flapping model [4].

According to implicit first order model, there is a high correlation between the flapping motion of the tip-path plane and the body angular accelerations. For example, for helicopters with rigid rotors and high hinge offsets, roll acceleration and lateral flapping can be expressed as,

$$\dot{p} = L_{\beta_{1s}} \beta_{1s} \tag{2.20}$$

$$\ddot{p} = L_{\beta_{1s}} \dot{\beta}_{1s} \tag{2.21}$$

19

$$\dot{\beta}_{1s} = -\frac{1}{\tau_f}\beta_{1s} - p + \frac{Lf_{\delta_{lat}}}{\tau_f}\delta_{lat} \tag{2.22}$$

$$\ddot{p} = L_{\beta_{1s}}\dot{\beta}_{1s} = -\frac{\dot{p}}{\tau_f} - L_{\beta_{1s}}p + L_{\beta_{1s}}\frac{Lf_{\delta_{lat}}}{\tau_f}\delta_{lat} \tag{2.23}$$

$$\ddot{p} = \tilde{L}_{\dot{p}}\dot{p} + \widetilde{L_p}p + \widetilde{L_{\delta_{lat}}}\delta_{lat} \tag{2.24}$$

where $\tilde{L}$ represents the new lateral system parameter, τ_f is the flapping time constant and δ_{lat} is the control input at the root of the blade. These equations mean that step control input leads to a first order response of the rotor itself. Moreover, control input couples with the body response driven by the rotor flapping [4]. Similarly, these equations can be changed for the longitudinal flapping motion. After these implementations, the new state terms are appeared as $\dot{p}$ and $\dot{q}$ hence, tip-path-plane dynamics is modeled implicitly.

Tip-path plane dynamics can also be modeled explicitly. Actually these dynamics have three second order flapping modes. Two of them are the lower frequency mode and the higher frequency mode which are related to longitudinal and lateral flap angle, respectively. Third mode comes from the coning flap response. However second mode, which is the higher frequency mode about $\omega_{f_c} \approx 2\Omega$, for UH-60 $\omega_{f_c} = 54\ rad/sec$, is much higher than flight dynamics and control mode frequencies. Third mode is the important mode for the flight dynamics and controls especially the vertical degree of freedom. [5]. However first order zero flap response gives the nearly same results as the second order flapping mode in the on–axis. Hence flapping response can be accurately modeled as two coupled first order equations [5, 26, 27]. According to this result, tip-path plane equations can be rewritten by dropping the flap and fuselage angular accelerations.

$$\dot{\beta}_{1s} = -\frac{1}{\tau_f}\beta_{1s} + \frac{Lf_{\beta_{1c}}}{\tau_f}\beta_{1c} + p + \frac{Lf_{\delta_{long}}}{\tau_f}\delta_{long} + \frac{Lf_{\delta_{lat}}}{\tau_f}\delta_{lat} \tag{2.25}$$

$$\dot{\beta}_{1c} = -\frac{1}{\tau_f}\beta_{1c} + \frac{Mf_{\beta_{1s}}}{\tau_f}\beta_{1s} + q + \frac{Mf_{\delta_{long}}}{\tau_f}\delta_{long} + \frac{Mf_{\delta_{lat}}}{\tau_f}\delta_{lat} \tag{2.26}$$

Here $Lf_{\beta_{1c}}$, $Mf_{\beta_{1s}}$, $Lf_{\delta_{long}}$ and $Mf_{\delta_{lat}}$ are coupling terms.

Rotor time constant, τ_f, can be calculated theoretically. Time constant is a function of the hinge offset and effective Lock number and it can be expressed as in [27],

$$\frac{1}{\tau_f} = \frac{\gamma\Omega}{16}\left(1 - \frac{8e}{3R}\right) \tag{2.27}$$

where e is the hinge offset, R is radius of the rotor, Ω is the angular velocity of the rotor and γ is the Lock number. Unit of the time constant is second. Lock number is a nondimensional parameter which represents the ratio of the aerodynamic forces to centrifugal forces.

$$\gamma = \frac{\rho a c R^4}{I_b} \tag{2.28}$$

where

ρ, atmospheric density
a, lift curve slope
c, balde chord
I_b, moment of the inertia of the blade about the flapping axis

However time constant should be corrected for the influence of dynamic inflow. [5] Curtiss [28] replaces the geometric Lock number to an effective or reduced Lock number for taking into consideration of the dynamic inflow. Effective Lock number denoted as γ^*.

$$\gamma^* = \frac{\gamma}{1 + \frac{a\sigma}{16\overline{v_0}}} \qquad (2.29)$$

where σ is the rotor solidity and $\overline{v_0}$ is the nondimensional inflow ratio.

Solidity can be calculated as,

$$\sigma = \frac{n_b c}{\pi R} \qquad (2.30)$$

Here n_b is the number of the blades. Trim inflow ratio is obtained from momentum theory and it can be expressed as, [25]

$$\overline{v_0}_{hover} = \sqrt{\frac{C_{T_0}}{2}} \qquad (2.31)$$

where C_{T_0} is the trim thrust coefficient.

In hover case, effects of the correction on the time constant are important. In hover with correction, the rotor time constant is increasing about %50. Moreover most hovering helicopters have the time constant between 0.10 and 0.15 depending on the hinge offset. If the time constant is closer to 0.10 helicopter can be classified as a small hinge offset helicopter and if the time constant is closer to 0.15, helicopter can be classified as a large hinge offset helicopter [5].

UH-60 helicopter has the 0.1265 time constant for hover condition. So it can be classified as small hinge offset helicopter.

In the identification process rotor time constant is a free parameter to estimate. Rotor time constant has a single value for the longitudinal and lateral flapping equations, so the constraint for the time constant can be used in the identification process. Moreover at the beginning of the identification, time constant which is calculated from previous formulations can be used as initial value of the identified time constant. [29]

The rotor fuselage coupling terms are the rotor force and moment stiffness which are $L_{\beta_{1s}}$ and $Y_{\beta_{1s}}$ for the roll and lateral degrees of freedom and $M_{\beta_{1c}}$ and $X_{\beta_{1c}}$ for the pitch and longitudinal degrees of freedom. There is a relation between the longitudinal and lateral force springs terms as,

$$Y_{\beta_{1s}} = -X_{\beta_{1c}} \qquad (2.32)$$

Moreover, these force stiffness terms theoretically equal to gravity constant. However these terms can be free to identify because of the uncertainty of the vertical center of gravity location [5]. In this study, the vertical center of gravity location is assumed to be known.

In this explicit flapping model, there are important points. First, the quasi-steady derivatives and lateral and longitudinal inputs in the state equations are omitted. These derivatives are quasi-steady rotor moment derivatives which are $L_p, L_q, M_p,$ and M_q, quasi-steady rotor force and moment derivatives which are $L_{\delta_{long}}, L_{\delta_{lat}}, M_{\delta_{long}}, M_{\delta_{lat}}, X_{\delta_{long}}, X_{\delta_{lat}}, Y_{\delta_{long}}$ and $Y_{\delta_{lat}}$. As mentioned before, omitting classical quasi-steady terms are a result of the 6 DoF assumptions that models the rotor with a simple time delay. Hence by using the explicit flapping model, these quasi-steady derivatives are not necessary in the 8 DoF model. Moreover, there is no need for using the longitudinal and lateral cyclic input terms because they are modeled as longitudinal flapping angle, β_{1c}, and lateral flapping angle, β_{1s}. Forces and moments are transmitted by these longitudinal and lateral flapping responses to the fuselage with associated flap spring terms which are $X_{\beta_{1c}}$ and $Y_{\beta_{1s}}$, respectively. However there is a quasi-steady force angular derivative Y_p which is retained to account for the tail-rotor effects even though the explicit flapping model is used. [5, 8, 17, 18, 19]

Second, in the explicit flapping model, instead of the all rotor equations, only angular shaft motions are taken into account. Hence, flapping response to translational velocities and effects of the rotor force and moments resulting from translational dynamics on the fuselage are remaining in the 8 DoF model. These speed derivatives, such as X_u, Y_v, M_u, L_v etc., are related to low frequency responses, so that rotor time lag is not important here. [5, 8, 17, 18, 19]

Finally, if explicit flapping model is added to the quasi-steady 6 DoF model, 8 DoF model is obtained as,

$$
\dot{x} = \begin{bmatrix}
X_u & X_v & X_w & 0 & -W_0 & X_r + V_0 & 0 & -gcos\theta_0 & X_{\beta_{1c}} & 0 \\
Y_u & Y_v & Y_w & Y_p + W_0 & 0 & Y_r - U_0 & gcos\theta_0 & 0 & 0 & Y_{\beta_{1s}} \\
Z_u & Z_v & Z_w & Z_p & Z_q & Z_r & 0 & 0 & Z_{\beta_{1c}} & Z_{\beta_{1s}} \\
L_u & L_v & L_w & 0 & 0 & L_r & 0 & 0 & 0 & L_{\beta_{1s}} \\
M_u & M_v & M_w & 0 & 0 & M_r & 0 & 0 & M_{\beta_{1c}} & 0 \\
N_u & N_v & N_w & N_p & N_q & N_r & 0 & 0 & N_{\beta_{1c}} & N_{\beta_{1s}} \\
0 & 0 & 0 & 1 & 0 & 0 & 0 & 0 & 0 & 0 \\
0 & 0 & 0 & 0 & 1 & 0 & 0 & 0 & 0 & 0 \\
0 & 0 & 0 & 0 & 1 & 0 & 0 & 0 & -\frac{1}{\tau_f} & \frac{Mf_{\beta_{1s}}}{\tau_f} \\
0 & 0 & 0 & 1 & 0 & 0 & 0 & 0 & \frac{Lf_{\beta_{1c}}}{\tau_f} & -\frac{1}{\tau_f}
\end{bmatrix} x +
$$

$$
\begin{bmatrix}
0 & 0 & X_{\delta_{coll}} & X_{\delta_{pedal}} \\
0 & 0 & Y_{\delta_{coll}} & Y_{\delta_{pedal}} \\
0 & 0 & Z_{\delta_{coll}} & Z_{\delta_{pedal}} \\
0 & 0 & L_{\delta_{coll}} & L_{\delta_{pedal}} \\
0 & 0 & M_{\delta_{coll}} & M_{\delta_{pedal}} \\
0 & 0 & N_{\delta_{coll}} & N_{\delta_{pedal}} \\
0 & 0 & 0 & 0 \\
0 & 0 & 0 & 0 \\
\frac{Mf_{\delta_{long}}}{\tau_f} & \frac{Mf_{\delta_{lat}}}{\tau_f} & 0 & 0 \\
\frac{Lf_{\delta_{long}}}{\tau_f} & \frac{Lf_{\delta_{lat}}}{\tau_f} & 0 & 0
\end{bmatrix} u
\qquad\qquad \textbf{(2.33)}
$$

where state vector and input vector are,

$$x' = [u \quad v \quad w \quad p \quad q \quad r \quad \varphi \quad \theta \quad \beta_{1c} \quad \beta_{1s}]$$

$$u = [\delta_{long} \quad \delta_{lat} \quad \delta_{coll} \quad \delta_{pedal}]$$

And the output vector is,

$$y' = [u \quad v \quad w \quad p \quad q \quad r \quad \varphi \quad \theta \quad \beta_{1c} \quad \beta_{1s}]$$

Here subscript 0 represents the trim values of the parameters.

In this thesis final model, which is 8 DoF with flapping dynamics, the unknown system parameters are 56. The number of the unknown parameters can be much higher to identify the parameters correctly. In addition to identifying these parameters with output-error method their initial values are very important for identifying the best values of the parameter. Hence, in the identification procedure, proper constraints may be applied to some unknown parameters. Moreover, known system parameters are taken as fixed parameters to reduce the number of the unknown parameters.

CHAPTER 3

IDENTIFICATION METHODS

There are two main system identification methods in the literature: Frequency domain method and time domain method. In time domain, system identification methods can be classified under two main headings. They are filter output error and output error methods. In this study, output error method is used for system identification. Furthermore, classical least square method is used to find the initial values of the parameters which are subsequently used in the output error method. In this section, the general structure of output error method, cost function calculation and optimization, statistical accuracy approaches and the least square method are explained.

3.1 OUTPUT ERROR METHOD

Output error method often used in system identification methods. In the 1970s, Taylor and Iliff [6, 7] used this method and has been successful in identification of the parameters of an aircraft. Later, Jatagoankar [4] and Morelli [21] used the Output error method in their studies for the identification of linear and nonlinear systems. In the literature, although most of the studies are done in the time domain identification for the fixed wing aircraft identification, in the time domain output error method is also used for the helicopter identification proccess.

In this part, output error algorithm and the formulation are described. In addition to these, optimization of the cost function used for Gauss-Newton method is also explained here. Finally statistical measurements of the accuracy of the parameters and least square method are presented.

Figure 3- 1 shows the output error method. System identification inputs are applied to the FLIGHTLAB non-linear model and then non-linear responses are gathered. Moreover, identification inputs are applied to 8 DoF linear model in hover flight condition. These responses are compared with the non-linear simulation responses to calculate the errors. By using these output errors and optimization algorithm, parameter values are calculated. Unknown parameters are updated and these updated parameters are used identification model so that identification model responses are updated. Output errors are again calculated and cost function is optimized. This cycle is continued up to obtaining minimum cost function.
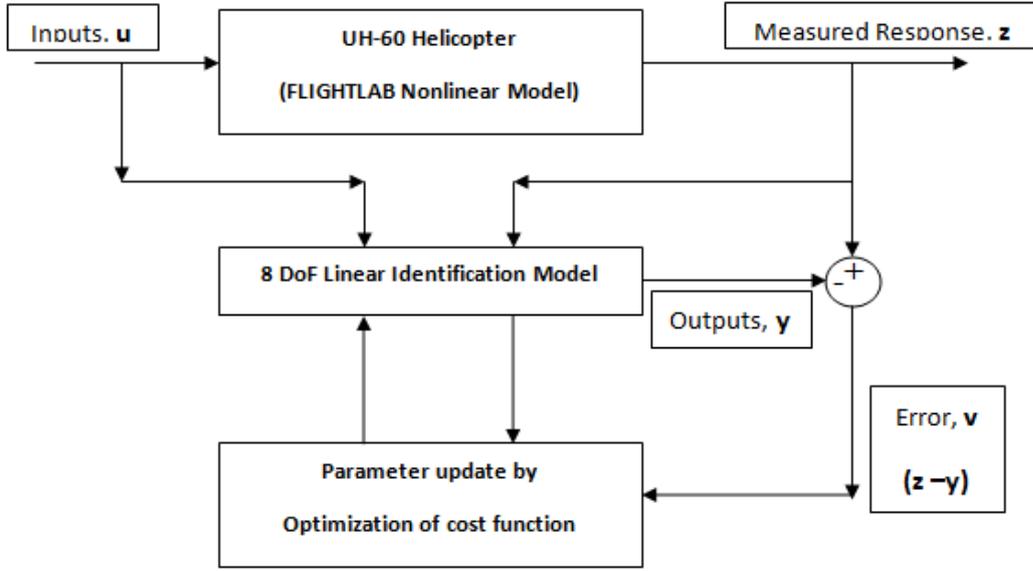
Figure 3- 1 : Output Error Method Diagram [4]

3.1.1 THE MAXIMUM LIKELIHOOD FUNCTION FOR ESTIMATION OF PARAMETERS IN DYNAMIC SYSTEM

System identification is a statistical method and it depends on the estimation theory. The probability density function of a x which has a Gaussian distribution and a real random variable is written as,

$$p(x) = \frac{1}{\sqrt{2\pi}\sigma} e^{\left(-\frac{(x-m)^2}{2\sigma^2}\right)} \qquad (3.1)$$

Here, $p(x)$ represents the probability of x. m and σ^2 are represent the mean and variance respectively. Mean and variance can be also expressed as [4, 21, 30],

$$m = E\{x\}$$

$$\sigma^2 = E\{(x-m)^2\}$$

where E is the expected value.

If the variables are more than one, joint probability distribution function is used and these variables are independent variables. The joint probability distribution function for n variable can be written as,

$$p(x_1, \cdots, x_n) = \frac{1}{(2\pi)^2\sqrt{|R|}} exp\left[-\frac{1}{2}(x-m)^T R^{-1}(x-m)\right] \qquad (3.2)$$

where $(x_1, \cdots, x_n) = x^T$ represents the variables and $(m_1, \cdots, m_n) = m^T$ represents the mean values of the variables. Moreover, R is the covariance matrix and its elements are calculated as [4, 21],

$$R_{ij} = E\{(x_i - m_i)(x_j - m_j)\} = \sigma_i \sigma_j \rho_{ij}$$

26

ρ_{ij} are called as correlation coefficients.

For nonparametric system identification, maximum likelihood function which is based on the Fisher Estimation Model is widely used. According to this model likelihood function can be defined as the conditional probability density function and it can be written as follows [4],

$$p(z \mid \theta) = p(z_1 \mid \theta) \cdot p(z_2 \mid \theta) \cdots p(z_N \mid \theta) \tag{3.3}$$

Here z represents the given N samples of random observations and θ is the unknown value of the parameter vector. $p(z \mid \theta)$ is the probability of z given θ. According to The Maximum Likelihood Method which is also known as Fisher Model Estimator, optimal solution for the unknown parameters vector θ probability of z given θ should be maximized. Thus the solution can be estimated as following expression [4, 21].

$$\hat{\theta} = \arg\left[\min_{\theta} \ln p(z \mid \theta)\right] \tag{3.4}$$

Assuming that probability density function of z given θ is twice differentiable function and according to estimation method its first differential function should be equal to zero. Then the linear Taylor series expansion can be applied around θ_0 to first differential function of the probability density function of z given θ. These expressions can be written as,

$$\frac{\partial \ln p(z \mid \theta)}{\partial \theta} = 0 \tag{3.5}$$

$$\frac{\partial \ln p(z \mid \theta_1)}{\partial \theta} \approx \frac{\partial \ln p(z \mid \theta_0)}{\partial \theta} + \frac{\partial^2 \ln p(z \mid \theta_0)}{\partial \theta^2}\Delta\theta \tag{3.6}$$

where $\theta_1 = \theta_0 + \Delta\theta$ is the improved approximation of the θ. These two expressions can be combined and then written as follows,

$$\frac{\partial \ln p(z \mid \theta_0)}{\partial \theta} = -\frac{\partial^2 \ln p(z \mid \theta_0)}{\partial \theta^2}\Delta\theta \tag{3.7}$$

This system of equation can be solved by using any optimization technique to find the improvement vector $\Delta\theta$. Expected value of the coefficient of $\Delta\theta$ is called as the Fisher Information Matrix. [4, 21]

Assuming that parameter vector θ and error which is expressed as $v = z - y$, has a Gaussian distribution so that the mean and covariance matrix can completely determined. Moreover assuming the error is independent at different time points. Then mean and variance of the error are,

$$E(v) = 0$$

$$\text{Cov}(v) = R$$

For the Gaussian distribution of the parameter vector and error, the conditional probability density function takes the form as [4],

$$p(z \mid \theta, R) = [(2\pi)^{n_0}|R|]^{-N/2}\exp\left[-\frac{1}{2}\sum_{i=1}^{N}\left(z(i) - y(i)\right)^{T}R^{-1}(z(i) - y(i))\right] \tag{3.8}$$

where n_0 is the dimension of measurement vector and N is the number of measurements.

Jatagaonkar [4] and Morelli [21] suggest that when doing minimization to find the optimal solution negative logarithm of the likelihood function, $\mathbb{L}(z \mid \theta, R)$, can be used. Because the negative logarithm of the likelihood function is simpler than the density function itself. Moreover the differential of these

density functions are equal. So that when constructing the output error algorithm negative logarithm of the likelihood function is used. It can be written as,

$$
\begin{aligned}
p(z \mid \theta, R) \equiv \mathbb{L}(z \mid \theta, R) \\
= \frac{1}{2} \sum_{i=1}^{N} [z(i) - y(i)]^{T} R^{-1} [z(i) - y(i)] + \frac{N}{2} \ln[\det(R)] \\
+ \frac{Nn_0}{2} \ln(2\pi)
\end{aligned}
\tag{3.9}
$$

Application Maximum Likelihood Function to Output-Error Method:

As discussed before, the mathematical system identification model of the helicopter can be expressed as linear state space dynamic system. In this case there is no process noise and the system can be described as following expressions.

$$
\dot{x}(t) = Ax(t) + Bu(t) \tag{3.10}
$$

$$
y(t) = Cx(t) + Du(t) \tag{3.11}
$$

$$
z(i) = y(i) + \upsilon(i) \tag{3.12}
$$

where z is the measurement outputs, $x(t_0) = x_0$ is the initial condition and υ is the error which as zero mean with covariance matrix R, that is [4],

$$
E\{v(i)\} = 0 \text{ and } E\{v(i)v^{T}(j)\} = R\delta_{ij}
$$

where δ_{ij} is the Kronecker delta which means that $\delta_{ij} = 1$ for $i = j$ and $\delta_{ij} = 0$ for $i \neq j$.

Now negative logarithm of the maximum likelihood function, $\mathbb{L}(z \mid \theta, R)$, can be used to find the unknown parameters of the system identification system. For general convenience negative logarithm of the maximum likelihood function, $\mathbb{L}(z \mid \theta, R)$ renamed as the cost function as J. To obtain the optimal unknown parameters solution, cost function can be minimized like mentioned before as Maximum Likelihood function by differentiated twice. The likelihood cost function or negative logarithm of the likelihood function is [4, 21],

$$
\begin{aligned}
\mathbb{L}(z \mid \theta, R) = J(\theta) \\
= \frac{1}{2} \sum_{i=1}^{N} [z(i) - y(i)]^{T} R^{-1} [z(i) - y(i)] + \frac{N}{2} \ln[\det(R)] \\
+ \frac{Nn_0}{2} \ln(2\pi)
\end{aligned}
\tag{3.13}
$$

3.1.2 COST FUNCTION OPTIMIZATION

Cost function optimization is based on the known measurement noise covariance and unknown measurement covariance matrix. In this thesis measurement covariance matrix is unknown and the optimization is done according to this case.

First, likelihood cost function, equation *3.13*, is differentiated with respect to R and setting the result to zero and then the following equation is obtained.

$$
R = \frac{1}{N} \sum_{i=1}^{N} [z(i) - y(i)][z(i) - y(i)]^{T} \tag{3.14}
$$

For obtaining the measurement covariance matrix, likelihood cost function can be expressed again as [4],

$$J(\theta) = \frac{1}{2}Nn_0 + \frac{N}{2}\ln[\det(R)] + \frac{Nn_0}{2}\ln(2\pi) \qquad \textbf{(3.15)}$$

There will be applied as assumption that the measurement noise sequences for the n_0 measured outputs are uncorrelated with one another. [21] With this assumption the calculation efficiency is higher than before. Hence the first and last terms become a constant and they can be neglected without affecting the minimization results. Final likelihood cost function becomes as,

$$J(\theta) = \det(R) \qquad \textbf{(3.16)}$$

When this cost function minimized with respect to θ by using the optimization algorithm the unknown parameter vector θ can be determined. In this thesis optimization method is chosen as Modified Newton-Raphson Method. It is detailed explained next topic.

3.1.3 MODIFIED NEWTON-RAPHSON METHOD

Modified Newton-Raphson method is an iterative optimization technique to find the zero points of the nonlinear function. In this case this method can be used to minimize the cost function.

Partial differential equation of the cost function with respect to parameter vector is,

$$\frac{\partial J}{\partial \theta} = -\sum_{i=1}^{N}\left[\frac{\partial y(i)}{\partial \theta}\right]^T R^{-1}[z(i) - y(i)] = 0 \qquad \textbf{(3.17)}$$

The system response y can be expand by using the two term Taylor's series expansions like,

$$y(\theta) \cong y(\theta_0) + \left(\frac{\partial J}{\partial \theta}\right)\Delta\theta \qquad \textbf{(3.18)}$$

where

$$\Delta\theta = \theta_{k+1} - \theta_k \qquad \textbf{(3.19)}$$

This quasi-linearized (first order approximation) equation is substituted to the first partial differential cost function equation and then the equation becomes,

$$\sum_{i=1}^{N}\left[\frac{\partial y(i)}{\partial \theta}\right]^T R^{-1}[z(i) - y(i)] - \sum_{i=1}^{N}\left[\frac{\partial y(i)}{\partial \theta}\right]^T R^{-1}\left[\frac{\partial y(i)}{\partial \theta}\right]\Delta\theta = 0 \qquad \textbf{(3.20)}$$

After these manipulations system consists of the linear equations and they can be solved easier than before. The first term of the left hand side is the gradient vector and the coefficient of the parameter change vector, $\Delta\theta$, is the Fisher information matrix. Hence to find the updated parameter, firstly gradient and then information matrices are calculated and then parameter change vector can be solved by using these matrices [4, 5, 21].

3.1.4   STATISTICAL ACCURACY OF PARAMETER ESTIMATES

After the all unknown parameters are calculated, accuracy of the parameters should be checked by using the statistical properties. These properties can also be used for the validation of the system identification model results. Cramer–Rao bound, or standard deviation and also correlation coefficients are usually used for determining the parameter accuracy in the system identification procedure.

Cramer-Rao bound shows the maximum achievable statistical accuracy of the estimated parameters [5]. In the time domain, maximum likelihood estimator is used the available data very efficiently, so that maximum likelihood estimator has the asymptotic efficiency which means that the maximum likelihood estimates converge in probability to the true values of the parameters. [4] The standard deviations and correlation coefficients are calculated by using the parameter error covariance matrix. It is calculated by taken the inverse of the Fisher information matrix. It can be represented as follows [4],

$$\text{PCOV} = \left[\sum_{i=1}^{N} \left[\frac{\partial y(i)}{\partial \theta} \right]^{T} R^{-1} \left[\frac{\partial y(i)}{\partial \theta} \right] \right]^{-1} \tag{3.21}$$

In statistics and probability theory standard deviation is the measure of the variation from the mean or expected value. If the standard deviation is low, estimated parameters are close to the expected value and if it is high, estimated parameters are spread out over a large range of expected values. The diagonal elements of the square root of the parameter error covariance matrix show the standard deviation of the estimated parameters. In statistics, it is showed by σ, sigma notation and can be represented as [4],

$$\sigma_{ii} = \sqrt{\text{PCOV}_{ii}} \tag{3.22}$$

Correlation coefficient is widely used to show the linear dependence between two variables. It has the value between -1 and 1. If the correlation coefficient closes the 1 means the estimated output fit measurement output very good. For different correlation coefficient examples of different scatter diagrams are shown at Figure 3- 2. It is unitless parameter [4, 21].

$$r_{ij} = \frac{\text{PCOV}_{ii}}{\sqrt{\text{PCOV}_{ii} \text{PCOV}_{jj}}} \tag{3.23}$$

In addition to these statistical accuracy parameters, t statistics is used for determining the significance of the parameter. It has a simple calculation as [21],

$$t_0 = \frac{\hat{\theta}}{s(\hat{\theta})} \tag{3.24}$$

where $\widehat{\theta}$ indicates the estimated parameter and $s(\hat{\theta})$ represents the standard error of the estimated parameter. In regression analysis, standard error of the mean is the standard deviation and it is unitless parameter.
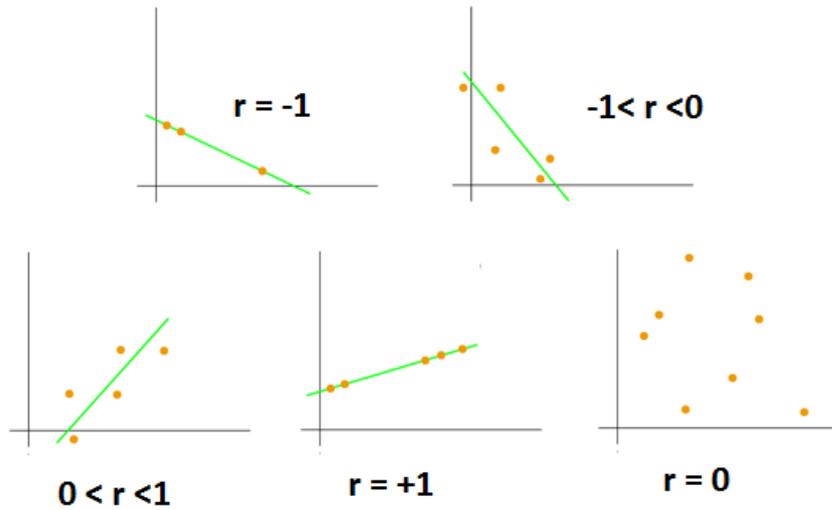
Figure 3- 2 : Examples of scatter diagrams with different values of correlation coefficient [22]

3.2 LEAST SQUARE METHOD

In this thesis, parameter estimation is done by using the output-error method however the initial values of the parameters are required to estimate the parameters correctly and also prevent the any singular value error. At the beginning of the system identification with output error method, to find the initial parameter values least square method is used at the translational and angular dynamics. Least square method is also known as the one of the equation error method.

General least square model can be written as,

$$y = X\theta \tag{3.25}$$

$$z = X\theta + \upsilon \tag{3.26}$$

Here again y is the estimated output and θ is the unknown parameter vector. **z** is the measurement vector, **X** is the regression vector and υ is the measurement error vector. Assume that measurement error has the zero mean and constant uncorrelated variance. Least square model may be constructed by using the measured states and their derivatives. Hence, measurement output vector may consist of the state vector and derivative of the state vector.

To find the unknown parameter vector, sum of the squares of the residuals (errors) should be minimized. In this case the cost function can be written as follows, [4, 21]

$$J(\theta) = \frac{1}{2}\sum_{i=1}^{N}[z(i) - y(i)]^T[z(i) - y(i)] = \frac{1}{2}[z - X\theta]^T[z - X\theta] \tag{3.27}$$

The derivative of the cost function with respect to the parameters which minimizes the cost function is given by,

$$\frac{\partial J}{\partial \theta} = -X^T z + X^T X \hat{\theta} = 0 \tag{3.28}$$

where $\hat{\theta}$ best parameter solution to minimize the cost function. So that the least square estimation solution can be expressed as follows,

$$\hat{\theta} = (X^T X)^{-1} X^T z \tag{3.29}$$

If the $X^T X$ matrix becomes a singular, there will be multiple solutions. For aircraft system identification applications, this matrix is generally nonsingular. For the least square estimation, information matrix is the $X^T X$ matrix, since this matrix is the measure of the information content of the measurement. [4]

In addition to the statistical accuracy parameters which are explained before part, coefficient of determination, R^2, is used for the determine the matching of the model to measurement data for least square estimation. The coefficient of determination defines as the ratio of the regression sum of squares SS_R to total sum of squares, SS_T. These parameters are defining according to mean value of the measured output data. It is expressed as [21],

$$\bar{z} = \frac{1}{N} \sum_{i=1}^{N} z(i) \tag{3.30}$$

where N is the number of data and I is the sampling number of the data. Then the regression sum of squares and total sum of squares are calculated as [21],

$$SS_R = \sum_{i=1}^{N} (y(i) - \bar{z})^2 \quad \text{and} \quad SS_T = \sum_{i=1}^{N} (z(i) - \bar{z})^2 \tag{3.31}$$

Hence coefficient of determination is,

$$R^2 = \frac{SS_R}{SS_T} \tag{3.32}$$

Another statistical parameter is the fit error. It indicates how close the estimated outputs are to the measured values. It is the square root of the measurement error variance, $\hat{\sigma}^2$. Fit error is calculated as, [21]

$$s = \sqrt{\hat{\sigma}^2} = \sqrt{\frac{1}{N - n_p} \sum_{i=1}^{N} [z(i) - y(i)]^2} \tag{3.33}$$

where n_p is the number of the parameter.

Parameter covariance matrix is estimated by using the fit error and information matrix for least square estimation. Then, it is obtained as follows,

$$PCOV = s^2 [X^T X]^{-1} \tag{3.34}$$

CHAPTER 4

SYSTEM IDENTIFICATION APPROACH AND IDENTIFIED MODEL VALIDATION

In this part, system identification approach used to identify a linear model of the UH-60 Black Hawk helicopter using FLIGHTLAB simulation data is examined. As mentioned in chapter one, system identification procedure have same basics namely, maneuver, measurements, methods, models and validation. In this chapter, first which maneuver is done and data compatibility of the gathering data from simulation are explained. Identification models and methods was explained the before chapters. In chapter two linear system identification model is explained and in chapter three the output error and least square methods in time domain are introduced. Hence after data compatibility analysis, system identification approach is explained. Finally, model validation is carried out by comparing simulation data with system identification model results.

4.1   EXPERIMENT AND DATA GATHERING

In this thesis, FLIGHTLAB UH-60 Black Hawk helicopter model is used to generate flight data instead of actual flight test data. Open loop system identification is carried out. Thus Stability Augmentation System was turned off. UH-60 helicopter has the mixer unit which mixes the inputs before the swashplate mechanism. Therefore swashplate angles are used instead of the pilot inputs to represents the system characteristic more accurately. In the literature, when Fetcher [18] were modeling the UH-60 helicopter for system identification purpose, he used to mixer control matrix to convert to pilot inputs to the swashplate angles. However, in FLIGHTLAB environment these angles can be selected as outputs and there is no need to convert the pilot inputs to swashplate angles.

For the successful system identification, inputs should excite the helicopter stability and control modes and to yield good data compatibility. For this reasons the input design is the important part of the system identification procedure. In the literature optimal input design is the subject of the many research. Jategaonkar [4], studied the maximum likelihood parameter estimation with using the 3-2-1-1, modified 3-2-1-1, doublet and step inputs in the time domain analysis. Moreover, Morelli [21] also investigated on the time domain system identification with optimal input designs. On the other hand, Tischler [5] investigated the frequency domain system identification with the sine sweep inputs. Tischler [5], Jategaonkar [4] and Morelli [21] suggests that for the time domain system identification 3-2-1-1 multistep input or the modified 3-2-1-1 step input may be used for frequency domain system identification sine sweep or Schroerder-phased signal are reported to be most effective.

At the beginning of this study, although the time domain method is selected to identify the helicopter, sine sweep input was also employed. However in this case data collinearity was not as good as expected. In addition, the analysis time was long compared to the 3-2-1-1 input. Tischler [5] also mentioned that the simulation sine sweep input does not have sufficient spectral richness because it did not have any irregularities in the input shape. Some noise components are also added to the sine sweep input and the other off-axis inputs. However in this case, some problems were observed related to the simulation convergence, since the system is open loop and helicopter is an unstable system. To obtain convergence results of the nonlinear simulation, input amplitude and the frequency range were

reduced. However this resulted in lower coherence values than required. For example, coherence values of the swashplate controls with longitudinal sine sweep and 3-2-1-1 inputs are shown at Figure 4- 1. As a result of these situations, 3-2-1-1 multistep input is used for identification in this study instead of sine sweep input.
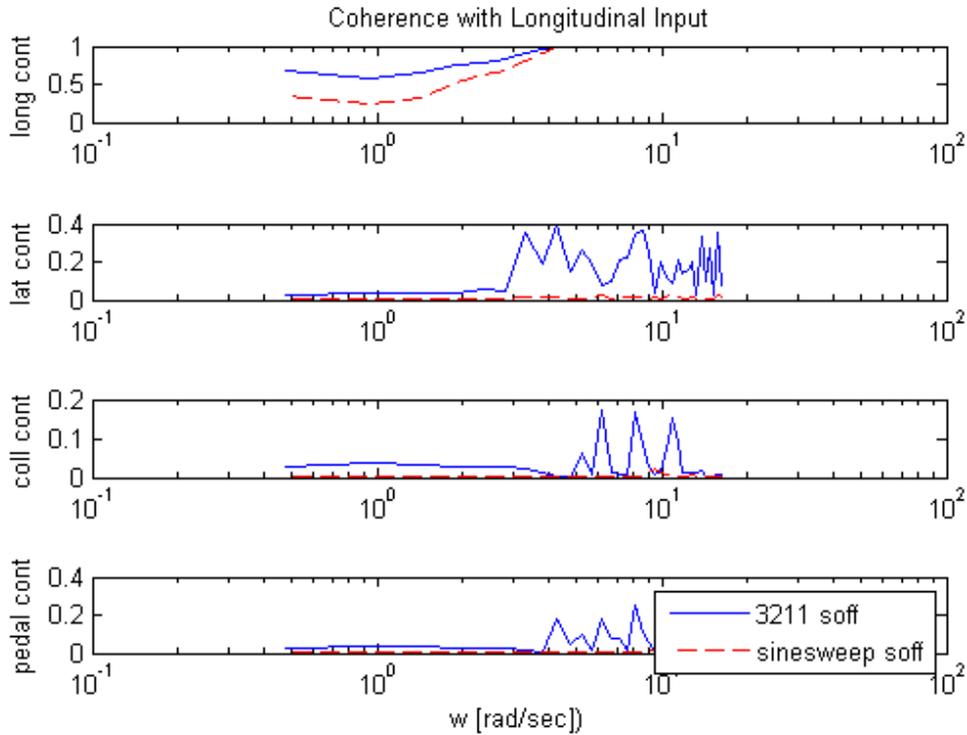
Figure 4- 1 : Comparison of the coherence value of the swasplate controls with longitudinal input (Hover, SAS off (soff))

4.2   DATA COLLINEARITY

When doing the simulation, 3-2-1-1 input is applied to each of the controls of the helicopter, namely, longitudinal, lateral, collective and pedal controls. These identification inputs are shown at Figure 4- 2. After gathering the output data corresponding to the each controls, data collinearity can be checked between variables before doing system identification.

As shown Figure 4- 2, lateral 3-2-1-1 input has the smaller step time than other inputs. Step time of the longitudinal, collective and pedal inputs is chosen as 1 second. However, step time of the lateral input is 0.3 seconds, since data collinearity problem is observed when using the 3-2-1-1 lateral input with 1 second step time. Moreover input which has smaller step time covers the wider frequency range. Hence lateral 3-2-1-1 input with 0.3 second step time is decided to be appropriate for system identification. All of the inputs have 0.2 second rise time and fall time to approximate the pilot input except for lateral input. Since, 3-2-1-1 lateral input has 0.3 second step time, its rise time and fall time are taken as zero.
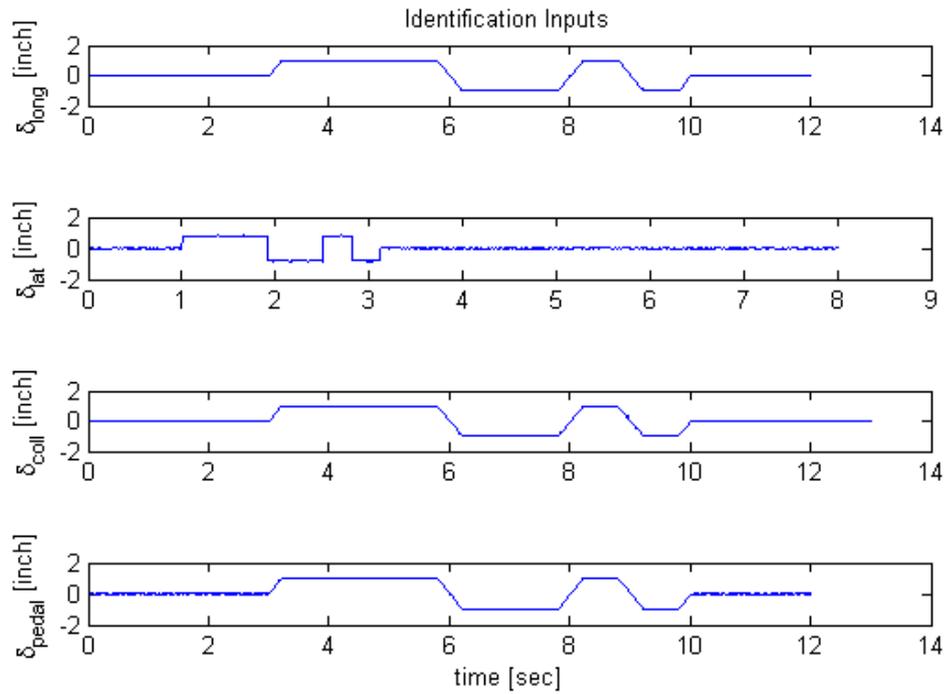
Figure 4- 2 : Identification Inputs

For successful system identification, correlation between the output data should be minimum, since the fundamental assumption of the maximum likelihood function is that input is independent of the system output. Thus after doing the experiment, data collinearity should be checked for linearity between variables. Correlation between data can be measured by using different statistical techniques. One of them is looking at the correlation matrix of the data. Obtaining the correlation matrix was explained in chapter two. Correlation matrix gives the information about the linearity between two variables. For the air vehicle system identification, absolute value of the correlation matrix should be less than the 0.9. Data collinearity is also used for determining the system identification model parameters [4,21]. Linearity of the data may also be determined by using graphical method. For example, Figure 4- 3 shows the uncorrelated relation with angular pitch and roll rates for lateral input.

For longitudinal, lateral, collective and pedal inputs, the correlation matrices for the states are calculated as Table 4- 1, Table 4- 2, Table 4- 3 and Table 4- 4 respectively. Elements of correlation matrix are unitless. These matrices are the symmetric matrices according to diagonal elements. Correlations between states are generally low and suitable for the identification. Some correlations are greater than 0.9 but these parameters are eliminated in the identification procedure. For example, for collective input, correlation coefficient of the pitch (θ) and roll (φ) attitudes is greater than 0.9. However pitch and roll attitudes are not related parameters in the system identification model. Their coefficients are not identified in system identification procedure. Hence collinearity of the simulation data is suitable for system identification.
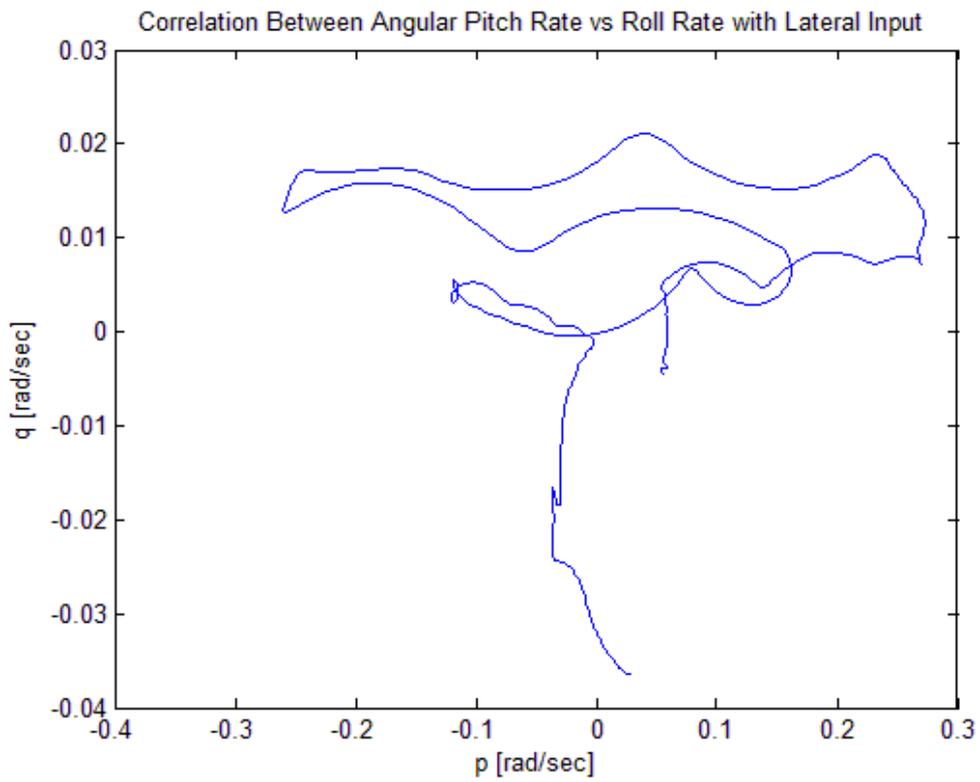
Figure 4- 3 : Uncorrelated Relation with Angular Pitch Rate and Roll Rate for Lateral Input

Table 4- 1 : Correlation Matrix of the States for the Longitudinal 3-2-1-1 Input

	p	q	r	φ	θ	u	V	w	β_{1c}	β_{1s}
p	1,00	-0,62	-0,26	0,46	-0,52	0,12	-0,48	-0,03	0,26	-0,70
q	-0,62	1,00	-0,19	0,17	0,06	0,60	0,82	-0,39	-0,11	0,78
r	-0,26	-0,19	1,00	-0,10	-0,25	-0,23	-0,28	0,55	0,28	0,05
φ	0,46	0,17	-0,10	1,00	-0,91	0,83	0,37	0,14	0,56	-0,06
θ	-0,52	0,06	-0,25	-0,91	1,00	-0,65	-0,07	-0,28	-0,63	0,18
u	0,12	0,60	-0,23	0,83	-0,65	1,00	0,72	-0,30	0,27	0,41
v	-0,48	0,82	-0,28	0,37	-0,07	0,72	1,00	-0,26	-0,01	0,73
w	-0,03	-0,39	0,55	0,14	-0,28	-0,30	-0,26	1,00	0,60	-0,45
β_{1c}	0,26	-0,11	0,28	0,56	-0,63	0,27	-0,01	0,60	1,00	-0,44
β_{1s}	-0,70	0,78	0,05	-0,06	0,18	0,41	0,73	-0,45	-0,44	1,00

Table 4- 2 : Correlation Matrix of the States for the Lateral 3-2-1-1 Input

	p	q	r	φ	θ	u	V	w	β_{1c}	β_{1s}
p	1,00	0,21	-0,18	0,09	-0,40	0,36	-0,51	0,28	0,55	-0,25
q	0,21	1,00	0,02	0,90	0,30	0,92	-0,02	0,93	-0,49	-0,11
r	-0,18	0,02	1,00	0,14	0,89	-0,20	0,87	0,08	-0,22	0,13
φ	0,09	0,90	0,14	1,00	0,45	0,72	0,23	0,73	-0,55	-0,26
θ	-0,40	0,30	0,89	0,45	1,00	0,03	0,92	0,30	-0,56	0,17
u	0,36	0,92	-0,20	0,72	0,03	1,00	-0,33	0,94	-0,34	-0,14
v	-0,51	-0,02	0,87	0,23	0,92	-0,33	1,00	-0,07	-0,43	0,19
w	0,28	0,93	0,08	0,73	0,30	0,94	-0,07	1,00	-0,42	0,05
β_{1c}	0,55	-0,49	-0,22	-0,55	-0,56	-0,34	-0,43	-0,42	1,00	-0,09
β_{1s}	-0,25	-0,11	0,13	-0,26	0,17	-0,14	0,19	0,05	-0,09	1,00

Table 4- 3 : Correlation Matrix of the States for the Collective 3-2-1-1 Input

	p	q	r	φ	θ	u	V	w	β_{1c}	β_{1s}
p	1,00	0,54	0,03	0,37	0,27	-0,27	-0,51	0,09	0,80	-0,81
q	0,54	1,00	-0,46	0,58	0,42	-0,28	-0,15	0,50	0,06	-0,55
r	0,03	-0,46	1,00	-0,77	-0,67	0,71	-0,60	-0,96	0,36	-0,18
φ	0,37	0,58	-0,77	1,00	0,94	-0,83	0,10	0,73	-0,02	-0,26
θ	0,27	0,42	-0,67	0,94	1,00	-0,84	-0,04	0,56	-0,10	-0,18
u	-0,27	-0,28	0,71	-0,83	-0,84	1,00	-0,12	-0,62	-0,07	0,20
v	-0,51	-0,15	-0,60	0,10	-0,04	-0,12	1,00	0,65	-0,42	0,68
w	0,09	0,50	-0,96	0,73	0,56	-0,62	0,65	1,00	-0,20	0,13
β_{1c}	0,80	0,06	0,36	-0,02	-0,10	-0,07	-0,42	-0,20	1,00	-0,61
β_{1s}	-0,81	-0,55	-0,18	-0,26	-0,18	0,20	0,68	0,13	-0,61	1,00

Table 4- 4 : Correlation Matrix of the States for the Pedal 3-2-1-1 Input

	p	q	r	φ	θ	u	V	w	β_{1c}	β_{1s}
p	1,00	-0,10	-0,34	0,35	0,01	-0,38	-0,10	-0,25	0,88	-0,89
q	-0,10	1,00	-0,74	0,70	0,08	-0,22	0,38	-0,06	-0,14	-0,03
r	-0,34	-0,74	1,00	-0,54	-0,16	0,51	-0,14	0,52	-0,17	0,35
φ	0,35	0,70	-0,54	1,00	0,19	-0,27	0,59	0,30	0,51	-0,59
θ	0,01	0,08	-0,16	0,19	1,00	-0,79	0,04	-0,09	0,19	-0,22
u	-0,38	-0,22	0,51	-0,27	-0,79	1,00	0,30	0,53	-0,39	0,50
v	-0,10	0,38	-0,14	0,59	0,04	0,30	1,00	0,71	0,14	-0,08
w	-0,25	-0,06	0,52	0,30	-0,09	0,53	0,71	1,00	0,10	0,04
β_{1c}	0,88	-0,14	-0,17	0,51	0,19	-0,39	0,14	0,10	1,00	-0,96
β_{1s}	-0,89	-0,03	0,35	-0,59	-0,22	0,50	-0,08	0,04	-0,96	1,00

In addition to the 3-2-1-1 input, when obtaining the initial parameter values by using the least square method sine sweep inputs are also used for the identification. Figure 4- 4 shows the sine sweep inputs are used for the longitudinal and lateral translational dynamics. They are generated in FLIGHTLAB. They have small amplitude to avoid instability, since SAS is turned off. To obtain the simulation data amplitudes are taken small with compared to the 3-2-1-1 inputs. Lateral sine sweep input is taken shorter than longitudinal input. Low frequencies are very important to estimate the dominant parameters in translational dynamics. To observe this phenomenon, longitudinal sine sweep input is selected to have a wider frequency, 0.05 to 2 Hz than lateral sine sweep input which runs from 0.05 to 0.2 Hz.
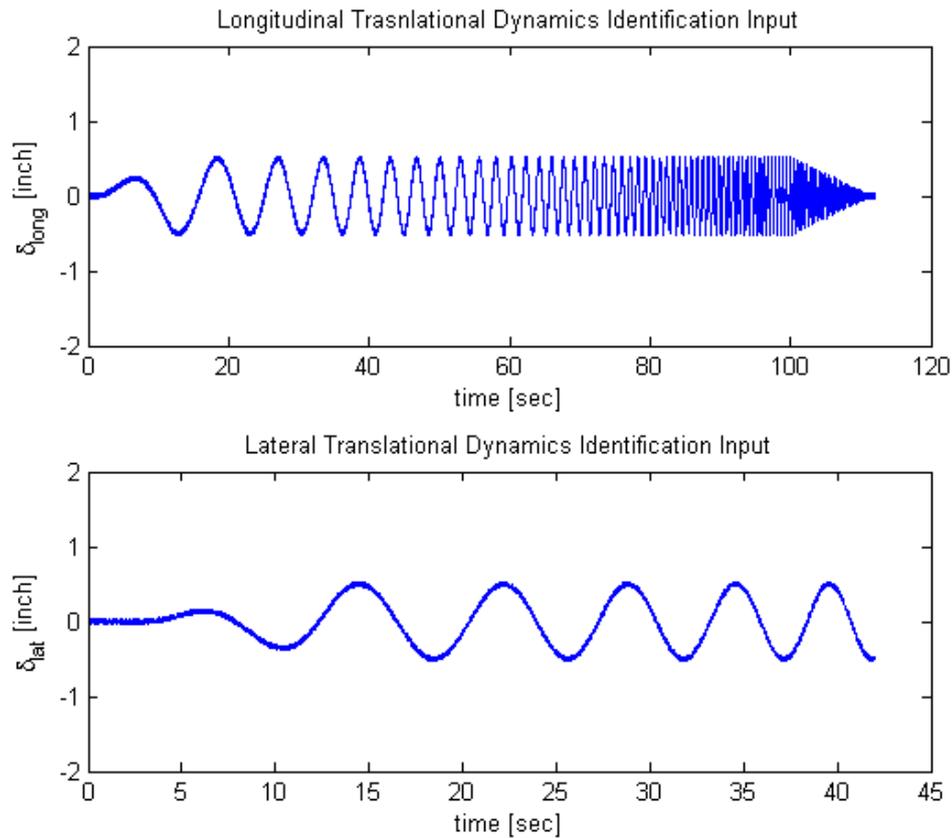
Figure 4- 4 : Identification Inputs for Longitudinal and Lateral Translational Dynamics

Correlation matrices for longitudinal and lateral sine sweep inputs are shown Table 4- 5 and Table 4- 6, respectively. It can be seen that correlation values are lower than 0.9 so that these inputs may be used for identification of translational parameters.

Table 4- 5 : Correlation Matrix for the Longitudinal Sine Sweep Input

	θ	u	β_{1c}
θ	1,00	-0,72	-0,52
u	-0,72	1,00	0,37
β_{1c}	-0,52	0,37	1,00

Table 4- 6 : Correlation Matrix for the Lateral Sine Sweep Input

	φ	v	β_{1s}
φ	1,00	-0,18	-0,31
v	-0,18	1,00	0,42
β_{1s}	-0,31	0,42	1,00

4.3   SYSTEM IDENTIFICATION APPROACH

As presented before, 8 DoF linear helicopter system identification model, which consists of 6 DoF fuselage and 2 DoF flapping dynamics, is used to identify the UH-60 helicopter at hover condition. Good starting values are needed to successfully identify unknown parameters. Another challenge of the identification is the number of parameters to be identified. As the number of the parameters is increased, accuracy of the estimation may decrease and in some cases there is no solution is found. If it is needed to identify the more parameters, more informative data are required. [21]

In the 8 DoF linear system identification model, there are 36 unknown system parameters with no initial condition information for these unknown parameters. However initial parameter values may be determined to start the identification. Yuan [29] and Mettler [31] suggested to use partition system identification procedure to find the initial parameter values and to identify the complex systems. According to this approach systems can be divided to some meaningful dynamical parts, and then these parts are solved. After that each part of the system is solved, build up process is begun and finally full system is identified with initial parameter values which are computed in the previous step. In this way, especially coupled parameters can be found after obtaining the dominant parameters of the system.

Yuan [29] identified the full model of the miniature rotorcraft at the nine steps as shown Figure 4- 5. This procedure is called partitioned system identification procedure. It may be divided three main steps. First, the parameters of the translational and angular dynamics are identified. In the first part of this procedure, least square method is used, since this method does not require the initial conditions to estimate the parameters. Hence, the dominant parameters are obtained without any initial parameter values, and then these parameters are used as the initial parameter values for identification of the uncoupled and coupled dynamics. Second, the uncoupled pitch and roll dynamics are acquired by using the output error method. Third, coupled dynamics and complete model dynamics were solved after obtaining the uncoupled dynamics. The complete dynamic model is obtained by combining the coupled pitch and roll dynamics and the coupled heave and yaw dynamics. Output error method is used to identify the coupled dynamics and the complete dynamic models. Estimated parameters of the coupled dynamics are used as the initial parameter values of the complete dynamic model. The complete dynamic model is solved for finding the remaining coupled parameters. In addition, complete dynamic model is again identified to refine all the unknown parameters.
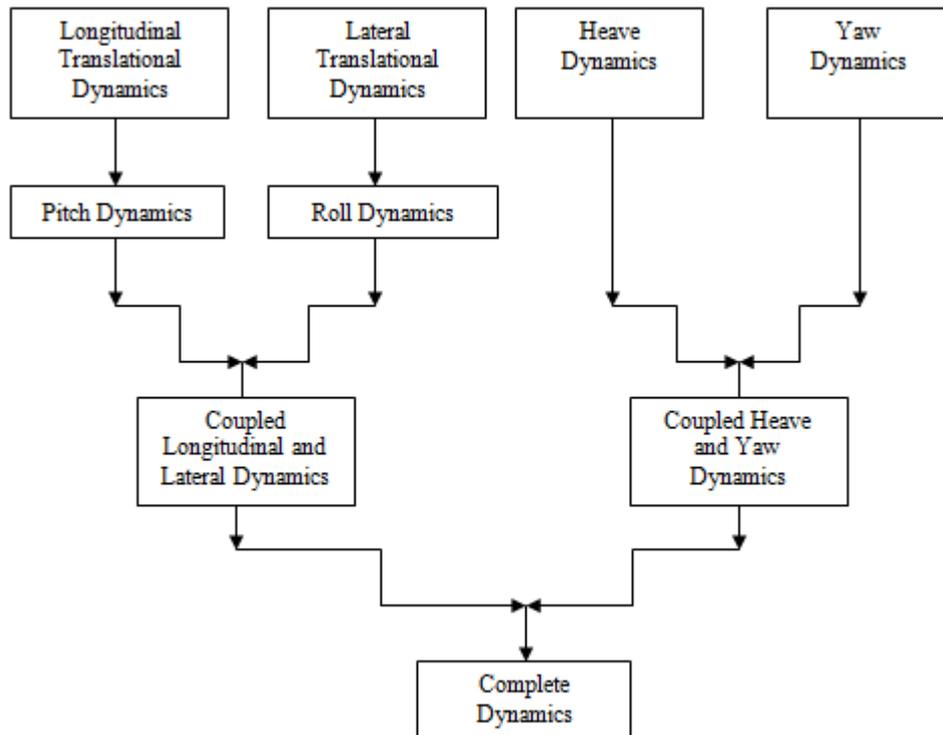
Figure 4- 5 : Partitioned System Identification Procedure

Similar to the study described above, in this study, 8 DoF UH-60 linear identification hover model is identified at the three main steps. These steps are translational and angular dynamics, uncoupled dynamics and coupled dynamics. In order to find the initial conditions of the dominant parameters, least square method is used. By taking results of the previous steps, output error method is used to identify the uncoupled and coupled dynamics. As shown Figure 4- 5, at the partition method, coupled heave and yaw dynamics is identified separately. However, in this study this coupled dynamics is estimated in the complete dynamic model as shown Figure 4- 6. The estimated parameters of the heave and yaw dynamics are used as initial parameter values for further identification step. Afterwards, parameters of the coupled heave and yaw dynamics and the coupled pitch and roll dynamics are estimated at the estimation of the complete 8 DoF model step. At the final step, all of the unknown 36 parameters are refined again to take effects of the complete system dynamics into account.
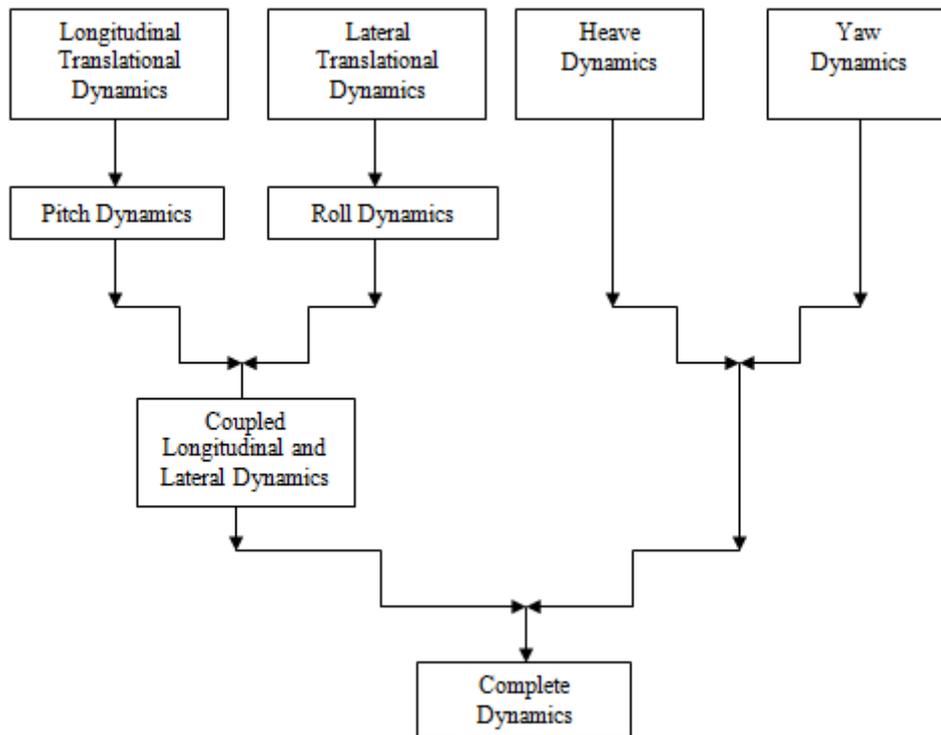
Figure 4- 6 : System Identification Procedure Used In This Study

Translational and angular dynamic steps consist of the longitudinal, lateral, heave and yaw dynamics with some simplifications, which is explained at the related parts. After that, by using the identification solution of the translational and angular dynamics, the uncoupled pitch and roll dynamics are identified. The uncoupled pitch dynamics has four states namely, u, q, θ and β_{1c}. The uncoupled roll dynamics has also four states namely, v, p, φ and β_{1s}. Identified parameters of the uncoupled pitch and roll dynamics are used as the initial parameter, when identifying the coupled pitch and roll dynamics, which has the eight states, $u, v, p, q, \varphi, \theta, \beta_{1c}$ and β_{1s}. Finally, parameters of the complete 8 DoF linear identification model are estimated by using the previous identified parameter values by making use of the output error method.

4.3.1 TRANSLATIONAL AND ANGULAR DYNAMICS

In order to begin the identification process with output error method, initial parameter values of the unknown parameters should be meaningful and close to their real values to obtain successful results. Hence, identification process begins with the simple translational and angular equations with least square method. As discussed before, least square method is independent of the initial conditions of parameters, in other words initial parameter values are not necessary to obtain results. The drawback of the least squares method, however is that the translational and rotational accelerations must be available.

After extending the 6 DoF rigid body dynamics to 8 DoF with the addition of the flapping dynamics, longitudinal translational equations can be written as,

$$\dot{u} = X_u u + X_v v + X_w w + X_r r - g\theta + X_{\beta_{1c}}\beta_{1c} + X_{\delta_{coll}}\delta_{coll} + X_{\delta_{pedal}}\delta_{pedal} \quad \textbf{(4.1)}$$

However, this equation involves the coupled terms. To simplify this equation, coupled terms can be ignored, so that the dominant parameters remain on the on-axis. After this simplification, (4.1 can be rewritten as,

$$\dot{u} = X_u u - g\theta + X_{\beta_{1c}}\beta_{1c} \quad \textbf{(4.2)}$$

Then, it remained the only dominant parameters, X_u and $X_{\beta_{1c}}$. $X_{\beta_{1c}}$ has been constrained as explained in the flapping model section. $X_{\beta_{1c}}$ has the value of the negative gravity constant theoretically. That is, if the vertical center of gravity is known, its exact value can be calculated. Because of that, all data obtained from the non-linear simulation are defined in the body axes. Therefore it can be said that $X_{\beta_{1c}}$ has the value of the negative gravity constant and in the calculations, its value is fixed. Finally, the only remaining parameters, X_u and the bias term, B_u are identified. X_u is the speed force derivative and it should be physically negative.

After the least square method is applied to this simple equation, obtained results are shown at the Table 4- 7. It may be concluded that X_u has the small standard error and its coefficient of determination is close to 0.9. Furthermore, it has the relatively small t_o, inverse of the relative parameter standard error. Hence, it is justifiable to use it as initial parameter value for output error method. Figure 4- 7 shows the result of the longitudinal translational dynamics. Straight line shows non-linear simulation result and dashed line shows identified result. As shown in the Figure 4- 7, model fit is better at the low frequency region than high frequency region. Main aim of this step is fitting the low frequency content of the non-linear simulation response. It is enough for the beginning of the system identification procedure.

Table 4- 7 : Longitudinal Translational Dynamics, Least Square Estimation Results

Parameters	$\widehat{\theta}$	Standard Error, $s(\widehat{\theta})$	% Error	$|t_o|$
X_u	-3,13E-02	1,44E-03	4,60E+00	2,17E+01
B_u	3,32E+00	1,97E-02	5,95E-01	1,68E+02
s (fit error)	1,72E+00			
R^2 (coeficient of determination, %)	8,38E-01			

Lateral translational dynamic equation is also obtained as longitudinal dynamic case. After using the same simplifications, lateral translational equation becomes,

$$\dot{v} = Y_v v + Y_p p + g\varphi + Y_{\beta_{1s}}\beta_{1s} \quad \textbf{(4.3)}$$

In this equation Y_p is coupled parameter, since it represents the tail rotor contribution. Hence, it can be ignored at this step. Then equation rewritten as,

$$\dot{v} = Y_v v + g\varphi + Y_{\beta_{1s}}\beta_{1s} \quad \textbf{(4.4)}$$
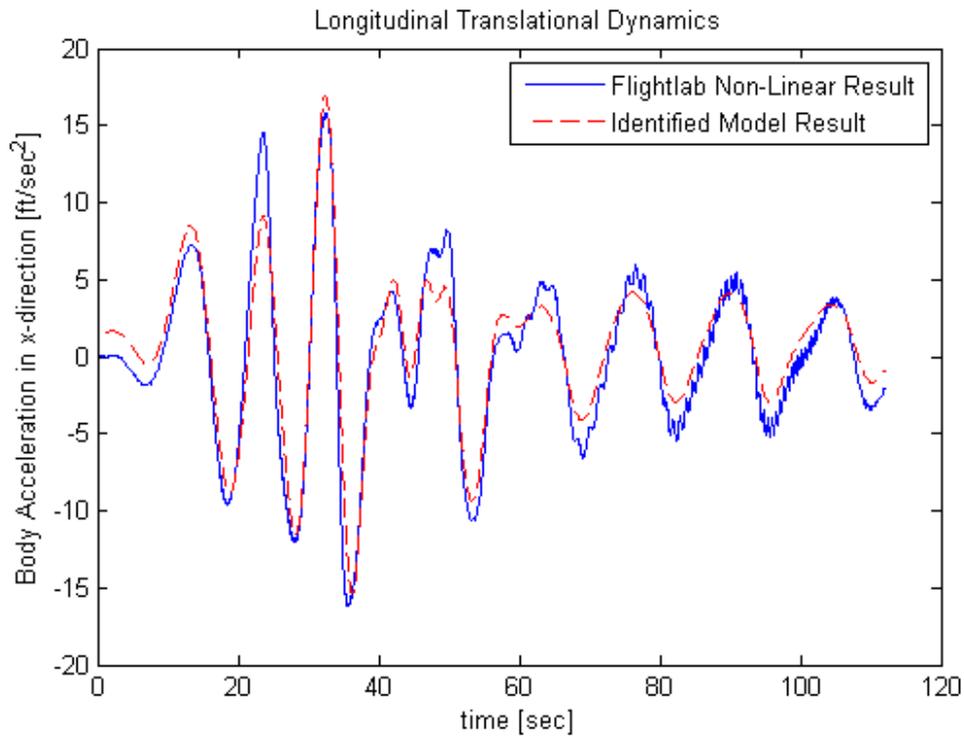
Figure 4- 7 : Body Acceleration in x-direction result with Least Square Method

Finally, lateral translational dynamic has one unknown parameter, Y_v at this step. Again the unknown parameters are estimated using the least square method. Estimated parameters are tabulated in Table 4 - 8. Like longitudinal case, Y_v has small standard error and its coefficient of determination is close to 1. Hence, identified model response shows good agreement with non-linear simulation model result. It has relatively high percentage error, but it is accepted for simplified lateral translational dynamic equation. Y_v is the speed force damping derivative. It should have the negative value physically. Estimated result is negative. Hence it may be used as initial parameter value for the further estimations. B_v is the bias parameter to take the effects of the non-linearity into account. Comparison of the non-linear simulation model and identified body acceleration in y-direction are shown at the Figure 4 - 8. In this figure, solid line shows non-linear simulation response and dashed line shows identified model response.

Table 4 - 8 : Lateral Translational Dynamics, Least Square Estimation Results

Parameters	$\widehat{\boldsymbol{\theta}}$	Standard Error, $s(\widehat{\boldsymbol{\theta}})$	% Error	$|t_o|$
Y_v	-4,44E-02	2,76E-03	6,22E+00	1,61E+01
B_v	1,20E+00	6,54E-02	5,46E+00	1,83E+01
s (fit error)	1,33E+00			
R^2 (coeficient of determination, %)	9,89E-01			

44
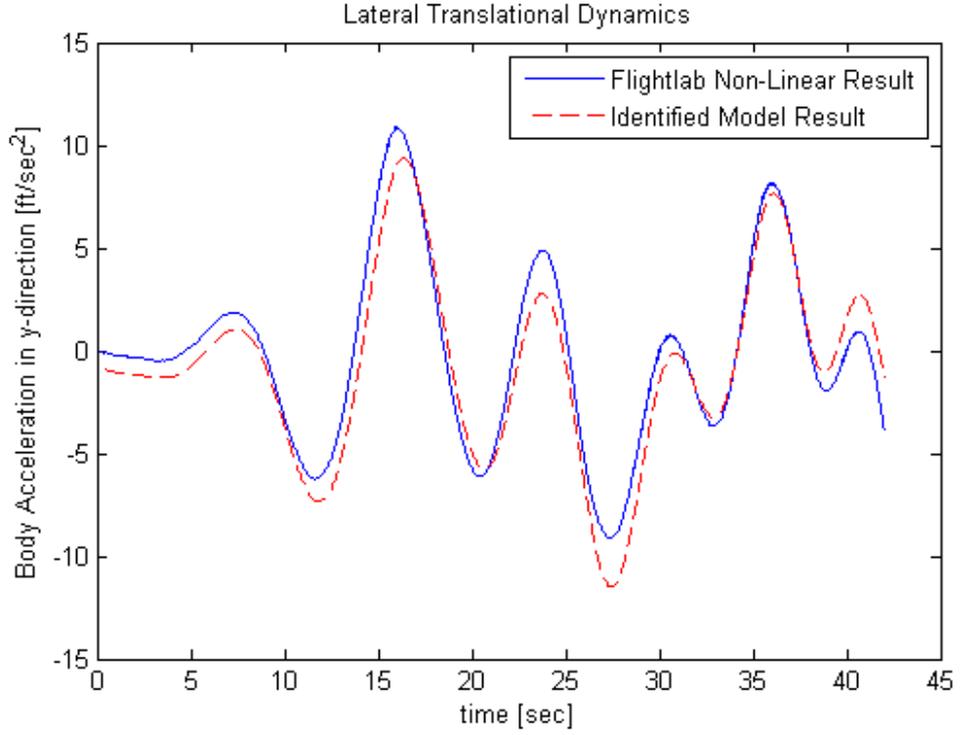
Figure 4 - 8 : Body Acceleration in y-direction result with Least Square Method

Heave translational dynamic equation may be written as,

$$\dot{w} = Z_u u + Z_v v + Z_w w + Z_q q + Z_r r + Z_{\beta_{1c}}\beta_{1c} + Z_{\beta_{1s}}\beta_{1s} + Z_{\delta_{coll}}\delta_{coll}$$
$$+ Z_{\delta_{pedal}}\delta_{pedal} \qquad (4.5)$$

In this equation heave dynamic is directly affected from heave damping derivative, Z_w, and gain for the heave dynamics from collective input, $Z_{\delta_{coll}}$. Other terms represent the coupling effects and they may be ignored at this step to examine the dominant parameters. Then this equation becomes as follows,

$$\dot{w} = Z_w w + Z_{\delta_{coll}}\delta_{coll} \qquad (4.6)$$

There are two unknown system parameter to estimate at this step. Estimated values of these unknown parameters and their statistical parameters are seen in Table 4 - 9. Heave damping derivative must have a negative value. Estimated value is negative with small standard error. Moreover fit error is very small and coefficient of determination is also close to 1. Hence, fitting is acceptable. Figure 4 - 9 shows non-linear simulation result and estimated body acceleration in z direction. It is seen that low frequency responses are matched better than high frequency responses. However estimated parameters are used as initial parameter values to identify the full 8 DoF linear hover identification model.

Table 4 - 9 : Heave Translational Dynamics, Least Square Estimation Results

Parameters	$\hat{\theta}$	Standard Error, $s(\hat{\theta})$	% Error	$|t_o|$
Z_w	-2,41E-01	2,85E-03	1,18E+00	8,45E+01
$Z_{\delta_{coll}}$	-2,44E+02	7,15E-01	2,94E-01	3,40E+02
B_w	7,86E+01	2,31E-01	2,93E-01	3,41E+02
s (fit error)	5,77E-01			
R^2 (coeficient of determination, %)	9,83E-01			

Last step of the identification of the translational and angular dynamics is yaw angular dynamics. Yaw angular rate equation can be written as,

$$\dot{r} = N_u u + N_v v + N_w w + N_p p + N_q q + N_r r + N_{\beta_{1c}}\beta_{1c} + N_{\beta_{1s}}\beta_{1s} + N_{\delta_{coll}}\delta_{coll} + N_{\delta_{pedal}}\delta_{pedal} \tag{4.7}$$

In this equation, N_r and $N_{\delta_{pedal}}$ are directly related to yaw axis. Other parameters affect the yaw dynamic indirectly and they are coupled terms. Hence, in this step, N_r and $N_{\delta_{pedal}}$ are estimated by using the least square method. Final equation is obtained as,

$$\dot{r} = N_r r + N_{\delta_{pedal}}\delta_{pedal} \tag{4.8}$$
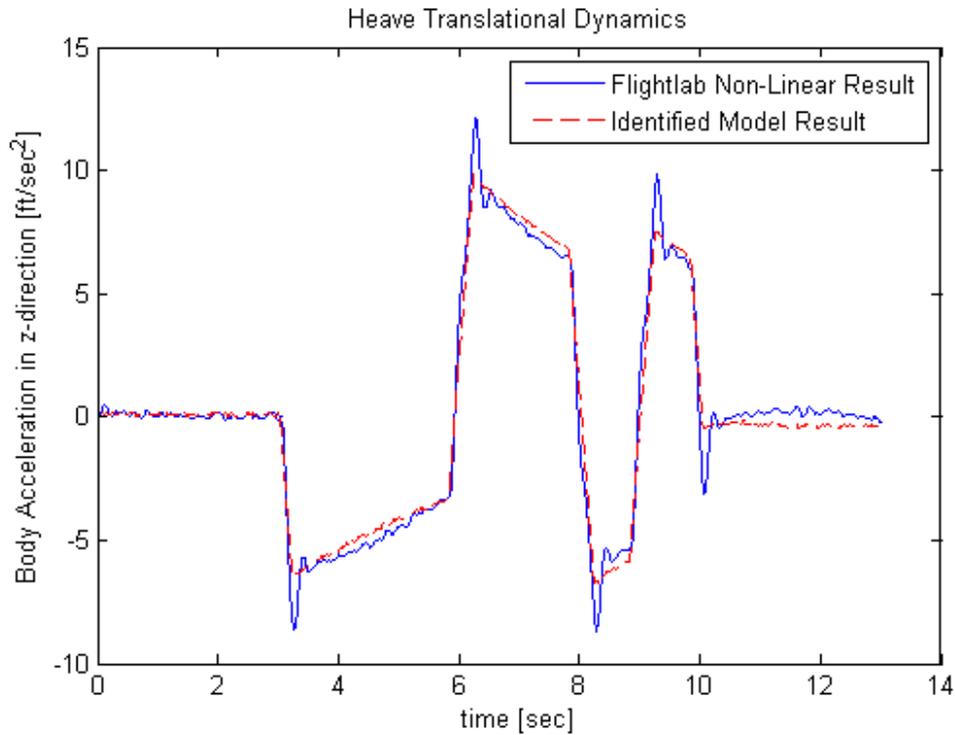
Figure 4 - 9 : Body Acceleration in z-direction result with Least Square Method

Estimated parameter values and their errors are shown at the Table 4 - 10. The results are good enough, since error, namely fit error, standard errors and percentage errors are small. Furthermore, coefficient of determination and t_0 values are sufficiently high values. Moreover, non-linear simulation response and estimated angular yaw acceleration are shown with respect to time at the Figure 4 - 10. Straight line shows the non-linear simulation model response and dashed line shows the identified model response. It seems a very good fitting. After ten seconds, error is growing up. However, estimated parameters are acceptable to take as initial parameter values for the complete 8 DoF linear coupled identification model. Since, fitting of the low frequency region is important for this step.

Table 4 - 10 : Angular Yaw Dynamics, Least Square Estimation Results

Parameters	$\widehat{\boldsymbol{\theta}}$	Standard Error, $s(\widehat{\boldsymbol{\theta}})$	% Error	$|t_o|$
N_r	-3,71E-01	2,31E-03	6,23E-01	1,60E+02
$N_{\delta_{pedal}}$	-4,04E+00	8,40E-03	2,08E-01	4,81E+02
B_N	1,65E+00	3,55E-03	2,15E-01	4,66E+02
s (fit error)	2,92E-02			
R^2 (coeficient of determination, %)	9,92E-01			
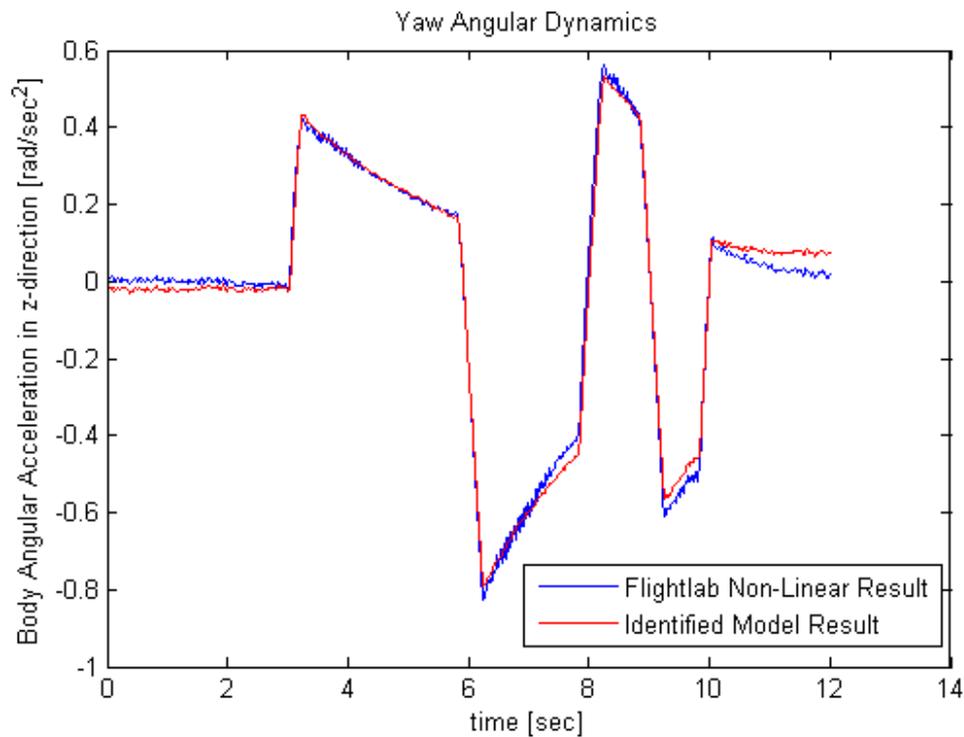
Figure 4 - 10 : Angular Yaw Acceleration in z-direction result with Least Square Method

4.3.2 UNCOUPLED DYNAMICS

After estimating dominant parameters of the translational and angular dynamics which are mentioned previous part of this chapter, remaining uncoupled parameters may be estimated by using the output error method. In this study, uncoupled dynamics means pitch and roll dynamics.

Pitch dynamics may be obtained from the complete 8 DoF model by making use of the u, q, θ and β_{1c} states without cross coupling terms. Coupled terms are ignored. Then, the following state space form of the pitch dynamics is obtained.

$$
\begin{bmatrix} \dot{u} \\ \dot{q} \\ \dot{\theta} \\ \dot{\beta}_{1c} \end{bmatrix} = \begin{bmatrix} X_u & 0 & -g & X_{\beta_{1c}} \\ M_u & 0 & 0 & M_{\beta_{1c}} \\ 0 & 1 & 0 & 0 \\ 0 & 1 & 0 & -\dfrac{1}{\tau_f} \end{bmatrix} x + \begin{bmatrix} 0 \\ 0 \\ 0 \\ A_{long} \end{bmatrix} \delta_{long} \qquad (4.9)
$$

In these equations, there are four unknown parameters which are M_u, $M_{\beta_{1c}}$, τ_f, and A_{long}. M_u represents the effects of the changing helicopter longitudinal velocity to the pitching motion of the helicopter. $M_{\beta_{1c}}$ is relating to the flapping model and represents the rotor dynamics cross coupling. τ_f is the rotor time constant and its theoretical value is 0,127 second, which is calculated at the flapping model part. A_{long} is the gain from longitudinal input. X_u and $X_{\beta_{1c}}$ are taken as a fixed parameters with estimating values of the translational dynamic step. Here A_{long} represents the ratio of the rotor pitch moment derivative to the rotor time constant, $\dfrac{Mf_{\delta_{long}}}{\tau_f}$.

Estimated parameters and their statistical parameters are tabulated at the Table 4 - 13. In order to estimate these unknown parameters, output error method is used. Estimated parameters have the reasonable values with small errors. Rotor time constant is estimated as 0,144 second and its theoretical value is 0,127 second. It is also tabulated at the Table 4 - 12. Its estimated value is close to its theoretical value.

Table 4 - 11 : Pitch Dynamics, Output Error Method Results

Parameters	$\hat{\theta}$	Standard Error, $s(\hat{\theta})$	% Error	$|t_o|$
M_u	6,91E-03	1,65E-05	2,39E-01	4,18E+02
$M_{\beta_{1c}}$	9,05E+00	5,73E-02	6,33E-01	1,58E+02
τ_f	1,44E-01	8,63E-03	6,01E+00	1,66E+01
A_{long}	-6,82E+00	9,63E-02	1,41E+00	7,08E+01

Table 4 - 12 : Comparison of Theoretical and Estimated Rotor Time Constants at Pitch Dynamics Step

Parameter	Estimated Value	Theoretical Value
τ_f [sec]	0,144	0,127

Identified model responses and non-linear simulation model responses are shown at Figure 4 - 11. Solid line represents the non-linear simulation responses and dashed line represents the non-linear analysis results. In order to determine the linearity between the estimated and measured outputs, data correlation matrix is calculated. Its diagonal elements are tabulated at the Table 4 - 13. Diagonal elements of the correlation matrix represent the correlation of the identified model results and non-linear simulation responses. All of them are greater than 0.9 thus their linearity is very good. Hence these estimated parameters may be used as initial parameter values at the identification of the coupled pitch and roll dynamics step.
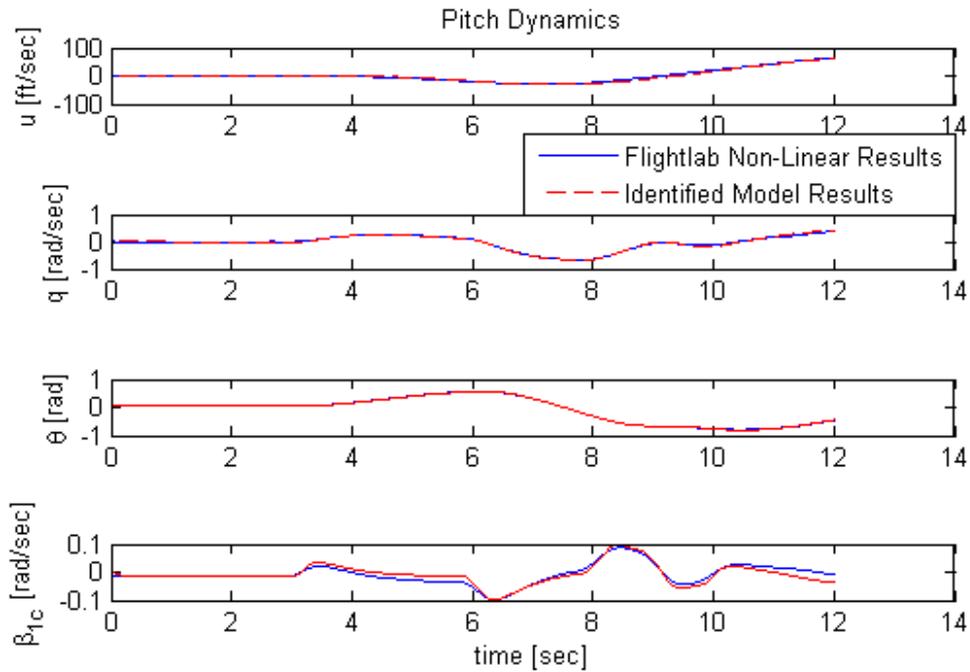
Figure 4 - 11 : Uncoupled Pitch Dynamics result with Output Error Method

Table 4 - 13 : Correlation Coefficient Matrix for Pitch Dynamics

Outputs	Correlation Coefficients
u	0,99
q	1,00
θ	1,00
β_{1c}	0,94

Roll dynamics equations may be obtained likewise. If cross coupling terms are ignored, state space form of the roll dynamics may be written as (4.10. Roll dynamics has four states, which are v, p, φ and β_{1s}.

$$\begin{bmatrix} \dot{v} \\ \dot{p} \\ \dot{\varphi} \\ \dot{\beta}_{1s} \end{bmatrix} = \begin{bmatrix} Y_v & 0 & g & Y_{\beta_{1s}} \\ L_v & L_p & 0 & L_{\beta_{1s}} \\ 0 & 1 & 0 & 0 \\ 0 & 1 & 0 & -\dfrac{1}{\tau_f} \end{bmatrix} x + \begin{bmatrix} 0 \\ 0 \\ 0 \\ B_{lat} \end{bmatrix} \delta_{lat} \qquad (4.10)$$

This state space form involves quasi-steady force angular derivative, L_p. However, this parameter is ignored in the identification procedure. Since, its contribution to results is much smaller than other parameters. Hence final roll dynamics equation can be expressed as following,

$$\begin{bmatrix} \dot{v} \\ \dot{p} \\ \dot{\varphi} \\ \dot{\beta}_{1s} \end{bmatrix} = \begin{bmatrix} Y_v & 0 & g & Y_{\beta_{1s}} \\ L_v & 0 & 0 & L_{\beta_{1s}} \\ 0 & 1 & 0 & 0 \\ 0 & 1 & 0 & -\dfrac{1}{\tau_f} \end{bmatrix} x + \begin{bmatrix} 0 \\ 0 \\ 0 \\ B_{lat} \end{bmatrix} \delta_{lat} \qquad (4.11)$$

Yv is estimated by using the least square method at the identification of the lateral translational dynamic step. Moreover, $Y_{\beta_{1s}}$ has a fixed value. It is equal to gravity constant, g. Then four unknown parameters, namely L_v, $L_{\beta_{1s}}$, τ_f and B_{lat}, remain to estimate. Rotor time constant, τ_f, has the same value for pitch and roll dynamics case theoretically. However, in this step, it is also estimated. B_{lat} represents the ratio of the rotor roll moment derivative to the rotor time constant, $\dfrac{Lf_{\delta_{lat}}}{\tau_f}$.

Estimation values of the four unknown parameters are tabulated as Table 4 - 14 with their statistical accuracy parameters. The results are useful. Standard errors are small and t_0 statistics are sufficiently high to accept the parameter accuracy. In addition, rotor time constant is almost same with its theoretical value as seen at the Table 4 - 15.

Table 4 - 14 : Roll Dynamics, Output Error Method Results

Parameters	$\hat{\theta}$	Standard Error, $s(\hat{\theta})$	% Error	$|t_o|$
L_v	-5,40E-02	5,00E-04	9,25E-01	1,08E+02
$L_{\beta_{1s}}$	4,89E+01	2,49E-01	5,08E-01	1,97E+02
τ_f	1,28E-01	9,29E-04	7,24E-01	1,38E+02
B_{lat}	8,14E+00	3,06E-02	3,76E-01	2,66E+02

Table 4 - 15 : Comparison of Theoretical and Estimated Rotor Time Constants at Roll Dynamics Step

Parameter	Estimated Value	Theoretical Value
τ_f [sec]	0,128	0,127

Results of the roll dynamics are seen at the Figure 4 - 12. The non-linear simulation responses and identification results have good matching with each other. In addition, correlation of the non-linear simulation responses and identified model results are seen at the diagonal elements of the correlation coefficient matrix. Diagonal elements of the correlation coefficient matrix are tabulated at the Table 4 - 16. All of the diagonal elements of the correlation coefficient matrix are greater than 0,9. That is to say, non-linear simulation responses and identified results are almost same. As a result, estimated parameters may be used for estimating the other unknown parameters at the further step which is coupled pitch and roll dynamics.
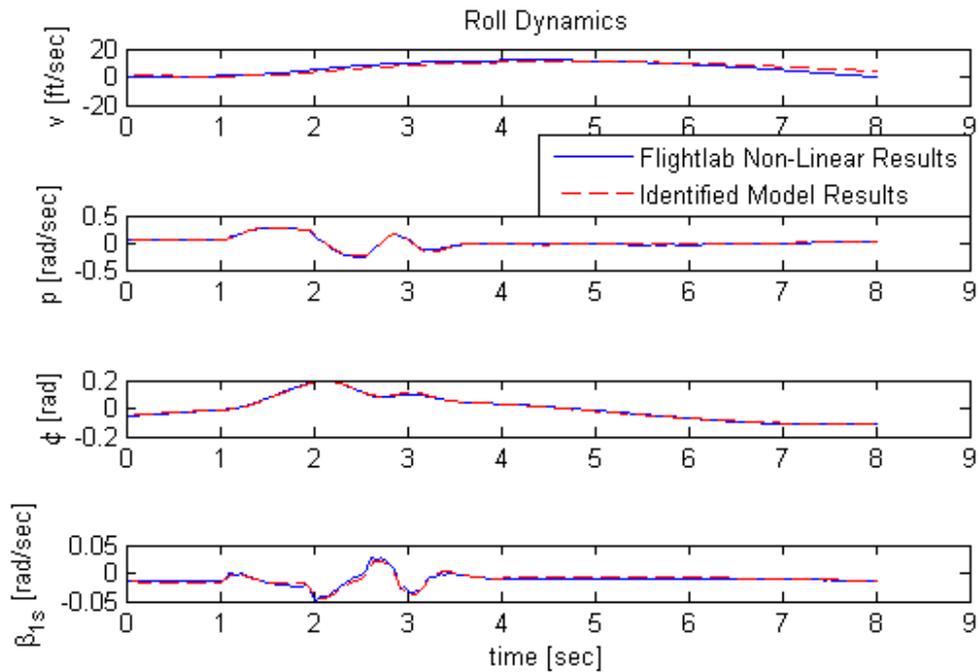
**Figure 4 - 12 : Uncoupled Roll Dynamics results with Output Error Method**

Table 4 - 16 : Correlation Coefficient Matrix for Roll Dynamics

Outputs	Correlation Coefficients
v	0,92
p	0,99
φ	1,00
β_{1s}	0,95

4.3.3 COUPLED DYNAMICS

At this part, first coupled pitch and roll dynamics is identified. Second, parameters of the complete 8 DoF linear model are estimated. In order to estimate the unknown parameters of the coupled pitch and roll dynamics, estimated parameters of the translational dynamics, angular dynamics and uncoupled dynamics are used. Moreover, to identify the complete 8 DoF linear identification model, results of the coupled pitch and roll dynamics model is used.

Coupled pitch and roll dynamics model with the four pitch dynamics states, u, q, θ, β_{1c}, and four roll dynamics states $v, p, \varphi, \beta_{1s}$, may be obtained from full 8 DoF linear identification model as follows,

$$
\begin{bmatrix} \dot{u} \\ \dot{v} \\ \dot{p} \\ \dot{q} \\ \dot{\varphi} \\ \dot{\theta} \\ \dot{\beta}_{1c} \\ \dot{\beta}_{1s} \end{bmatrix} =
\begin{bmatrix}
X_u & X_v & 0 & 0 & 0 & -g & X_{\beta_{1c}} & 0 \\
Y_u & Y_v & Y_p & 0 & g & 0 & 0 & Y_{\beta_{1s}} \\
L_u & L_v & 0 & 0 & 0 & 0 & 0 & L_{\beta_{1s}} \\
M_u & M_v & 0 & 0 & 0 & 0 & M_{\beta_{1c}} & 0 \\
0 & 0 & 1 & 0 & 0 & 0 & 0 & 0 \\
0 & 0 & 0 & 1 & 0 & 0 & 0 & 0 \\
0 & 0 & 0 & 1 & 0 & 0 & -\dfrac{1}{\tau_f} & A_b \\
0 & 0 & 1 & 0 & 0 & 0 & B_a & -\dfrac{1}{\tau_f}
\end{bmatrix} x +
\begin{bmatrix}
0 & 0 \\
0 & 0 \\
0 & 0 \\
0 & 0 \\
0 & 0 \\
0 & 0 \\
A_{long} & A_{lat} \\
B_{long} & B_{lat}
\end{bmatrix}
\begin{bmatrix} \delta_{long} \\ \delta_{lat} \end{bmatrix} \quad \textbf{(4.12)}
$$

However, some parameters are also dropped in the iteration process because of their small contributions. These parameters are X_v, Y_u and Y_p. Finally coupled pitch and roll dynamics can be expressed at the state space form as follows,

$$
\begin{bmatrix} \dot{u} \\ \dot{v} \\ \dot{p} \\ \dot{q} \\ \dot{\varphi} \\ \dot{\theta} \\ \dot{\beta}_{1c} \\ \dot{\beta}_{1s} \end{bmatrix} =
\begin{bmatrix}
X_u & 0 & 0 & 0 & 0 & -g & X_{\beta_{1c}} & 0 \\
0 & Y_v & 0 & 0 & g & 0 & 0 & Y_{\beta_{1s}} \\
L_u & L_v & 0 & 0 & 0 & 0 & 0 & L_{\beta_{1s}} \\
M_u & M_v & 0 & 0 & 0 & 0 & M_{\beta_{1c}} & 0 \\
0 & 0 & 1 & 0 & 0 & 0 & 0 & 0 \\
0 & 0 & 0 & 1 & 0 & 0 & 0 & 0 \\
0 & 0 & 0 & 1 & 0 & 0 & -\dfrac{1}{\tau_f} & A_b \\
0 & 0 & 1 & 0 & 0 & 0 & B_a & -\dfrac{1}{\tau_f}
\end{bmatrix} x +
\begin{bmatrix}
0 & 0 \\
0 & 0 \\
0 & 0 \\
0 & 0 \\
0 & 0 \\
0 & 0 \\
A_{long} & A_{lat} \\
B_{long} & B_{lat}
\end{bmatrix}
\begin{bmatrix} \delta_{long} \\ \delta_{lat} \end{bmatrix} \quad \textbf{(4.13)}
$$

First, estimated parameters of the translational dynamic, angular dynamic and uncoupled dynamics are taken as fixed values at the estimation of the coupled dynamics step. Hence, total six unknown coupled parameters namely, $M_v, L_u, A_b, B_a, A_{lat}$ and B_{long}, are estimated at this step with longitudinal and lateral inputs. Cross-coupling parameter A_b represents the ratio of the pitch moment stiffness to the rotor time constant, $\dfrac{Mf_{\beta_{1s}}}{\tau_f}$. B_a is the ratio of the roll moment stiffness to the rotor time constant, $\dfrac{Lf_{\beta_{1c}}}{\tau_f}$. A_{long} and B_{lat} are defined at the uncoupled dynamics section. A_{lat} and B_{long} indicate the ratio of the moment control derivatives to rotor time constant. They can be expressed as $\dfrac{Mf_{\delta_{lat}}}{\tau_f}$ and $\dfrac{Lf_{\delta_{long}}}{\tau_f}$, respectively.

Table 4 - 17 shows the estimated parameters of the coupled pitch and roll dynamics. Output error method is used to estimate the unknown parameters at this part. Standard errors of the estimated parameters are small and it is acceptable for successful fitting.

Figure 4 - 13 and Figure 4 - 14 show the results of the coupled pitch and roll dynamics. Fitting of the FLIGHTLAB non-linear simulation responses and identification results are acceptable except for the lateral flapping angle, β_{1s}.

Table 4 - 17 : Coupled Pitch and Roll Dynamics, Output Error Method Results

Parameters	$\widehat{\theta}$	Standard Error, $s(\widehat{\theta})$	% Error	$|t_o|$
M_v	2,52E-04	4,69E-05	1,86E+01	5,38E+00
L_u	3,21E-02	1,88E-04	5,87E-01	1,70E+02
A_b	4,36E-01	6,62E-02	1,52E+01	6,58E+00
B_a	-9,73E-01	3,86E-02	3,96E+00	2,52E+01
A_{lat}	-1,13E+00	2,59E-02	2,28E+00	4,38E+01
B_{long}	1,51E+00	2,13E-02	1,42E+00	7,06E+01

Diagonal elements of the correlation coefficient matrix are used to measure the linearity between non-linear simulation responses and identified results. They are tabulated as Table 4 - 18. The results of identification of the pitch dynamics u, q, θ and β_{1c} have greater than 0,9 correlation with non-linear simulation model responses. In addition, results of the roll dynamics v, p and φ have greater than 0,7 correlation factor. Estimated lateral flapping angle, β_{1s}, does not have good agreement with the non-linear simulation model result. However, all estimated results are adequate to use at the complete 8 DoF model.

Table 4 - 18 : Correlation Coefficient Matrix for Coupled Pitch and Roll Dynamics

| Outputs	Correlation Coefficients
u	0,98
v	0,98
p	0,87
q	0,97
φ	0,72
θ	0,97
β_{1c}	0,84
β_{1s}	0,26
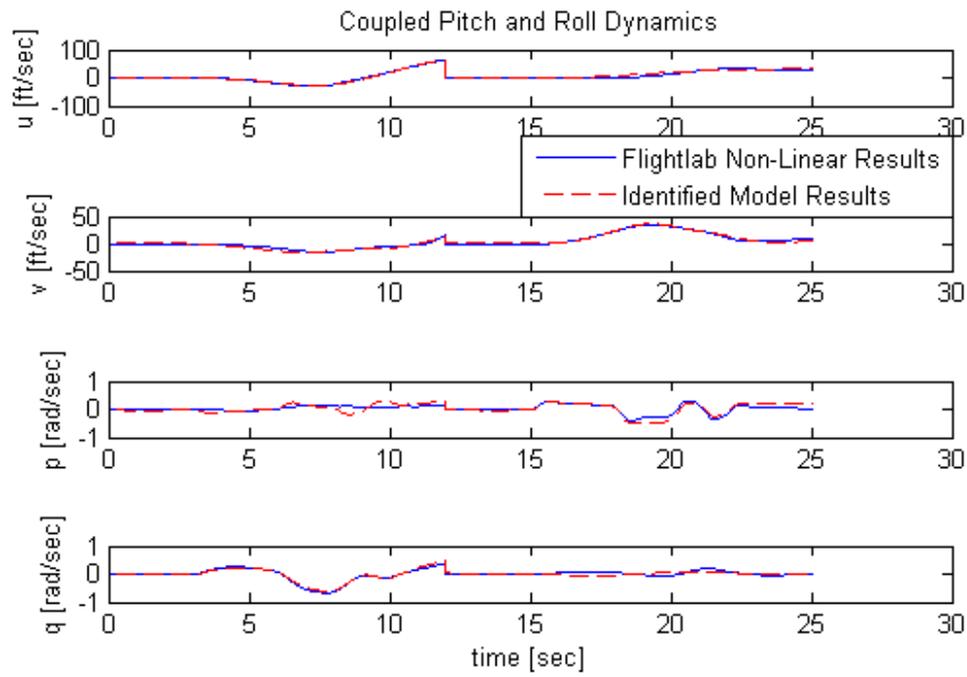
Figure 4 - 13 : Coupled Pitch and Roll Dynamics results with Output Error Method
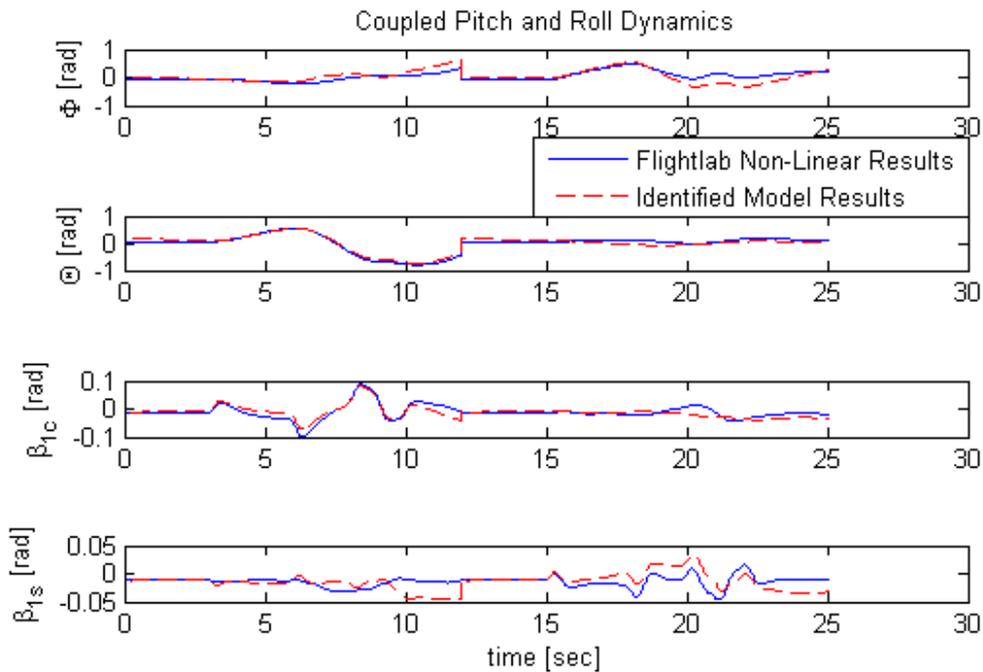

Figure 4 - 14 : Coupled Pitch and Roll Dynamics results (Cont.) with Output Error Method

Finally, complete 8 DoF model is identified by using all of the estimated parameters of the previous steps. Final model is obtained by adding the heave and yaw dynamics to coupled pitch and roll dynamics model with their coupled parameters. State space model of this model can be expressed as,

$$
\begin{bmatrix} \dot{u} \\ \dot{v} \\ \dot{w} \\ \dot{p} \\ \dot{q} \\ \dot{r} \\ \dot{\varphi} \\ \dot{\theta} \\ \dot{\beta}_{1c} \\ \dot{\beta}_{1s} \end{bmatrix} =
\begin{bmatrix}
X_u & 0 & X_w & 0 & 0 & X_r & 0 & -g & X_{\beta_{1c}} & 0 \\
0 & Y_v & Y_w & Y_p & 0 & Y_r & g & 0 & 0 & Y_{\beta_{1s}} \\
Z_u & Z_v & Z_w & Z_p & Z_q & Z_r & 0 & 0 & Z_{\beta_{1c}} & Z_{\beta_{1s}} \\
L_u & L_v & L_w & 0 & 0 & L_r & 0 & 0 & 0 & L_{\beta_{1s}} \\
M_u & M_v & M_w & 0 & 0 & M_r & 0 & 0 & M_{\beta_{1c}} & 0 \\
N_u & N_v & N_w & N_p & N_q & N_r & 0 & 0 & N_{\beta_{1c}} & N_{\beta_{1s}} \\
0 & 0 & 0 & 1 & 0 & 0 & 0 & 0 & 0 & 0 \\
0 & 0 & 0 & 0 & 1 & 0 & 0 & 0 & 0 & 0 \\
0 & 0 & 0 & 0 & 1 & 0 & 0 & 0 & -\frac{1}{\tau_f} & A_b \\
0 & 0 & 0 & 1 & 0 & 0 & 0 & 0 & B_a & -\frac{1}{\tau_f}
\end{bmatrix}
\begin{bmatrix} u \\ v \\ w \\ p \\ q \\ r \\ \varphi \\ \theta \\ \beta_{1c} \\ \beta_{1s} \end{bmatrix} +
$$

$$
\begin{bmatrix}
0 & 0 & X_{\delta_{coll}} & X_{\delta_{pedal}} \\
0 & 0 & Y_{\delta_{coll}} & Y_{\delta_{pedal}} \\
0 & 0 & Z_{\delta_{coll}} & Z_{\delta_{pedal}} \\
0 & 0 & L_{\delta_{coll}} & L_{\delta_{pedal}} \\
0 & 0 & M_{\delta_{coll}} & M_{\delta_{pedal}} \\
0 & 0 & N_{\delta_{coll}} & N_{\delta_{pedal}} \\
0 & 0 & 0 & 0 \\
0 & 0 & 0 & 0 \\
A_{long} & A_{lat} & 0 & 0 \\
B_{long} & B_{lat} & 0 & 0
\end{bmatrix}
\begin{bmatrix} \delta_{long} \\ \delta_{lat} \\ \delta_{coll} \\ \delta_{pedal} \end{bmatrix}
$$

(4.14)

with the output vector,

$$y' = \begin{bmatrix} u & v & w & p & q & r & \varphi & \theta & \beta_{1c} & \beta_{1s} \end{bmatrix}$$

Quasi steady force angular derivative, Y_p, is taken into account at this step. It represents the effect of the tail rotor. Longitudinal, lateral, pedal and collective inputs are used for identification of the model. X_w, X_r, $X_{\delta_{pedal}}$, Y_w, $Y_{\delta_{coll}}$, L_w, L_r, M_w, Z_u, Z_v, Z_p, $Z_{\beta_{1c}}$, $Z_{\beta_{1s}}$, N_v, N_p and $N_{\beta_{1c}}$ are taken as zero. Since, their contributions are small according to others parameters. Thus, final complete 8 DoF linear hover identification model may be written as follows,

$$
\begin{bmatrix} \dot{u} \\ \dot{v} \\ \dot{w} \\ \dot{p} \\ \dot{q} \\ \dot{r} \\ \dot{\varphi} \\ \dot{\theta} \\ \dot{\beta}_{1c} \\ \dot{\beta}_{1s} \end{bmatrix} =
\begin{bmatrix}
X_u & 0 & 0 & 0 & 0 & 0 & 0 & -g & X_{\beta_{1c}} & 0 \\
0 & Y_v & 0 & Y_p & 0 & Y_r & g & 0 & 0 & Y_{\beta_{1s}} \\
0 & 0 & Z_w & 0 & Z_q & Z_r & 0 & 0 & 0 & 0 \\
L_u & L_v & 0 & 0 & 0 & 0 & 0 & 0 & 0 & L_{\beta_{1s}} \\
M_u & M_v & 0 & 0 & 0 & M_r & 0 & 0 & M_{\beta_{1c}} & 0 \\
N_u & 0 & N_w & 0 & N_q & N_r & 0 & 0 & 0 & N_{\beta_{1s}} \\
0 & 0 & 0 & 1 & 0 & 0 & 0 & 0 & 0 & 0 \\
0 & 0 & 0 & 0 & 1 & 0 & 0 & 0 & 0 & 0 \\
0 & 0 & 0 & 0 & 1 & 0 & 0 & 0 & -\frac{1}{\tau_f} & A_b \\
0 & 0 & 0 & 1 & 0 & 0 & 0 & 0 & B_a & -\frac{1}{\tau_f}
\end{bmatrix}
\begin{bmatrix} u \\ v \\ w \\ p \\ q \\ r \\ \varphi \\ \theta \\ \beta_{1c} \\ \beta_{1s} \end{bmatrix} +
$$

(4.15)

$$\begin{bmatrix} 0 & 0 & X_{\delta_{coll}} & 0 \\ 0 & 0 & 0 & Y_{\delta_{pedal}} \\ 0 & 0 & Z_{\delta_{coll}} & Z_{\delta_{pedal}} \\ 0 & 0 & L_{\delta_{coll}} & L_{\delta_{pedal}} \\ 0 & 0 & M_{\delta_{coll}} & M_{\delta_{pedal}} \\ 0 & 0 & N_{\delta_{coll}} & N_{\delta_{pedal}} \\ 0 & 0 & 0 & 0 \\ 0 & 0 & 0 & 0 \\ A_{long} & A_{lat} & 0 & 0 \\ B_{long} & B_{lat} & 0 & 0 \end{bmatrix} \begin{bmatrix} \delta_{long} \\ \delta_{lat} \\ \delta_{coll} \\ \delta_{pedal} \end{bmatrix}$$

Complete 8 DoF identification model has 36 free unknown parameters and two fixed parameters as shown equation (4.15. Fixed parameters are $X_{\beta_{1c}}$ and $Y_{\beta_{1s}}$. They are associated with gravity constant. Except for the new coupled parameters such as $X_{\delta_{coll}}$, Y_p, Y_r, M_r, $N_{\delta_{pedal}}$ etc., initial values of the parameters are taken as estimated values at the previous steps. Furthermore, all of them are refined in this step with bias terms. Initial parameter values for the new unknown coupled parameters are taken as zero.

After estimating all unknown parameters, estimated parameter values are obtained as Table 4 - 19. Standard errors of the estimated parameters are small and except for the $Z_{\delta_{pedal}}$. t_0 statistics have sufficiently big values and this is good for parameter accuracy.

Identification of the complete 8 DoF linear hover identification model converged to a cost function J_{conv} = 8,38E-24. It is a very small value, so that this is acceptable for identification. In the identification procedure, number of the unknown parameters is reduced as much as possible. Briefly, 36 free parameters are estimated. All estimated parameters are shown at the Table 4 - 19. They are in terms of the English units. In addition to, all of them are taken as free parameter to identify the complete 8 DoF linear hover model, except for the $X_{\beta_{1c}}$ and $Y_{\beta_{1s}}$. They have constant values as explained related part.

Figure 4 - 15 shows the inputs which are used at the identification process. Inputs are applied to the FLIGHTLAB non-linear simulation model separately, and then all obtaining results are combined to use at the identification process. At the Figure 4 - 16, Figure 4 - 17 and Figure 4 - 18, twelve seconds of the responses correspond to response of the longitudinal input. Twelve to twenty seconds of the responses represent the lateral response. Twenty to thirty-three seconds of the responses represent the response of the collective input, and then last twelve seconds of the responses represent the pedal response.

Comparison of the non-linear simulation model responses and identified model results are shown Figure 4 - 16, Figure 4 - 17 and Figure 4 - 18. Figure 4 - 16 shows the translational velocities. It is seen that vertical velocity does not have a good matching with non-linear simulation response between five to twelve seconds. This region corresponds to the longitudinal input response. Since, it is the off-axis response and it may be required higher order modeling with inflow coning dynamics for perfect fitting. At the Figure 4 - 17, angular velocity responses of the identified model and non-linear simulation model responses are compared. Angular velocities have good matching with non-linear model responses. Responses of pitch and roll attitudes are shown at the Figure 4 - 18. Attitudes are very close to the non-linear simulation model responses. Longitudinal and lateral flapping angles are also shown at Figure 4 - 18. Flapping angles, especially lateral flap angle, have large errors according to others responses. However, these errors are seen at the off-axis response part. Fitting of the off axis response is much more difficult than on-axis response. To identify the off axis responses,

identification model and/or identification inputs may be enhanced. [5, 18, 8, 13, 15, 22] On the other hand, off-axis responses of the identified model are acceptable for this study.
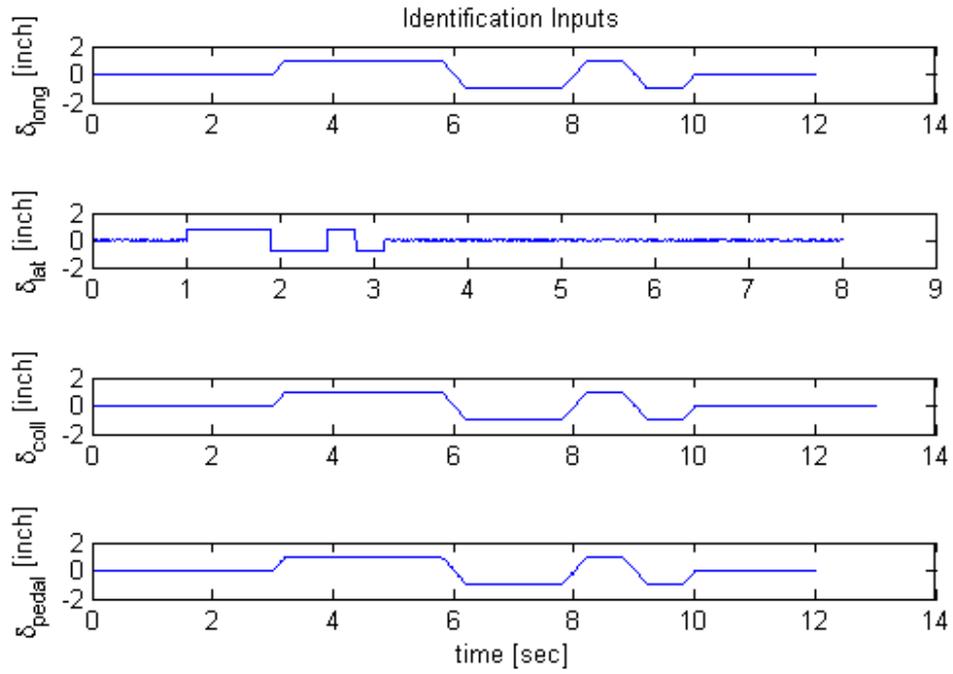

Figure 4 - 15 : Identification Inputs

Table 4 - 19 : Complete 8 DoF Model, Output Error Method Results

| Parameters	$\widehat{\theta}$	Standard Error, $s(\widehat{\theta})$	% Error	$|t_o|$
X_u	-1,37E-01	1,78E-03	1,30E+00	7,72E+01
$X_{\beta_{1c}}$	-32,17	-	-	-
Y_v	-1,44E-01	2,54E-03	1,76E+00	5,69E+01
Y_p	5,99E+00	3,06E-01	5,10E+00	1,96E+01
Y_r	3,41E+00	6,07E-02	1,78E+00	5,62E+01
$Y_{\beta_{1s}}$	32,17	-	-	-
Z_w	-4,53E-01	8,88E-03	1,96E+00	5,10E+01
Z_q	-1,01E+01	2,07E-01	2,05E+00	4,89E+01
Z_r	2,35E+00	1,24E-01	5,30E+00	1,89E+01
L_u	1,98E-02	1,88E-04	9,49E-01	1,05E+02
L_v	-4,46E-02	4,24E-04	9,50E-01	1,05E+02
$L_{\beta_{1s}}$	5,06E+01	4,55E-01	8,99E-01	1,11E+02
M_u	3,62E-03	5,12E-05	1,41E+00	7,07E+01
M_v	8,19E-03	1,06E-04	1,29E+00	7,74E+01
M_r	-4,25E-02	9,04E-04	2,13E+00	4,70E+01
$M_{\beta_{1c}}$	9,65E+00	4,13E-02	4,28E-01	2,34E+02
N_u	1,00E-03	4,58E-05	4,55E+00	2,20E+01
N_w	-6,06E-03	1,47E-04	2,43E+00	4,11E+01
N_q	-2,13E-01	3,81E-03	1,79E+00	5,59E+01
N_r	-2,76E-01	2,22E-03	8,04E-01	1,24E+02
$N_{\beta_{1s}}$	5,40E+00	7,96E-02	1,47E+00	6,78E+01
τ_f	1,22E-01	5,21E-04	4,28E-01	2,34E+02
A_b	-5,93E+00	1,20E-01	2,02E+00	4,95E+01
B_a	1,12E+00	1,50E-02	1,34E+00	7,47E+01
$X_{\delta_{coll}}$	5,43E+01	1,21E+00	2,24E+00	4,47E+01
$Y_{\delta_{pedal}}$	2,30E+01	2,67E-01	1,16E+00	8,64E+01
$Z_{\delta_{coll}}$	-2,93E+02	3,93E+00	1,34E+00	7,47E+01
$Z_{\delta_{pedal}}$	-4,85E+00	8,48E-01	1,75E+01	5,71E+00
$L_{\delta_{coll}}$	-4,22E+00	1,01E-01	2,39E+00	4,18E+01
$L_{\delta_{pedal}}$	2,58E+00	3,28E-02	1,27E+00	7,87E+01
$M_{\delta_{coll}}$	4,72E+00	2,92E-02	6,19E-01	1,61E+02
$M_{\delta_{pedal}}$	-2,34E+00	1,00E-02	0,428959	2,33E+02
$N_{\delta_{coll}}$	8,54E+00	6,15E-02	7,21E-01	1,39E+02
$N_{\delta_{pedal}}$	-3,63E+00	1,34E-02	3,68E-01	2,72E+02
A_{long}	-6,80E+00	1,08E-02	1,58E-01	6,32E+02
A_{lat}	3,84E+00	3,30E-02	8,58E-01	1,16E+02
B_{long}	1,54E+00	9,70E-03	0,630953	1,58E+02
B_{lat}	7,50E+00	3,58E-02	4,78E-01	2,09E+02
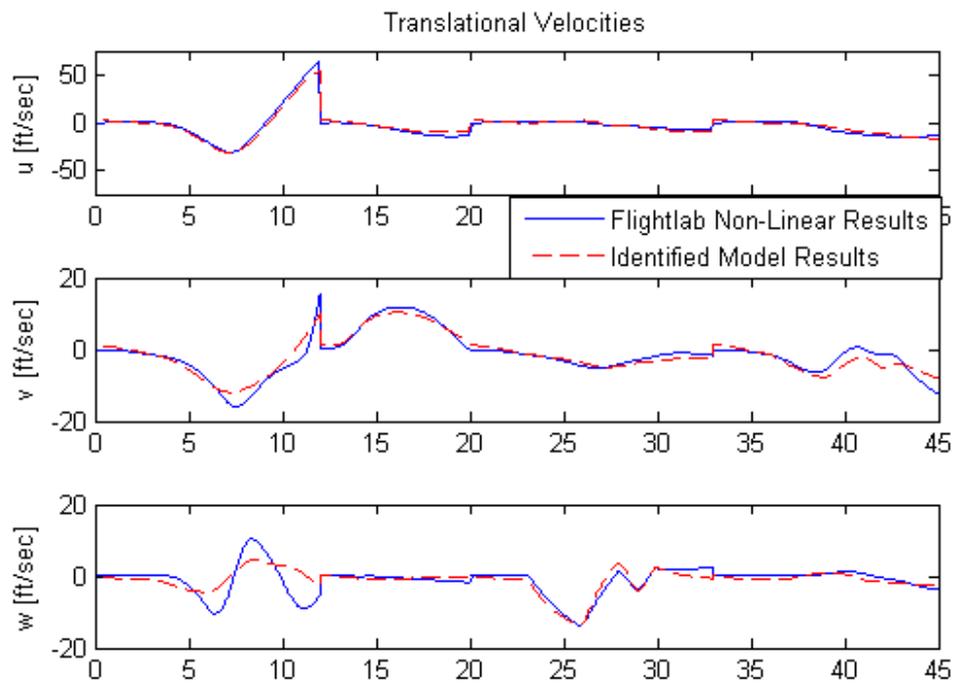
Figure 4 - 16 : Complete Model Velocity results with Output Error Method
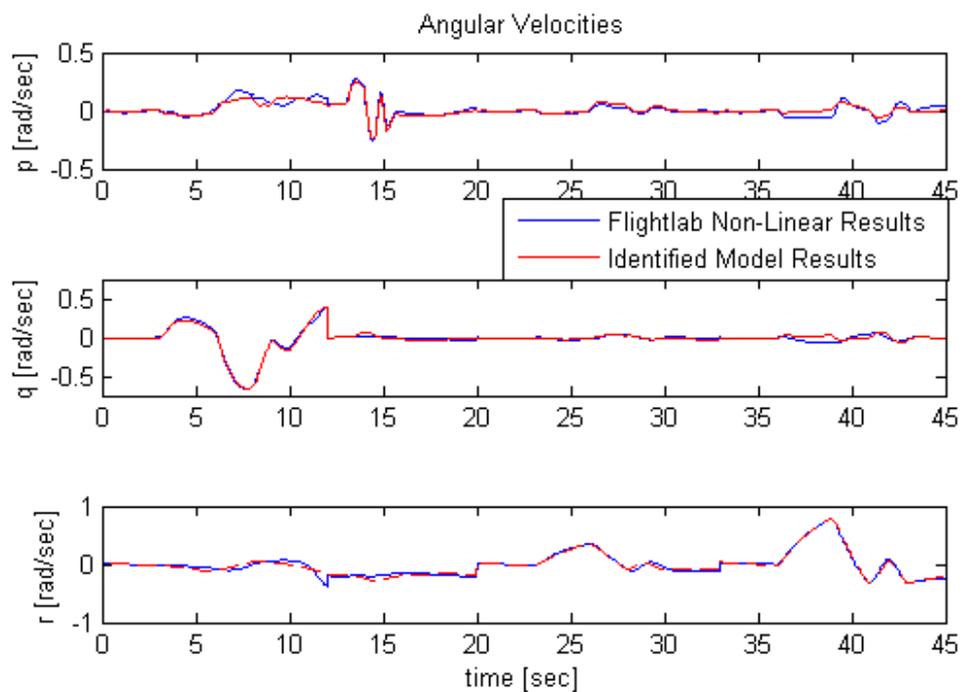

Figure 4 - 17 : Complete Model Angular Velocity results with Output Error Method

59
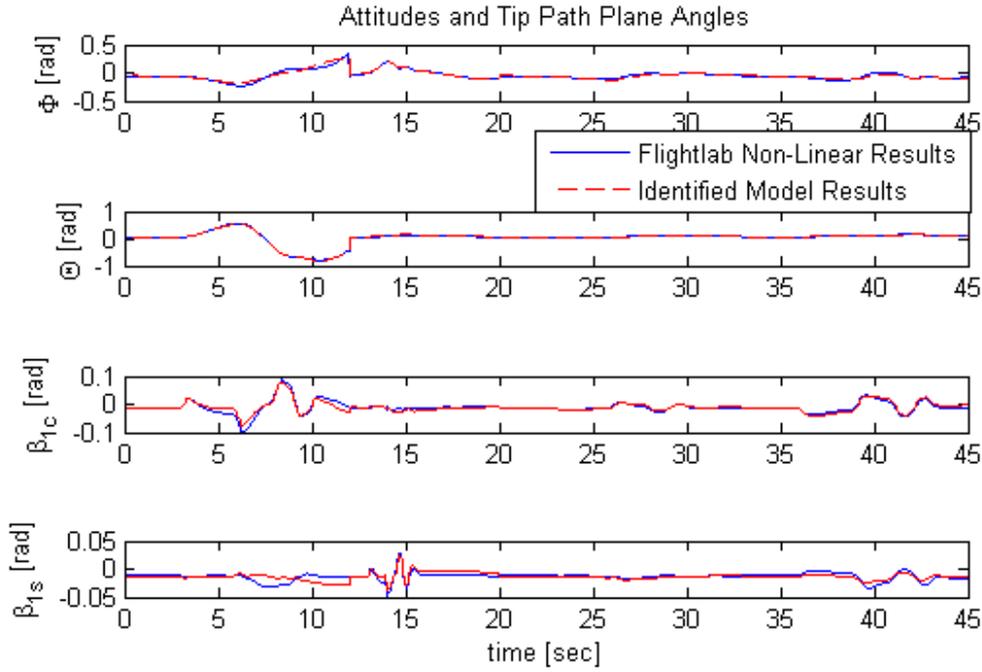
Figure 4 - 18 : Complete Model Attitudes and Flap Angles results with Output Error Method

As discussed before, in order to interpret the model fitting, correlation coefficient of determination matrix is used for complete 8 DoF linear hover identification model and FLIGHTLAB non-linear simulation model. Diagonal elements of the correlation matrix are shown at Table 4 - 20. Except of the vertical velocity and lateral swashplate angle, all of the outputs have greater than 0.9 correlation coefficient. This means that identification is successfully completed. For the vertical velocity and lateral swashplate angle, linearity of the responses are not very good because of the off-axis fitting results. However, these responses are acceptable for this study. Moreover at Table 4 - 21 shows the theoretical and identified values of the rotor time constant. Its theoretical value is the 0,127 second and its estimated value is 0,122 second. It shows agreeable prediction for time constant. The ratio of the pitch and roll stiffness terms, $\left|\dfrac{L_{\beta_{1s}}}{M_{\beta_{1c}}}\right|$, should be equal to the ratio of the pitch moment inertia to roll moment inertia. [5] Its comparison of the theoretical and estimated values also shown at the Table 4 - 21. Its theoretical value is 4,47 and estimated value is 5,24. Hence it may be claimed that parameters are successfully estimated.

In order to determine the helicopter static speed stability, the off axis controls should be fixed, so that the only control gradient parameter, $\dfrac{\Delta\delta_{long}}{\Delta u}$ is remaining. For positive static speed stability this gradient should be negative. Simplified equation for the longitudinal speed stability derivative is [5],

$$M_u = -M_{\delta_{long}}\left(\frac{\Delta\delta_{long}}{\Delta u}\right) + M_w\frac{Z_u}{Z_w} \qquad (4.16)$$

60

Table 4 - 20 : Correlation Coefficient Matrix for Complete 8 DoF Hover Model

Outputs	Correlation Coefficients
u	0,98
v	0,96
w	0,78
p	0,92
q	0,99
r	0,98
φ	0,96
θ	1,00
β_{1c}	0,94
β_{1s}	0,60

Table 4 - 21 : Comparison of Theoretical and Estimated Rotor Time Constants and The Ratio of The Pitch to Roll Flapping Stiffness for Complete 8 DoF Hover Model

Parameter	Estimated Value	Theoretical Value
τ_f [sec]	0,122	0,127
$\left| \dfrac{L_{\beta_{1s}}}{M_{\beta_{1c}}} \right|$	5,24	4,47

A positive is expected for M_u according to first principles analyses of the steady state response of an isolated rotor to speed perturbations. [5, 17, 25] As a result of these, M_u should have a positive value and result is consistent with the estimated value of the $M_u = 3.62\mathrm{E} - 03$.

Similarly lateral speed derivative L_v, may be expressed as follows, based on the non-linear simulation trim gradients, [5]

$$L_v = - \left[L_{\delta_{lat}} \left(\frac{\Delta \delta_{lat}}{\Delta v} \right) + L_{\delta_{pedal}} \left(\frac{\Delta \delta_{pedal}}{\Delta v} \right) \right] \qquad (4.17)$$

Hence, for the positive lateral dihedral stability, L_v should be negative. Moreover identification result of L_v is negative with value of -4.46E-02. Hence, identification parameters have good agreement with their theoretical values.

4.4   VERIFICATION

After estimated all of the unknown parameters of the complete 8 DoF hover model, time domain verification is done to observe the predictive capability of the identified model with step and doublet inputs. They are not used at the identification process. Here FLIGHTLAB simulation data represent

the flight data. At the figures, solid line represents the non-linear simulation responses, dashed line represents the identified model responses. All inputs are applied after the hover trim condition.

4.4.1   PILOT LONGITUDINAL CYCLIC RESPONSE VERIFICATION

For identified 8 DoF Hover model, stability and control derivatives are fixed and then step and doublet input are applied four control sticks, longitudinal, lateral, collective and pedal, respectively. Figure 4 - 19 shows the verification pilot inputs. Same inputs are also applied FLIGHTLAB non-linear simulation model to compare with identified model responses. These inputs have 0.2 second rise time and fall time.
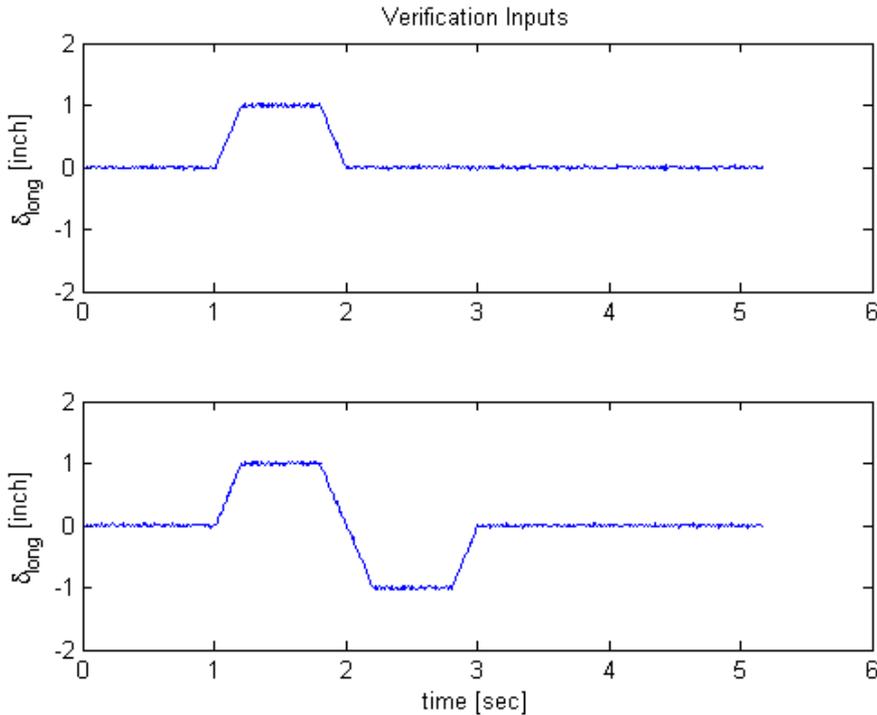

Figure 4 - 19 : Verification (Step and Doublet) Pilot Inputs for Longitudinal Responses

In order to compare the identified 8 DoF model responses and non-linear simulation model responses, correlation coefficients are used. If the correlation coefficient is 1, identified model response and simulation responses have a perfect match. Table 4 - 22 and Table 4 - 23 show the correlation coefficients for the step and doublet inputs, respectively.

Table 4 - 22 : Correlation Coefficients for Comparison of the Identified 8 DoF Model and Non-Linear Simulation Model for Longitudinal Step Input

Outputs	Correlation Coefficients
u	1,00
v	0,98
w	0,62
p	0,76
q	1,00
r	0,63
φ	0,93
θ	1,00
β_{1c}	0,99
β_{1s}	0,22

Table 4 - 23 : Correlation Coefficients for Comparison of the Identified 8 DoF Model and Non-Linear Simulation Model for Longitudinal Doublet Input

Outputs	Correlation Coefficients
u	0,89
v	0,96
w	0,83
p	0,68
q	1,00
r	0,92
φ	0,90
θ	1,00
β_{1c}	1,00
β_{1s}	0,43

Results of the longitudinal step response to identified model and nonlinear simulation model are compared. Correlation coefficients are calculated to compare identified 8 DoF model and non-linear simulation results. Longitudinal axis responses of the identified 8 DoF model which are u, q, θ and β_{1c} have greater than 0.9 correlations with non-linear simulation responses. These responses are the on-axis responses. The off-axis angular responses (p, r) and vertical velocity (w) responses have greater than 0.6 correlations with non-linear simulation results. Magnitudes of these off-axis responses are small. Figure 4 - 20, Figure 4 - 21 and Figure 4 - 22 show the responses of the longitudinal step input. It can be seen that non-linear simulation model and identified model responses are very close to each other.
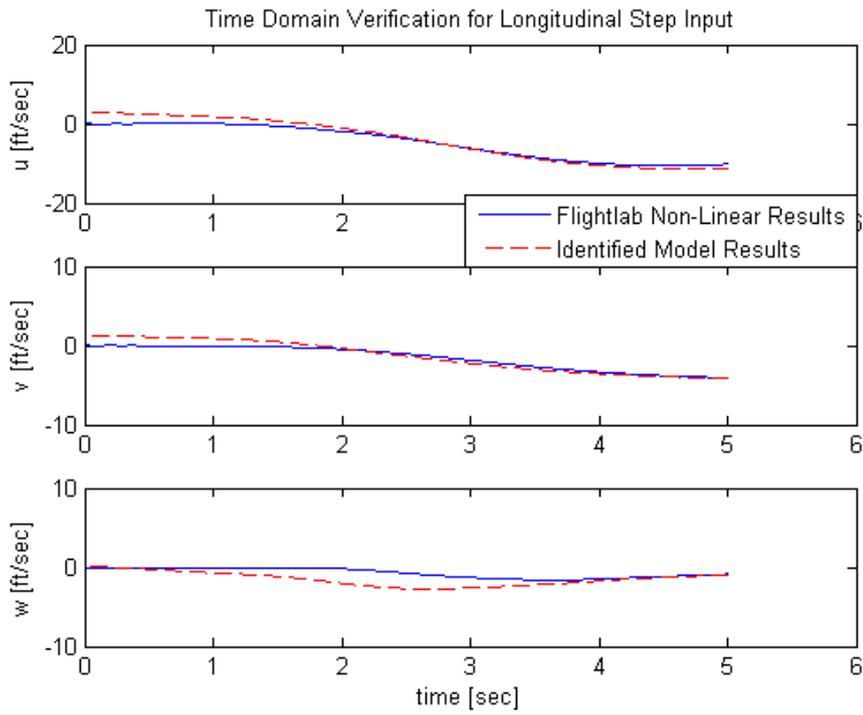
Figure 4 - 20 : Time Response Verification of Identified 8 DoF Hover Model for Longitudinal Step Response, Velocities
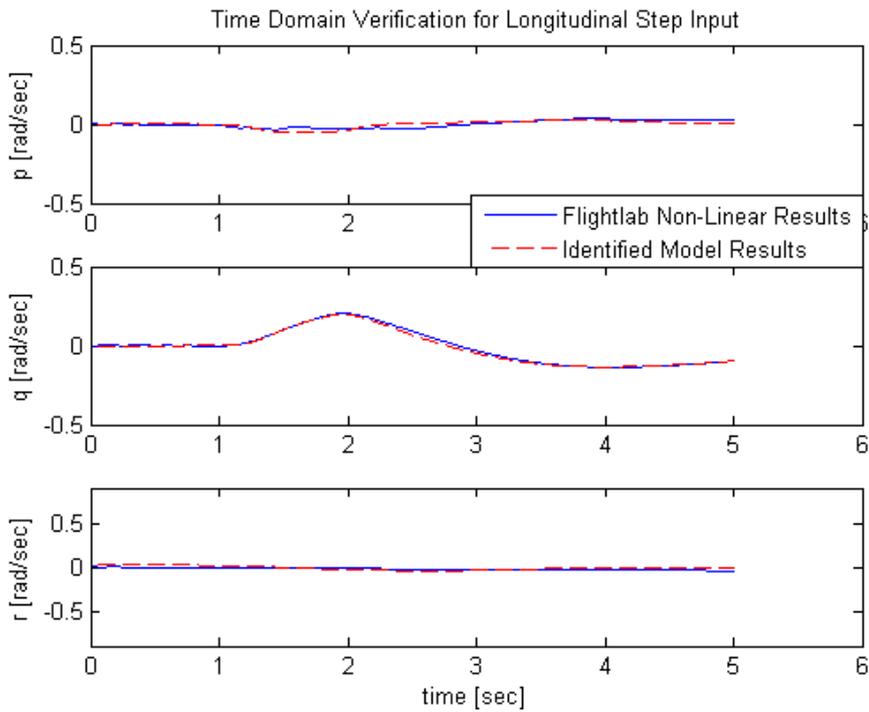

Figure 4 - 21 : Time Response Verification of Identified 8 DoF Hover Model for Longitudinal Step Response, Angular Velocities
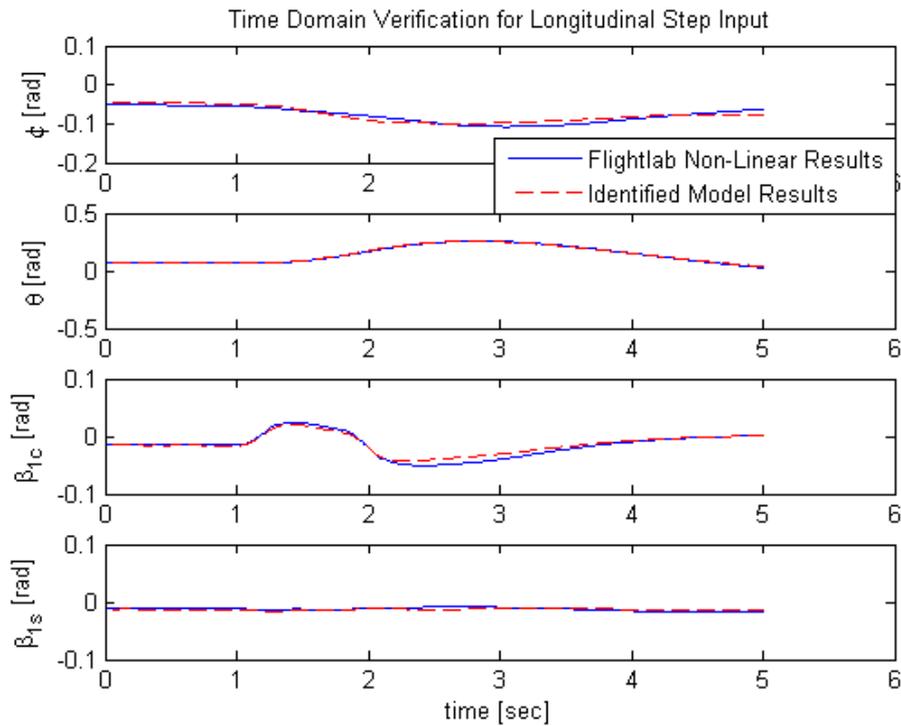
Figure 4 - 22 : Time Response Verification of Identified 8 DoF Hover Model for Longitudinal Step Response, Attitudes and FlapAngles

In addition to the step input, doublet input is also applied to the identified model. Comparison of the identified model response and non-linear simulation model response is done. Similar to step input responses, the on-axis responses of the identified model match better to non-linear simulation responses for doublet input. Correlation coefficients of the on-axis response are greater than 0,85. Figure 4 - 23 shows the responses of the body velocities. All body velocity responses of identified model have good matching with non-linear simulation model responses. Vertical body velocity has some deficiency, however it is acceptable. Angular velocities are shown at Figure 4 - 24. Pitch angular velocity response has perfect matching with non-linear simulation model. Its correlation coefficient is also equal to 1. Similarly, pitch attitude has also perfect matching. It can be seen at Figure 4 - 25. Flapping angles and roll attitude have also acceptable fitting with non-linear simulation model.
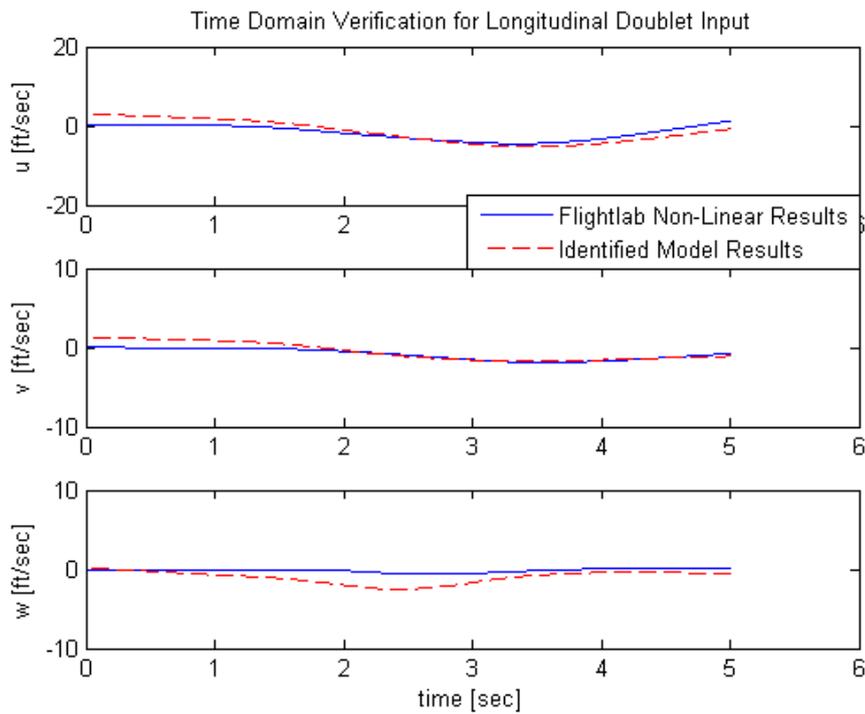
Figure 4 - 23 : Time Response Verification of Identified 8 DoF Hover Model for Longitudinal Doublet Response, Velocities
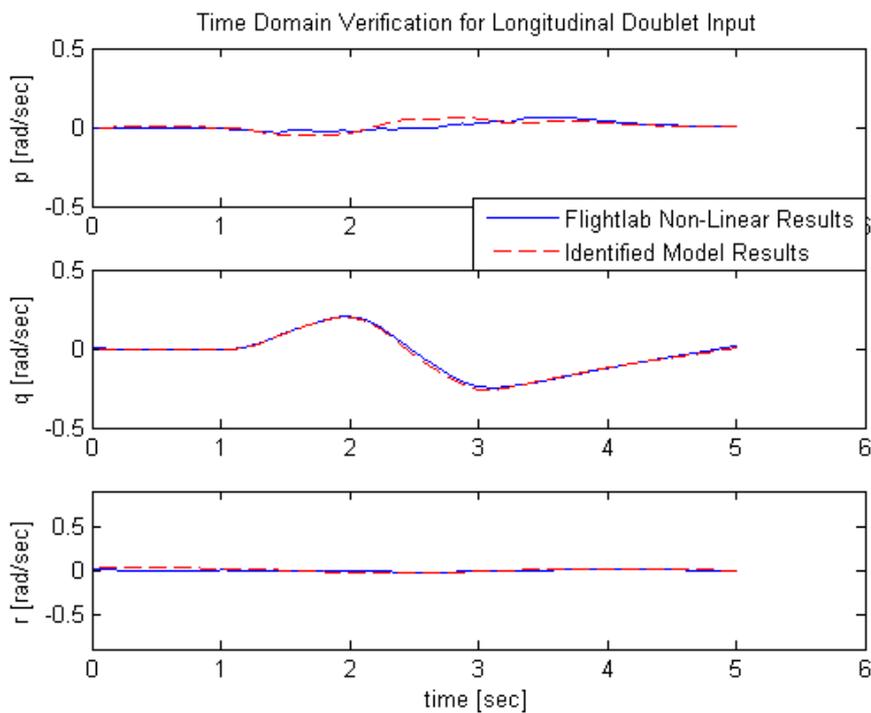

Figure 4 - 24 : Time Response Verification of Identified 8 DoF Hover Model for Longitudinal Doublet Response, Angular Velocities

66
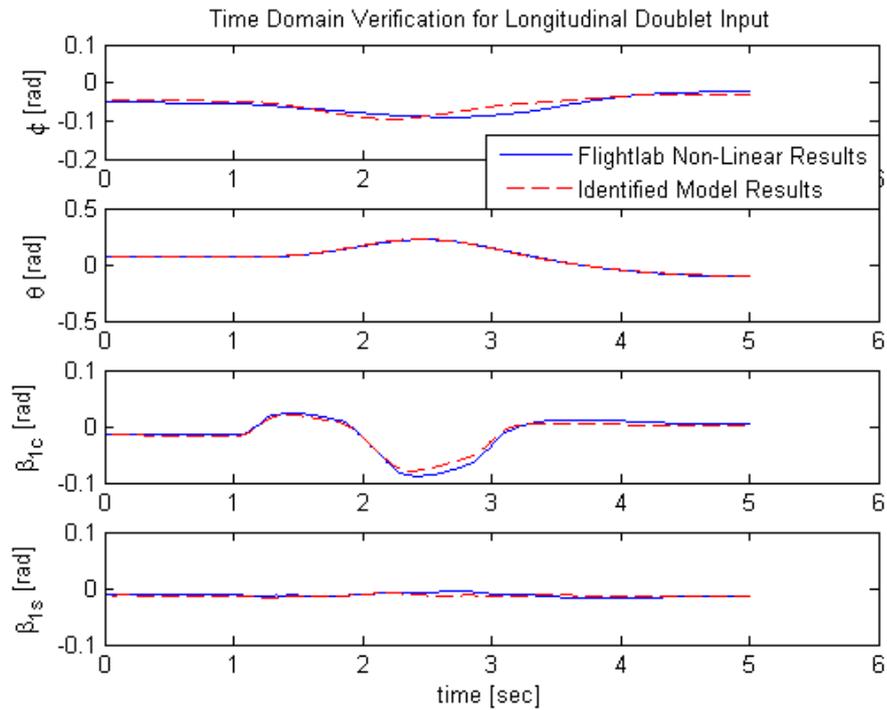
Figure 4 - 25 : Time Response Verification of Identified 8 DoF Hover Model for Longitudinal Doublet Response, Attitudes and FlapAngles

4.4.2 PILOT LATERAL CYCLIC RESPONSE VERIFICATION

Like longitudinal response verification, step and doublet inputs are also applied to identified 8 DoF complete model and FLIGHTLAB non-linear simulation model. Verification inputs are shown at the Figure 4 - 26. These step and doublet inputs have 0.2 second rise time and fall time.

Correlation coefficients of the identified 8 DoF model and non-linear simulation models responses are tabulated at the Table 4 - 24 and Table 4 - 25 for step and doublet inputs, respectively. For lateral step input responses, the on-axis responses are good matching with each other. Longitudinal body velocity response of the identified model has the lowest correlation with the non-linear simulation response. Moreover, vertical velocity and angular yaw rate responses have less correlation coefficient than other responses, since identified model has the only coupled flapping dynamics. Coupled inflow and coning dynamics are not modeled. When coupled inflow and coning dynamics are added to the identified model, this deficiency may be remedied. For lateral doublet input, the on-axis responses have also good matching. The off-axis responses have similar deficiencies. Longitudinal and vertical body velocity responses of the identified model have negative correlation with non-linear simulation responses. When longitudinal and vertical velocity of the identified model responses are decreasing, longitudinal and vertical velocity of the non-linear simulation model responses are increasing as shown in Figure 4 - 27. However, these responses have small magnitudes and they are acceptable for identified 8 DoF model. Lateral body velocity has good matching with 0,98 correlation coefficient.

67

Table 4 - 24 : Correlation Coefficients for Comparison of the Identified 8 DoF Model and Non-Linear Simulation Model for Lateral Step Input

Outputs	Correlation Coefficients
u	0,11
v	0,98
w	0,39
p	0,99
q	0,85
r	0,49
φ	0,95
θ	0,99
β_{1c}	0,74
β_{1s}	0,88

Table 4 - 25 : Correlation Coefficients for Comparison of the Identified 8 DoF Model and Non-Linear Simulation Model for Lateral Doublet Input

| Outputs	Correlation Coefficients
u	-0,29
v	0,79
w	-0,70
p	0,99
q	0,74
r	0,35
φ	1,00
θ	0,55
β_{1c}	0,77
β_{1s}	0,93
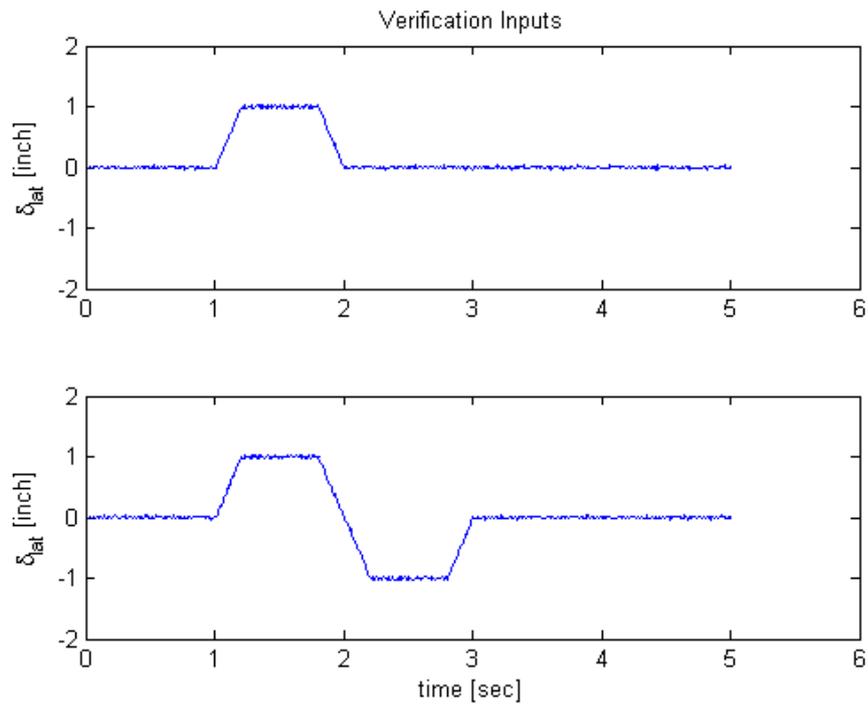
Figure 4 - 26 : Verification (Step and Doublet) Pilot Inputs for Lateral Responses

Figure 4 - 27, Figure 4 - 28 and Figure 4 - 29 show the responses of the lateral step input. It can be seen that non-linear simulation model and identified responses are close to each other. Correlation coefficients of the all responses are tabulated at Table 4 - 24. Longitudinal and vertical body velocities have some deficiencies and they are seen at Table 4 - 27. Angular velocities are shown at Figure 4 - 28. They have good agreement with non-linear simulation model response. Roll and pitch angular velocities have greater than 0.85 correlations with non-linear simulation model angular velocity responses. Figure 4 - 29 shows roll and pitch attitudes and flapping angles. These responses have also acceptable matching with non-linear simulation models responses. Pitch and roll attitude responses of identified model have greater than 0.95 correlations with non-linear simulation model responses. Flapping angles responses have also high correlation coefficients.
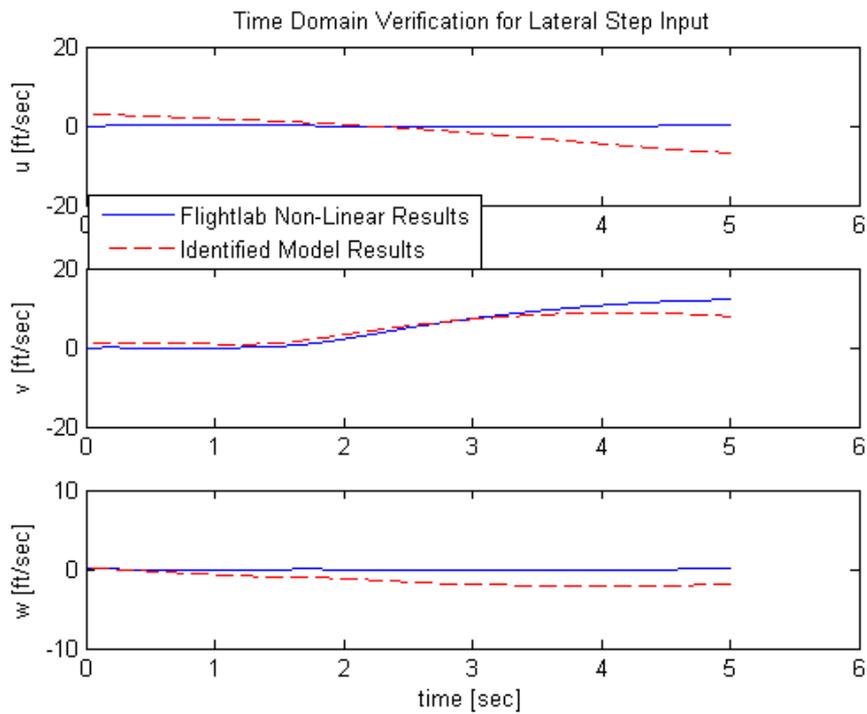
Figure 4 - 27 : Time Response Verification of Identified 8 DoF Hover Model for Lateral Step Response, Velocities
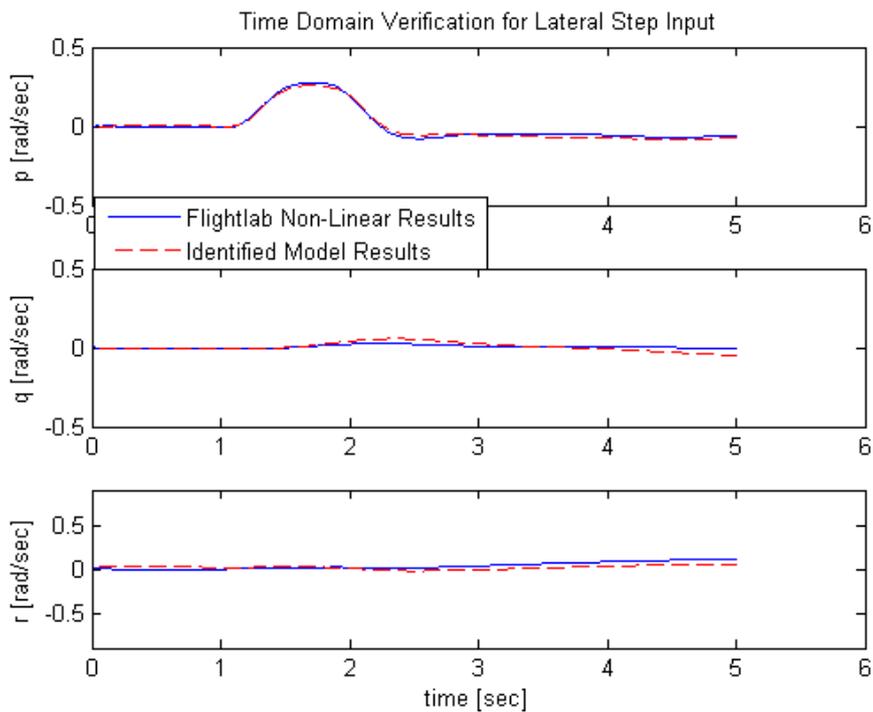

Figure 4 - 28 : Time Response Verification of Identified 8 DoF Hover Model for Lateral Step Response, Angular Velocities

70
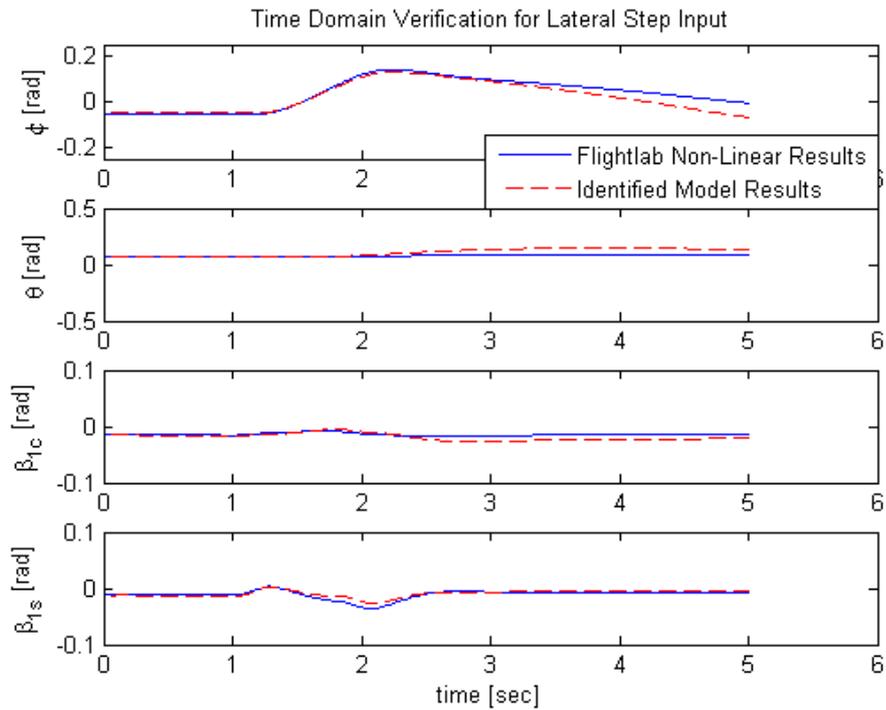
Figure 4 - 29 : Time Response Verification of Identified 8 DoF Hover Model for Lateral Step Response, Attitudes and FlapAngles

Doublet input is also applied to identified model and FLIGHTLAB non-linear simulation model. Comparison of the identified model response and non-linear simulation model response is done. Velocity responses are seen at Figure 4 - 30. Angular velocities are seen at Figure 4 - 31. Roll and yaw attitudes and also flapping angles are seen at Figure 4 - 32. Their correlation coefficients are tabulated at Table 4 - 25. Similar to lateral step input, longitudinal and vertical body velocity responses have some deficiencies for lateral doublet input. However, lateral body velocity has good matching with non-linear simulation model response. The off-axis velocity responses may be required to improve. Roll angular velocity response of identified model has approximately perfect matching. The off-axis angular velocity responses are acceptable matching for identified 8 DoF model. At Figure 4 - 32, roll attitude response have perfect matching. Longitudinal flapping angle response has 0,77 correlation coefficient. Moreover lateral flapping angle response have 0,93 correlation with non-linear simulation model response. Hence, identified 8DoF model is acceptable especially the on-axis responses for lateral inputs.
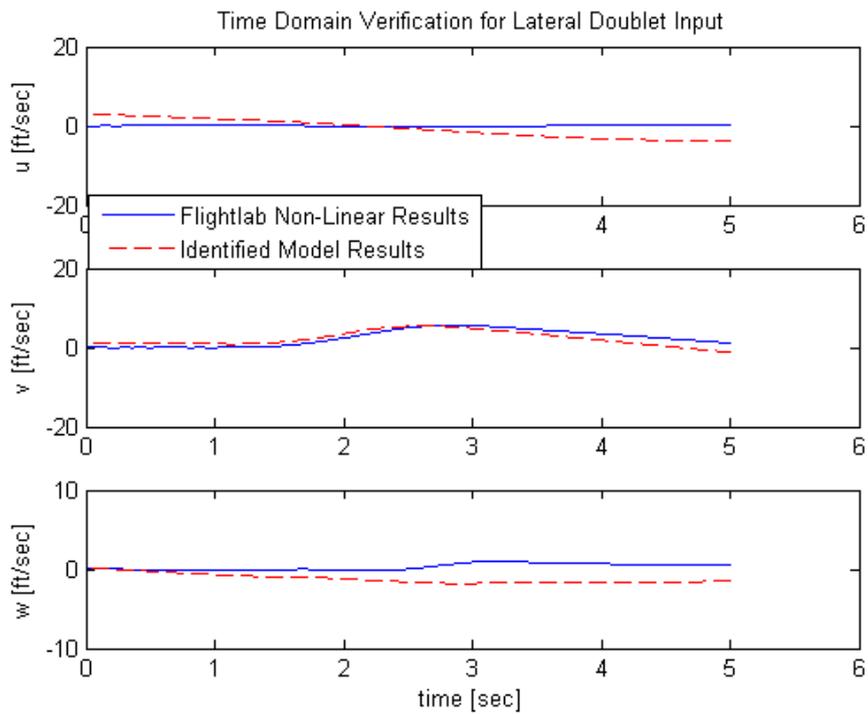
Figure 4 - 30 : Time Response Verification of Identified 8 DoF Hover Model for Lateral Doublet Response, Velocities
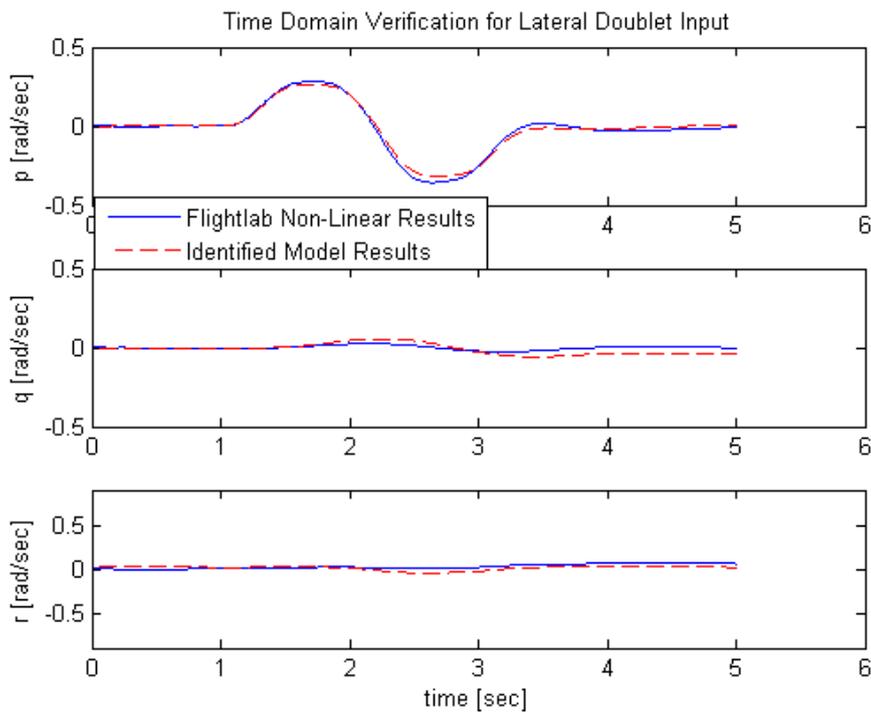

Figure 4 - 31 : Time Response Verification of Identified 8 DoF Hover Model for Lateral Doublet Response, Angular Velocities

72
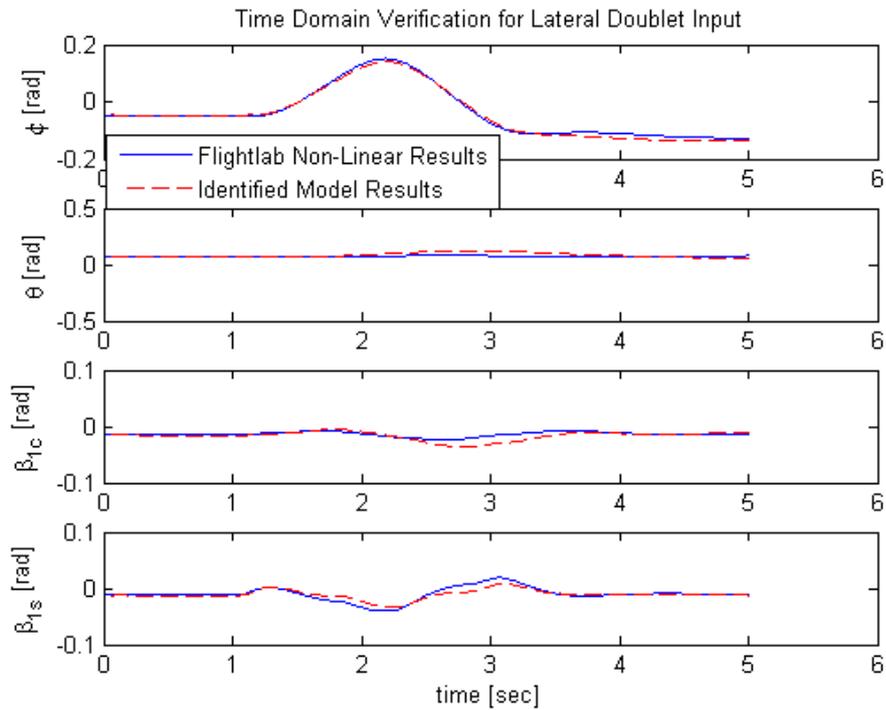
Figure 4 - 32 : Time Response Verification of Identified 8 DoF Hover Model for Lateral Doublet Response, Attitudes and FlapAngles

4.4.3   PILOT COLLECTIVE REPONSE VERIFICATION

Step and doublet collective inputs are also applied to identified 8 DoF complete model and FLIGHTLAB non-linear model. These inputs are shown at Figure 4 - 33. Inputs are applied at the 1 second with 0.2 second rise time and fall time.

Table 4 - 26 shows the correlation coefficients of the identified 8 DoF model and non-linear simulation model responses for step input. All responses have good fitting with each other, except for longitudinal body velocity. Longitudinal body velocity response has negative correlation coefficient. However, its magnitude is small.

Correlation coefficients of the identified model and non-linear simulation model responses for doublet input are shown at Table 4 - 27. Lateral, yaw and heave dynamics responses have greater than 0,8 correlation coefficient. Except for the longitudinal body velocity (u), longitudinal dynamic responses of the identified model have also greater than 0,8 correlation with non-linear simulation responses.

73

Table 4 - 26 : Correlation Coefficients for Comparison of the Identified 8 DoF Model and Non-Linear Simulation Model for Collective Step Input

Outputs	Correlation Coefficients
u	-0,40
v	0,98
w	0,93
p	0,98
q	0,90
r	0,95
φ	0,79
θ	0,79
β_{1c}	0,93
β_{1s}	0,93

Table 4 - 27 : Correlation Coefficients for Comparison of the Identified 8 DoF Model and Non-Linear Simulation Model for Collective Doublet Input

| Outputs	Correlation Coefficients
u	-0,27
v	0,90
w	0,97
p	0,99
q	0,81
r	0,80
φ	0,97
θ	0,83
β_{1c}	0,96
β_{1s}	0,95
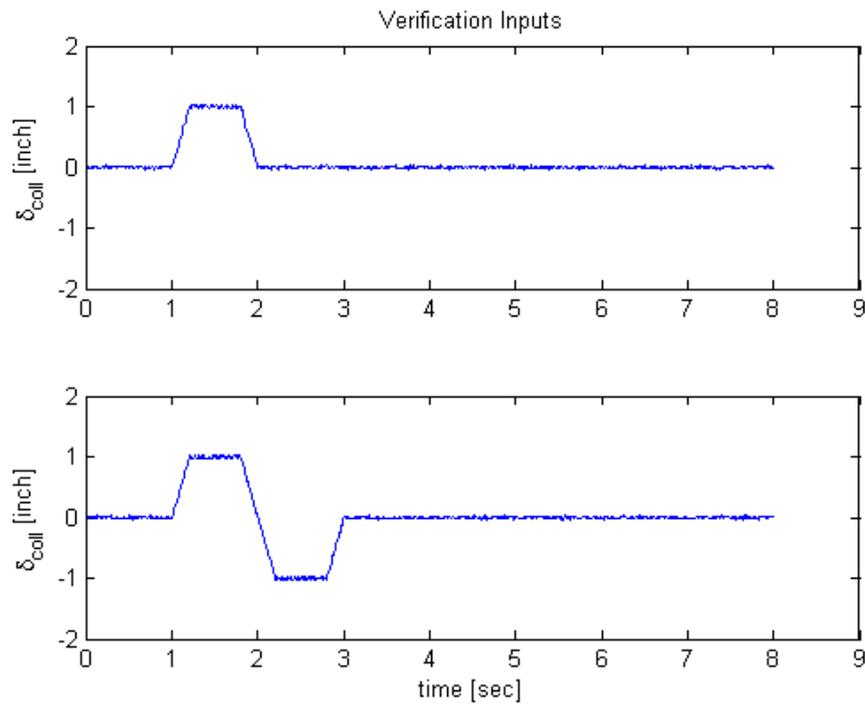
Figure 4 - 33 : Verification (Step and Doublet) Pilot Inputs for Collective Responses

Figure 4 - 34, Figure 4 - 35 and Figure 4 - 36 show the responses of the collective step input. It can be seen that non-linear simulation and estimated responses are close to each other except for the longitudinal body velocity response. Longitudinal body velocity has negative and small correlation with non-linear simulation model response. However, lateral and vertical body velocity responses of identified model have greater than 0,9 correlation with non-linear simulation model responses. These responses are seen at Figure 4 - 34. Figure 4 - 35 shows the angular velocity responses. Angular velocity responses have approximately perfect matching with non-linear simulation model responses. Roll and pitch attitude responses of identified model have also good agreement as shown Figure 4 - 36. Figure 4 - 36 shows also flapping angle responses to collective step input. Correlations of the flapping angles with non-linear simulation flapping angle responses are 0,93. Hence, identified 8 DoF model has good agreement with non-linear simulation model for collective step input.
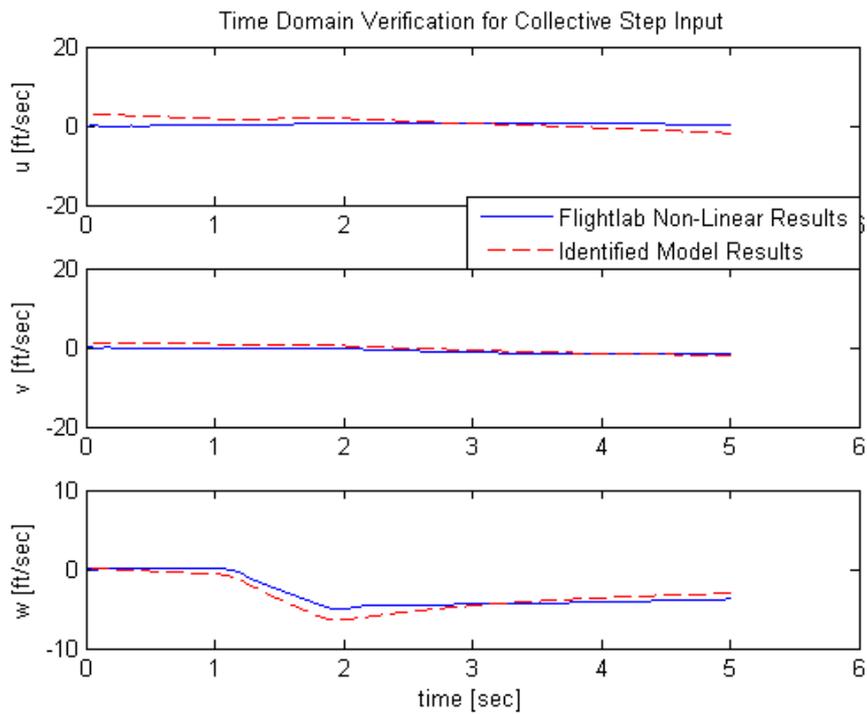
Figure 4 - 34 : Time Response Verification of Identified 8 DoF Hover Model for Collective Step Response, Velocities
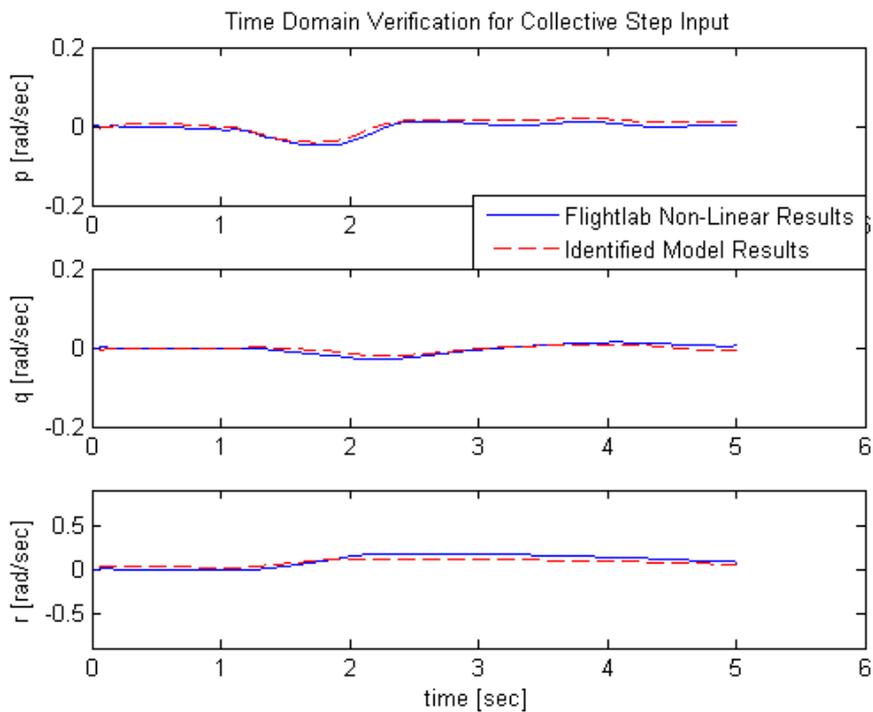

Figure 4 - 35 : Time Response Verification of Identified 8 DoF Hover Model for Collective Step Response, Angular Velocities

76
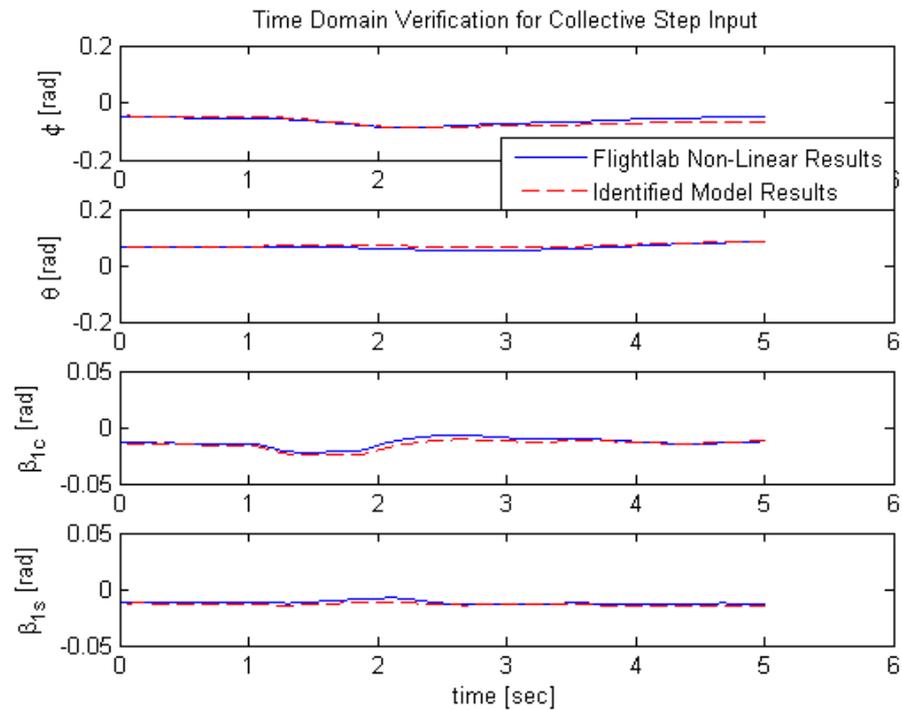
Figure 4 - 36 : Time Response Verification of Identified 8 DoF Hover Model for Collective Step Response, Attitudes and Flap Angles

Doublet input is also applied to identified model and then comparison of the identified model response and non-linear simulation model response is done. Agreement of the identified 8 DoF model responses with non-linear simulation model responses for collective step input is similar to responses for the collective doublet input. There is also some deficiency for longitudinal body velocity response. However, it is acceptable for this identified model. Body velocity responses are seen at Figure 4 - 37. The on-axis responses have good matching with non-linear simulation model responses. Vertical velocity response has 0,97 correlation coefficient. Angular velocities can be seen at Figure 4 - 38 and they have greater correlation coefficients. Roll and pitch attitudes have also good matching. They can be seen at Figure 4 - 39 with flapping angle responses. Flapping angles responses have greater than 0.95 agreement with non-linear simulation model responses.
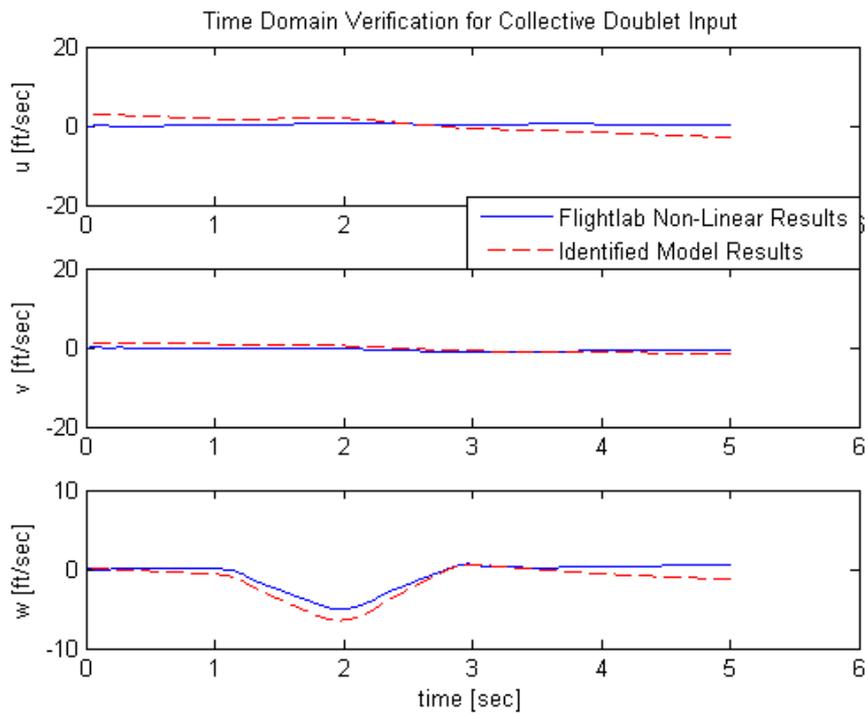
Figure 4 - 37 : Time Response Verification of Identified 8 DoF Hover Model for Collective Doublet Response, Velocities
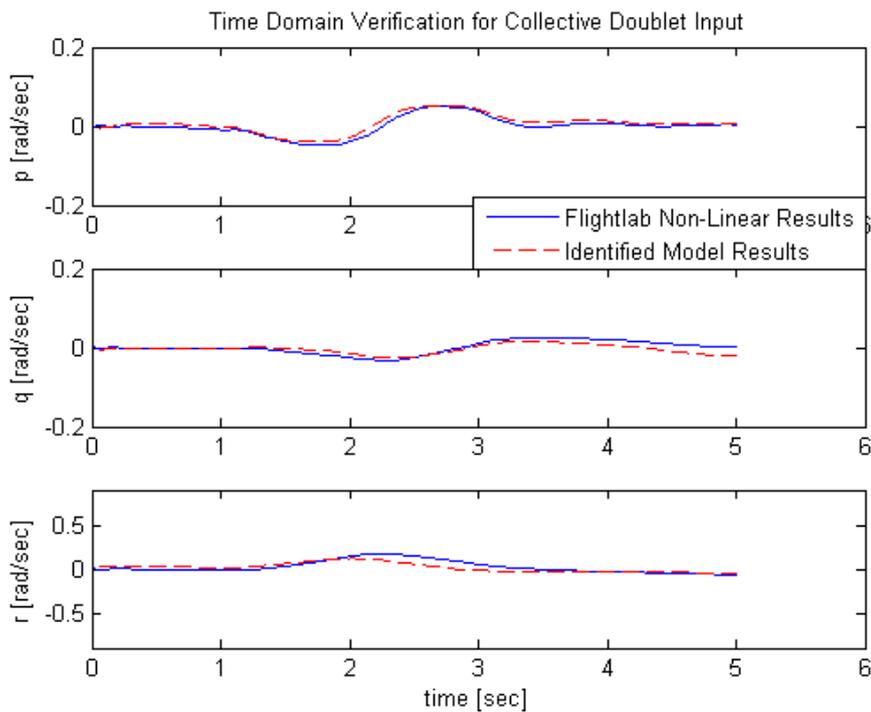

Figure 4 - 38 : Time Response Verification of Identified 8 DoF Hover Model for Collective Doublet Response, Angular Velocities

78
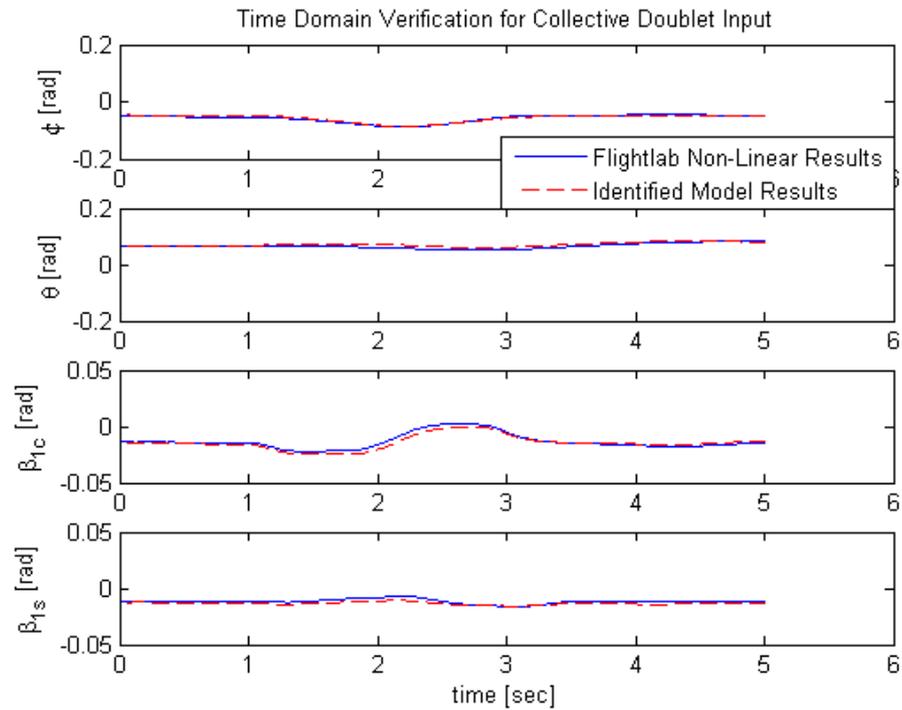
Figure 4 - 39 : Time Response Verification of Identified 8 DoF Hover Model for Collective Doublet Response, Attitudes and Flapping Angles

4.4.4   PILOT PEDAL RESPONSE VERIFICATION

In order to verify 8 DoF identification model, step and doublet inputs are applied to identified model and FLIGHTLAB non-linear simulation model. Inputs have 0.2 second rise time and fall time. Responses of these models are compared to each other.

For the pedal step and doublet inputs, correlation coefficients of the identified model and non-linear simulation model responses are calculated as Table 4 - 28 and Table 4 - 29, respectively. Vertical body velocity response of identified model has negative relation with the non-linear simulation response for pedal step and doublet inputs. Longitudinal body velocity has also negative relation with non-linear simulation result. However these responses have small magnitude. Except for these responses, other responses have good fitting.

Table 4 - 28 : Correlation Coefficients for Comparison of the Identified 8 DoF Model and Non-Linear Simulation Model for Pedal Step Input

Outputs	Correlation Coefficients
u	0,88
v	0,95
w	-0,71
p	0,97
q	0,80
r	1,00
φ	0,73
θ	0,50
β_{1c}	0,96
β_{1s}	0,93

Table 4 - 29 : Correlation Coefficients for Comparison of the Identified 8 DoF Model and Non-Linear Simulation Model for Pedal Doublet Input

| Outputs	Correlation Coefficients
u	-0,18
v	0,46
w	-0,86
p	0,98
q	0,55
r	0,99
φ	0,93
θ	0,49
β_{1c}	0,98
β_{1s}	0,92
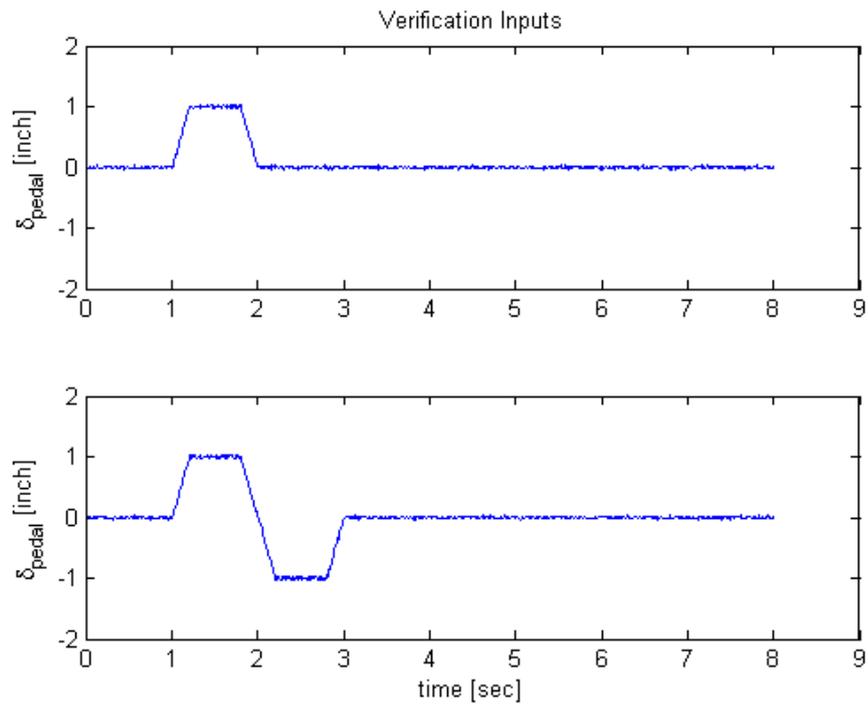
Figure 4 - 40 : Verification (Step and Doublet) Pilot Inputs for Pedal Responses

Figure 4 - 41, Figure 4 - 42, Figure 4 - 43 show the responses of the pedal step input. It is seen that vertical velocity response of the identified model have mismatch with non-linear simulation model at Figure 4 - 41. However its magnitude is small and it may be ignored. At Figure 4 - 42 and Figure 4 - 43, peaks of the angular rates and flapping angles do not have perfect match, but their response characteristics are similar with non-linear simulation responses. Direct response of the pedal input is angular yaw rate response. It is seen that at Figure 4 - 41 yaw rate response of the identified model have perfect match with non-linear simulation model response. Hence the on-axis response of the identified model is in good agreement with non-linear simulation model response. It has also largest correlation coefficient, as seen in Table 4 - 28.
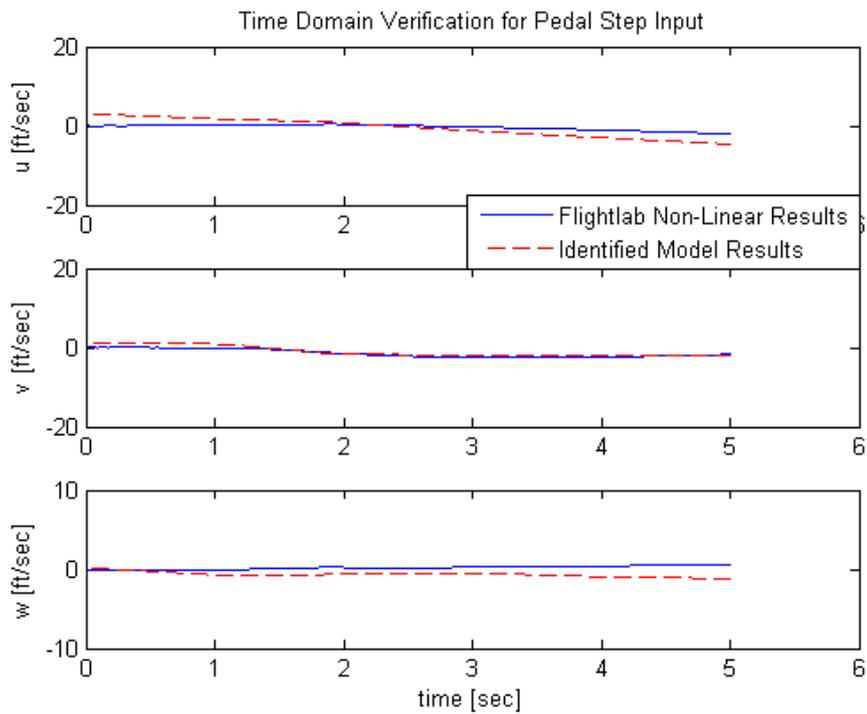
**Figure 4 - 41 : Time Response Verification of Identified 8 DoF Hover Model for Pedal Step Response, Velocities**
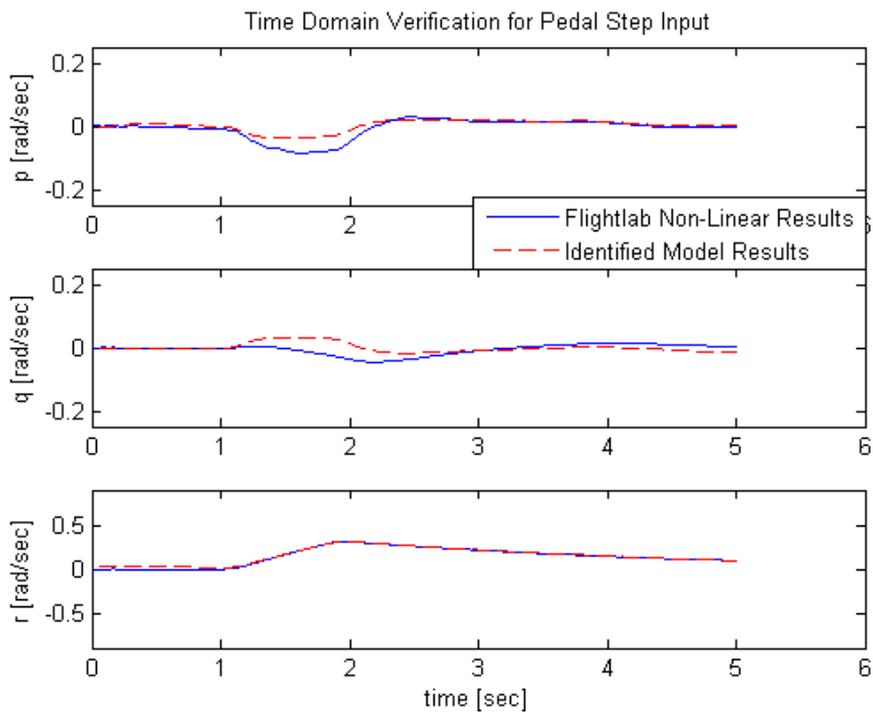
Figure 4 - 42 : Time Response Verification of Identified 8 DoF Hover Model for Pedal Step Response, Angular Velocities

82
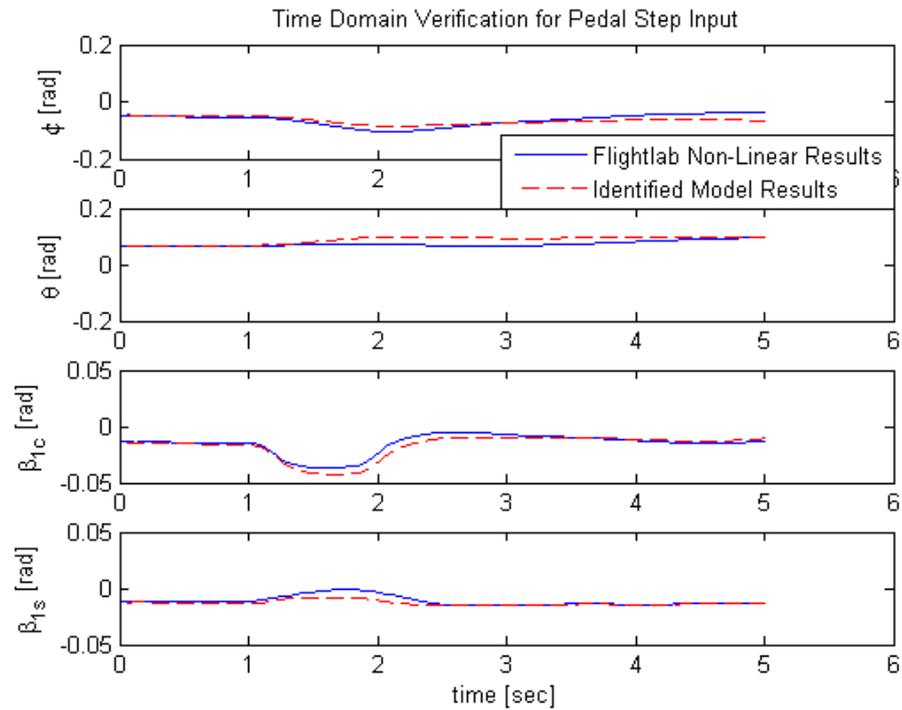
Figure 4 - 43 : Time Response Verification of Identified 8 DoF Hover Model for Pedal Step Response, Attitudes and Flapping Angles

Doublet input is also applied to identified model and then comparison of the identified model response and non-linear model response is done. Figure 4 - 44, Figure 4 - 45 and Figure 4 - 46 show the pedal doublet responses of the identified 8 DoF model and non-linear simulation model. At Figure 4 - 44, the longitudinal and vertical body velocities have different response characteristic from the non-linear simulation model response. These response characteristics may be improved by adding the coupled inflow-coning dynamics to identified model. Figure 4 - 45 show the angular velocities. Pitch and roll angular velocities have different peaks than non-linear simulation model responses. However these deficiencies are acceptable for this identified 8 DoF model. Yaw angular velocity has also perfect match with non-linear simulation model response. Attitudes and flapping angles are shown at Figure 4 - 46. These responses have also acceptable matching with non-linear simulation model.
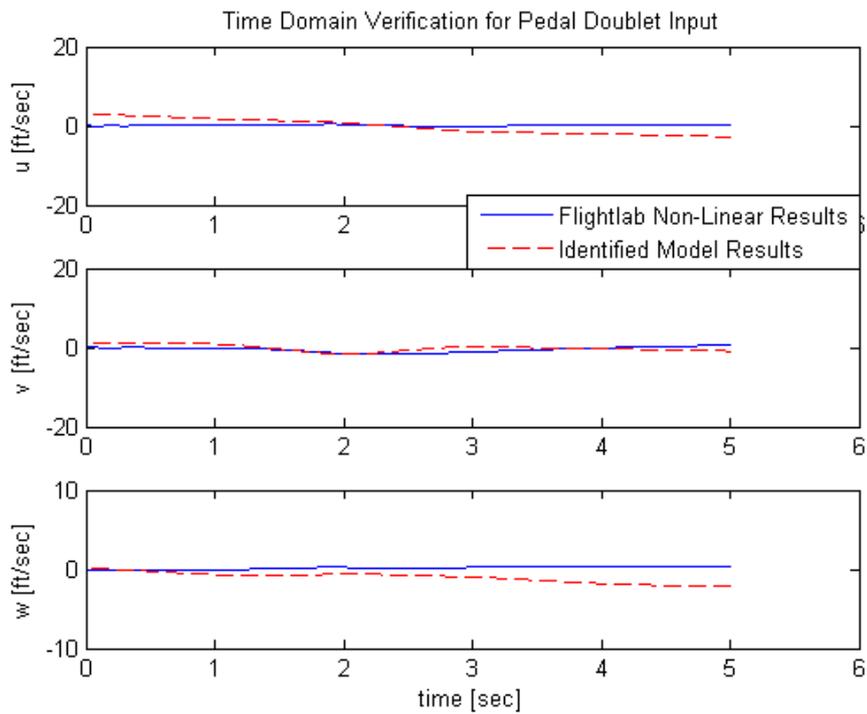
**Figure 4 - 44 : Time Response Verification of Identified 8 DoF Hover Model for Pedal Doublet Response, Velocities**
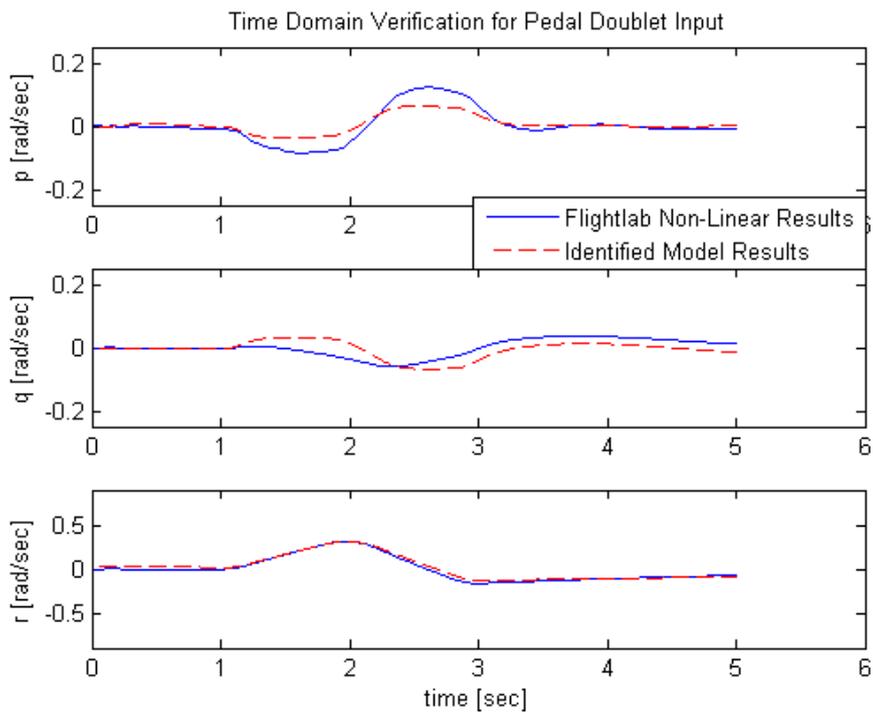

Figure 4 - 45 : Time Response Verification of Identified 8 DoF Hover Model for Pedal Doublet Response, Angular Velocities

84
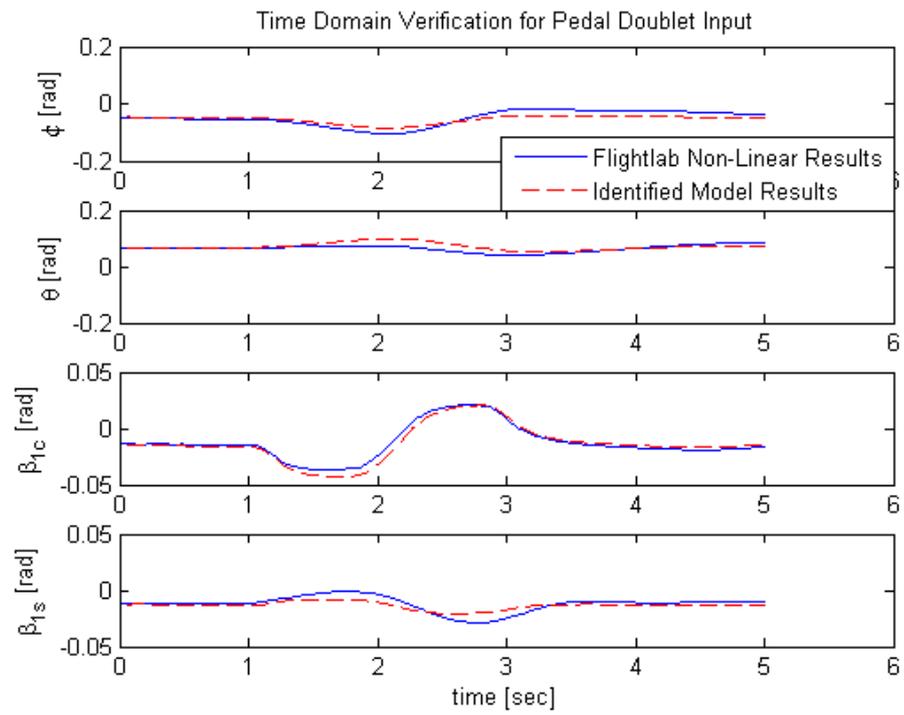
Figure 4 - 46 : Time Response Verification of Identified 8 DoF Hover Model for Pedal Doublet Response, Attitudes and Flapping Angles

85

CHAPTER 5

CONCLUSIONS AND FUTURE WORK

In this thesis, identification of an 8 DoF helicopter model in hover flight condition is carried out. Least square and output error methods are successfully applied in the time domain to determine the unknown stability and control derivatives of the 8 DoF linear identified hover model. In addition to, identification model results are compared with FLIGHTLAB non-linear simulation model responses.

The 8 DoF system identification model is obtained by adding the linearized 6 DoF fuselage dynamics to 2 DoF explicit flapping dynamics. Least square method is used to obtain the initial parameter values for this study.

The system identification is carried first starting from simple uncoupled models and successively including couplings and identifying these more complex models. At each step, the identification is started using the previously identified parameters. Finally, coupled linear model is identified. The success of the approach is demonstrated through simulations.After obtaining the complete helicopter identification model specific to UH-60 helicopter for hover case, its verification is done with step and doublet inputs. Identification model responses are compared the non-linear simulation model results to verify the identification model. Identified model responses successfully compare with the responses of FLIGHTLAB non-linear simulation model. Hence, partition system identification approach may be used to identify the helicopter dynamics. Moreover, identified model can be used for simulation of the hover condition to design the flight control system with limitations of the higher order responses.

5.1   FUTURE WORK

In the future 8 DoF linear model may be expanded to high fidelity such as, 9 to 14 DoF, model by adding and improving lead-lag, yaw-heave dynamics, coupled fuselage/coning-inflow dynamics, rotor wake modeling. Moreover, effects of the each additional complexity shall be be evaluated as well.

To improve the realism of the estimation approach, measurement noise shall also be added to the system approach. Furthermore, instead of the using the simulation model data, actual flight test data may be used for identification.

REFERENCES

1. Zadeh, L. A., From Circuit Theory to System Theory, Proceedings of the IRE, Vol. 50, May 1962

2. Anon., He Has a Question for Any Answer, Interview with K. Iliff by McCall, Antelope Valley Press, CA, Nov. 1, 1994

3. Ljung, Perspectives on System Identification, System Identification Applications and Examples

4. Jatagoankar, R. V., Flight Vehicle System Identification: A Time Domain Methodology, Vol. 216, Progress in Aeronautics and Astronautics, AIAA, 2006

5. Tischler, M. B., Remple, R. K., Aircraft and Rotorcraft Syatem Identification: Engineering Methods with Flight Test Examples, AIAA Education Series, 2006

6. Taylor, L. W., Iliff, K. W., System Identification Using A Modified Newton-Raphson Method – A Fortran Program. NASA TN D-6734, NASA Technical Note, May 1972.

7. Taylor, L. W., Iliff, K. W., Determination of Stability Derivatives From Flight Data Using A Newton-Raphson Minimization Technique. NASA TN D-6579, NASA Technical Note, March 1972.

8. Fletchler, J. W., Identification of UH-60 Stability Derivative Models in Hover from Flight Test Data, Journal of the American Helicopter Society

9. FLIGHTLAB Theory Manual I & II, Advanced Rotorcraft Technology Inc., July 2008

10. Vitale, A., Genito, N., Federico, L., Corraro F., Hybrid Approach for Rotorcraft Identification from Flight Data, American Helicopter Society, 67th Annual Forum, Virginia Beach, VA, May 3-5,2011

11. Wikipedia, http://en.wikipedia.org/wiki, last visited on 20.08.2012

12. Flight Line Supplement, UH-60L Blackhawk, 2-224th Aviation Regiment Sandston, VA 23150

13. Mettler, B., Kanade, T, Tischler, M.B, System Identification Modeling of a Model Scale Helicopter, CMU-RI-TR-00-03

14. Chang, Y. S., Kim, B. J., Keh, J. E., Rotorcraft Dynamics Model Identification and Hovering Motion Control Simulation

15. Ivler, C. M., Tischler, M. B., System Identificaion Modeling for Flight Control Design, Nov. 2008

16. Bhandari S., Colgren R., Lederbogen, P., Kowalchuk, S., six DoF Dynamic Modeling and Flight Testing of a UAV Helicopter, AIAA Modeling and Simulation Technologies Conference and Exhibit, August 2005

17. Prouty, W. R., Helicopter Performance, Stability, and Control, Krieger Publishing Company, Malabar, Florida, 2005

18. Fletchler, J. W., A Model Structure for Identification of Linear Models of the UH-60 Helicopter in Hover and Forward Flight, NASA Technical Memorandum 110362, August 1995

19. Zivan, L, Tischler, M.B., Devolopment of a Full Flight Envelope Helicopter Simulation Using System Identification

20. Hansen, R. S., Toward a Better Understanding of Helicopter Stability Derivatives, NASA Technical Memorandum 84227, August 1982

21. Morelli, E. A., Klein, V., Aircraft System Identification Theory and Practice, AIAA, 2006

22. http://en.wikipedia.org/wiki/Pearson_product-moment_correlation_coefficient

23. Tischler M. B., Tomashofski, C. A., Flight Test Identification of SH-2G Flapped-Rotor Helicopter Flight Mechanics Models, Journal of American Helicopter Society, October 2001

24. Chen, R. T., A Simplified Rotor System Mathematical Model for Piloted Flight Dynamics Simulation, NASA Technical Memorandum 78575, May 1979

25. Çalışkan, S., Development of Forward Flight Trim and Longitudinal Dynamic Stability Codes and Their Application to a UH-60 Helicopter, February 2009

26. Padfield, G. D., Helicopter Flight Dynamics : The Theory and Application of Fliying Qualities and Simulation Modeling, AIAA Education Series, 1999

27. Heffley, R. K., Bourne, S. M., Curtiss, H. C., Jr. Hindson, W.S., Hess, R.A., Study of Helicopter Roll Control Effectiveness Criteria, NASA CR 177404, April 1986

28. Curtiss, H. C., Stability and Control Modeling , Vertica, Vol. 12, No. 4, 1988, pp 381-394

29. Yuan, W., and Katupitiya, J., A Time Domain Grey-Box System Identification Procedure for Scale Model Helicopters, Proceedings to Australasian Conference on Robotics and Automation, 7-9 Dec 2011

30. Bialas, W.F., Lecture Notes in Applied Probability, University at Buffalo, Department of Industrial Engineering, 2005

31. Mettler, B., Identification Modeling and Characteristics of Miniature Rotorcraft, Kluwer Academic Publishers, 2003

32. Cicolani, L. S., Sahai R., Tucker, G. E., McCoy A. H., Tyson, P. H., Tischler M. B., Rosen A., Flight Test Identification and Simulation of a UH-60A Helicopter and Slung Load, NASA TM-2001-209619, USAAMCOM-TR-01-A-001, Jan. 2001

33. McCoy, A. H., Flight Testing and Real-Time System Identification Analysis of a UH-60A Black Hawk Helicopter with an Instrumented External Sling Load, December, 1997

34. Aponso, B. L., Johnston, D. E., Johnson, W. A., Magdaleno, R. E., Identification of Higher Orer Helicopter Dynamics Using Linear Modeling Methods, American Helicopter Society, May 1991

35. Talbot, P. D., Tinling, B. E., Decker, W. A, Chen, R. T., N., A Mathematical Model of a Single Main Rotor Helicopter for Piloted Simulation, NASA Technical Memorandum 84281, September 1982

36.   Chen, R. T. N., Hindson, W. S., Influence of Dynamic Inflow on the Helicopter Vertical Response, NASA Technical Memorandum 88327, June 1986